Extensive testing of an algorithm for travelling-wave-based directional detection and phase-selection by using TWONFIL and EMTP

Research Report
ISSN 0167-9708
Coden: TEUEDE

Eindhoven
University of Technology
Netherlands

Faculty of Electrical Engineering

Extensive Testing of an Algorithm for Travelling-Wave-Based Directional Detection and Phase-Selection by Using TWONFIL and EMTP

by
M.H.J. Bollen
and
G.A.P. Jacobs

EUT Report 88-E-206
ISBN 90-6144-206-0
October 1988

Eindhoven University of Technology Research Reports

EINDHOVEN UNIVERSITY OF TECHNOLOGY

Faculty of Electrical Engineering
Eindhoven The Netherlands

ISSN 0167- 9708 Coden: TEUEDE

EXTENSIVE TESTING OF AN ALGORITHM FOR TRAVELLING-WAVE-BASED DIRECTIONAL DETECTION AND PHASE-SELECTION BY USING TWONFIL AND EMTP

by

M.H.J. Bollen

and

G.A.P. Jacobs

EUT Report 88-E-206

ISBN 90-6144-206-0

Eindhoven

October 1988

CIP-GEGEVENS KONINKLIJKE BIBLIOTHEEK, DEN HAAG

Bollen, M.H.J.

Extensive testing of an algorithm for travelling-wave-based directional detection and phase selection, by using TWONFIL and EMTP / by M.H.J. Bollen and G.A.P. Jacobs. - Eindhoven: Eindhoven University of Technology, Faculty of Electrical Engineering. - Fig. - (EUT report, ISSN 0167-9708; 88-E-206)
Met lit. opg., reg.
ISBN 90-6144-206-0
SISO 661.5 UDC 621.311.1.015.3.001.57 NUGI 832
Trefw.: elektriciteitsnetten / elektrische overgangsverschijnselen.

Abstract

An algorithm for travelling-wave-based directional detection (including phase selection) has been studied for over 10,000 fault and non-fault situations by using a relatively simple network model called TWONFIL. Additional testing on an EMTP model has been performed for the most frequently occuring faults as well as for dangerous cases found from the TWONFIL-study.
From these studies threshold settings and cut-off frequencies needed for a reliable protection have been found, as well as detection and selection times needed.
A few situations showed not to be detectable, others might lead to the generation of false tripping signals.

Bollen, M.H.J. and G.A.P. Jacobs
EXTENSIVE TESTING OF AN ALGORITHM FOR TRAVELLING-WAVE-BASED DIRECTIONAL DETECTION AND PHASE-SELECTION, by using TWONFIL and EMTP.
Faculty of Electrical Engineering, Eindhoven University of Technology, 1988.
EUT Report 88-E-206

Adress of the authors:

ing. G.A.P. Jacobs,
Eindhoven University of Technology,
Faculty of Electrical Engineering,
P.O. Box 513,
5600 MB Eindhoven, The Netherlands.

ACKNOWLEDGEMENT

Thanks are due to Ir. W.F.J. Kersten and Prof.Dr.Ir. W.M.C. van den Heuvel for their assistance during the realization of this report.
Thanks are also to Marijke van de Wijdeven and Yvonne Gallé for the typing.
The EMTP-package was obtained from the

EMTP European Users Group,
K.U. Leuven EMTP Center,
Kard. Mercierlaan 94,
B-3030 Heverlee,
Belgium

Contents.

1. Introduction
1.1. Fast protection.....1
1.2. Different methods for travelling-wave-based protection.....2
1.3. Travelling-wave-based directional detection; the original algorithm.
1.3.1. Superimposed quantities.....4
1.3.2. Fault detection.....6
1.3.3. Phase selection.....8

2. Travelling-wave-based directional detection; the new algorithm.
2.1. Fault detection.....9
2.2. Phase selection.....10
2.3. Protection philosophy.....11

3. The network models used.
3.1. The simple network : TWONFIL.....15
3.2. The complex network : EMTP.....20
3.3. Relay settings.....23

4. Results of the study.
4.1. Derivation of the superimposed quantities.....24
4.2. Low pass filter.....25
4.3. Backward faults and faults on the parallel circuit.....28
4.4. Line energizing.....33
4.5. Lightning strokes.....35
4.6. Thresholds.
4.6.1. Fault detection.....36
4.6.2. Phase selection.....37
4.7. Faults around voltage zero.....38
4.8. Inter-circuit faults.
4.8.1. Non-detectable inter-circuit faults.....40
4.8.2. Failure of phase selection during inter-circuit faults.....41
4.9. Delayed phase selection.....43
4.10. What happened to the homopolar detection functions ?.....44
4.11. A summary of the results.....46

5. Conclusions.....47

References.....48

Appendix A : EMTP results of fault detection.....51
Appendix B : EMTP results of phase selection.....66
Appendix C : TWONFIL results.....75
Appendix D : EMTP input files.....81
Appendix E : Situations studied by using EMTP.....99
Appendix F : Multiple reflections.....100

1. Introduction.

1.1. Fast protection.

To assure a continued supply of electricity in public supply networks, it is neccessary to disconnect all short-circuits within a short time. If a short-circuit occurs this will be detected by one or more protection relays. These relays give tripping signals to a number of power breakers isolating the fault from the healthy part of the h.v network. The disconnected part of the network must be kept as small as possible. If a short circuit occurs on a h.v. line only the faulted line (or the faulted circuit in case of a multi-circuit line) needs to be disconnected.

Nowadays the protection of h.v. lines is largely achieved by means of power frequency distance relays. From the power frequency voltage and current an impedance is determined. If this impedance is below a preset value a tripping signal will be generated. The time between fault-initiation and the generation of a tripping signal is, in general, a few cycles of the power frequency. The fault disconnection time is about five cycles.

Since about ten years there is a call for shorter fault detection (and clearing) times. Three causes for this can be given.

- The increasing power exchange in h.v. networks calls for an increasing number of h.v. lines or a decreasing fault-clearing time. The latter solution is preferable from economic and environmental point of view. A fault clearing time of one or two cycles is needed in some situations to prevent transient instability [1]. Utilizing 3/4-cycle breakers this leaves about 5 milliseconds for fault detection.
- For the usefulness of current limiting devices, the fault must be detected within one or two milliseconds [2].
- The availability of fast and cheap microprocessors brought fast protection within reach. This triggers the call for fast protection (a well-known law in economics).

1.2. Different algorithms for travelling-waved-based protection.

When a fault-detection time of a few milliseconds is needed the power frequency voltages and currents can no longer be used as decisive quantities [3]. The fastest protection relay possible would be one that immediately recognizes travelling waves coming from a fault. In the past some algorithms for travelling-wave-based protection have been proposed. They can be divided into two groups: algorithms using voltages and currents from one line terminal only and those using information from both sides.

Three algorithms have been proposed in the first group:

- The determination of the time delay between forward and backward waves at the relay position. This time delay is a measure for the distance to the fault. To determine the time delay a cross correlation is used [4]. A fault close to the relay position is difficult to detect, so are faults close to the remote line terminal as well as faults around voltage-zero. In some situations the algorithm cannot distinguish between a fault on the line to be protected and a fault on another line [5]. Some problems can be solved by introducing a time derivative [6] or two different time windows [7]. But still no satisfying solution has been found.
- Another algorithm calculates voltages along the line from voltages and currents measured at the relay position. A fault will show up as a place where the voltage remains zero [8]. The second derivative to the position along the line, of the mean-square voltage or current, can be used as a detection function according to [9]. The fault position will show up as a non-zero value of the detection function. But that second derivative will make the algorithm very sensitive to disturbances. Therefore [10] uses the mean square voltage itself, together with the voltage at the suspected fault position.

  Problems with this algorithm are faults close to the relay or close to the remote line-terminal as well as the complicated (time-consuming) calculations needed. A calculation time of about 1 second is reported in [10].

- Reference [29] uses successive reflections to determine the suspected fault distance and fault resistance. This will be repeated untill the fault resistance determined from the suspected fault distance fits the fault resistance determined from the initial voltage jump. Problems may arise for faults around voltage zero as well as because of the complicated calculations needed.

Algorithms of the second group all need a communication link between the line terminals. In the past this was considered to be a great disadvantage. But recent trends in telecommunication (glass fiber, error correcting codes) have brought the possibility of highly reliable communication links, even in the vicinity of h.v. lines.
Four different methods can be distinguished in this group.

- The algorithm for differential travelling-wave-based protection [11]. The waves entering the line at one terminal are compared with those leaving the line, one travel time later, at the other line terminal. When the difference is non-zero, a fault is concluded.
  This algorithm is the subject of a separate study, the results of this will be presented in later publications.

The other three methods determine the direction of origin of the first travelling waves arriving at the relay position. A communication link between the two line terminals is needed to exchange the directions found. If both relays observe a forward fault the line will be disconnected. If one or both observe a backward fault the line will not be disconnected and both relays will be blocked for about 100 milliseconds.

- The method proposed in reference [12] uses the time derivatives of voltage and current to get a "travelling wave discriminant" independent of the fault-initiation-angle. This will allow for a fault detection within a few microseconds. The method has been improved and extended with phase selection [13]. Although extremely fast, the method is not suitable for protection purposes because the time derivative used, makes the detection functions very sensitive to all kinds of disturbances. This will almost certainly lead to false tripping situations.
- The method proposed in reference [14] is, uptill now, the only travelling-wave-based protection algorithm implemented on a commercial relay. The signs of voltage and current-changes determine the direction of origin of a disturbance. The fault detection time is between 4 and 8 milliseconds.

- The basic principle studied in this report is the one proposed by Johns [15] and extended with phase selection by Johns and Mahmoud [16]. Relatively simple combinations of voltages and currents are used to calculate 6 fault-detection and 3 phase-selection functions. From these the direction of the fault and the fault type are determined. Details of this algorithm are given in the next section.

1.3. Travelling-wave-based directional detection ; the original algorithm.

This section describes the algorithm for fault detection including phase selection as proposed by Johns [15] and Johns and Mahmoud [16]. Their algorithm has been the basic idea for the one proposed and studied in this report. The latter will be described in detail in the chapters 2, 4 and 5 together with a justification for the improvements introduced. Chapter 3 will describe the methods used to investigate the proposed algorithm.

1.3.1. Superimposed quantities.

The algorithm does not make use of momentary values of voltages and currents but of so called superimposed quantities. Superimposed quantities are defined as the voltage and current part directly caused by the fault-initiation.
Consider the situation shown in figure 1a. At time-zero a fault is initiated at the position F. The voltages and currents everywhere in the network can be described as a superposition of the undisturbed quantities of figure 1b and the superimposed quantities of figure 1c.
The undisturbed values are the values of voltages and currents in the network without fault initiation. They are caused by the sources. The undisturbed voltage at the fault position F is denoted by $\tilde{V}_F(t)$

Superimposed quantities are caused by the voltage source $\bar{V}_F(t)$ at the fault position. This voltage source is related to the undisturbed voltage at F.

$$\begin{aligned} \bar{V}_F(t) &= 0 \qquad t<0 \\ &= -\tilde{V}_F(t) \qquad t>0 \end{aligned} \tag{1}$$

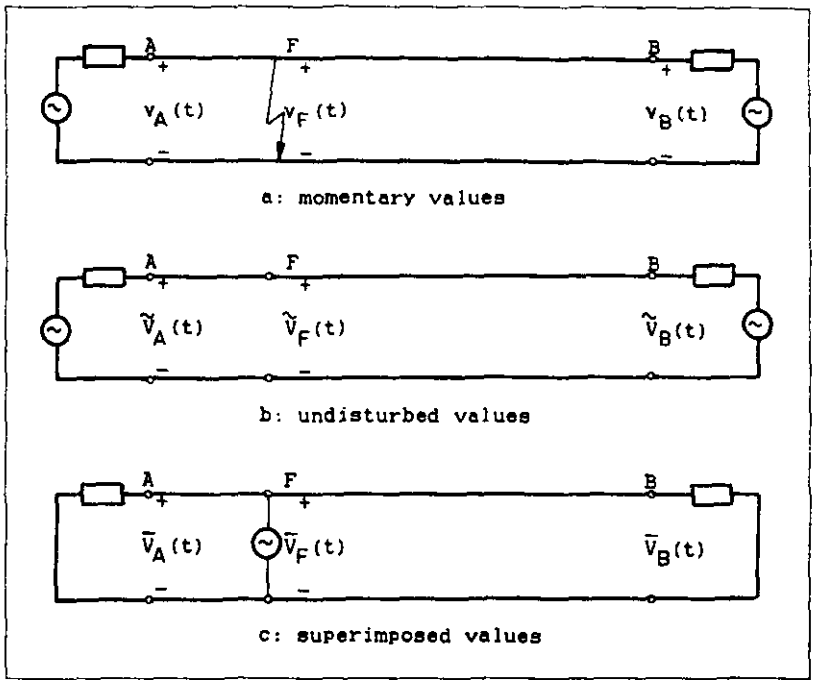

Figure 1 : The superposition principle.

The momentary values of voltages can be given as below.

$$v_A(t) = \tilde{v}_A(t) + \bar{v}_A(t) \qquad (2)$$

$$v_B(t) = \tilde{v}_B(t) + \bar{v}_B(t)$$

$$v_F(t) = \tilde{v}_F(t) + \bar{v}_F(t)$$

Analogue expressions apply for the currents.

1.3.2. Fault detection.

The input quantities of the relay are superimposed voltages and currents from three phase-conductors. The principle is based on the equations for a lossless completely balanced three-phase line. In the original version six detection functions are calculated from the input quantities .

$$D_0^{Fw} = (v_r + v_s + v_t) - R_0(i_r + i_s + i_t) \quad (3)$$

$$D_1^{Fw} = (3/2\, v_r - 3/2\, v_t) - R_1 (3/2\, i_r - 3/2\, i_t) \quad (4)$$

$$D_2^{Fw} = (1/2\, v_r - v_s + 1/2\, v_t) - R_1 (1/2\, i_r - i_s + 1/2\, i_t) \quad (5)$$

$$D_0^{Bw} = (v_r + v_s + v_t) + R_0(i_r + i_s + i_t) \quad (6)$$

$$D_1^{Bw} = (3/2\, v_r - 3/2\, v_t) + R_1 (3/2\, i_r - 3/2\, i_t) \quad (7)$$

$$D_2^{Bw} = (1/2\, v_r - v_s + 1/2\, v_t) + R_1 (1/2\, i_r - i_s + 1/2\, i_t) \quad (8)$$

v_r, v_s and v_t are phase voltages; i_r, i_s and i_t are phase currents, the positive direction is from the substation into the line; R_0 and R_1 are real approximations of the wave impedances for the ground wave and the aerial waves respectively.

The forward detection functions D_0^{Fw}, D_1^{Fw} and D_2^{Fw} are a measure for the amplitude of the travelling waves coming from the forward direction (out of the line, into the substation). The backward detection functions D_0^{Bw}, D_1^{Bw} and D_2^{Bw} are a measure for the amplitude of the waves coming from the backward direction (out of the substation, into the line).

After a forward fault (a fault somewhere in the forward direction) a wave from the forward direction reaches the relay position. The forward detection functions will obtain non-zero values. Almost immediately the travelling waves reflect at the substation, causing non-zero values of the backward detection functions.

If the fault occurs somewhere in the backward direction only a wave from the backward direction will reach the relay position. The forward detection functions will remain zero where the backward detection functions will become non-zero.

The algorithm concludes a backward fault if the backward detection functions become non-zero while the forward detection functions remain zero. A forward fault is concluded if the forward detection functions become non-zero and there has not been a backward fault for some time.

The relay gets into a blocking mode after the detection of a backward fault. This blocking period has to last untill all transients from a backward fault are damped. A period of 5-10 cycles of the power frequency is considered to be more than sufficient. During this blocking period the relay is not available for protection purposes. So a back-up relay will be needed to detect a fault during the blocking period.

A backward fault followed by a forward fault within 10 cycles (200 ms) may seem a very rare coincidence. But there are situations when the coincidence is not as rare.

- During a thunderstorm the chance of a fault is increased enormously, so is the chance of two faults within a short period.
- Line energizing will be detected as a backward fault. Due to this faults during line-energizing will not be detected.
- A fault on the parallel circuit will also lead to a blocking of the relay. If the fault evolves to the circuit-to-be-protected, this will not be detected.

A backward fault is concluded in the original algorithm if

$$\begin{aligned} &\{\ |D_0^{Fw}| < \delta \text{ and } |D_0^{Bw}| > \delta\ \} \\ \text{or } &\{\ |D_1^{Fw}| < \delta \text{ and } |D_1^{Bw}| > \delta\ \} \\ \text{or } &\{\ |D_2^{Fw}| < \delta \text{ and } |D_2^{Bw}| > \delta\ \} \end{aligned} \qquad (9)$$

After the detection of a backward fault the relay will be blocked during a few cycles of the power frequency. A blocking signal will be send to the relay at the remote line terminal as well.

If the relay is not in the blocking mode, a forward fault will be concluded if

$$\begin{aligned} &\{\ |D_0^{Fw}| > \delta \text{ or } |D_0^{Bw}| < \delta\ \} \\ \text{and } &\{\ |D_1^{Fw}| > \delta \text{ or } |D_1^{Bw}| < \delta\ \} \\ \text{and } &\{\ |D_2^{Fw}| > \delta \text{ or } |D_2^{Bw}| < \delta\ \} \\ \text{and } &\{\ |D_0^{Fw}| > \delta \text{ or } |D_1^{Fw}| > \delta \text{ or } |D_2^{Fw}| > \delta\} \end{aligned} \qquad (10)$$

If no blocking signal is received from the remote line-terminal, a tripping signal will be generated by the relay.

1.3.3. Phase selection.

From the superimposed voltages and currents the two following functions are calculated:

$$S_2 = K \{ {}^3/_2 \, v_r - {}^3/_2 \, v_t \} - R_1 \{ {}^3/_2 \, i_r - {}^3/_2 \, i_t \} \quad (11)$$

$$S_3 = K \{ {}^1/_2 \, v_r - v_s + {}^1/_2 \, v_t \} - R_1 \{ {}^1/_2 \, i_r - i_s + {}^1/_2 \, i_t \} \quad (12)$$

The "variable gain constant" K is used to "increase the S/N - ratio under genuine fault conditions". This is done by setting K = 5. From (11) and (12) three selection functions are calculated.

$$D_a = 3 \, S_3 - S_2 \quad (13)$$

$$D_b = 2 \, S_2 \quad (14)$$

$$D_c = 3 \, S_3 + S_2 \quad (15)$$

The following tripping scheme is used :

$|D_a| < \sigma$ and $|D_b| > \sigma$ and $|D_c| > \sigma$: trip phase R (16)

$|D_a| > \sigma$ and $|D_b| < \sigma$ and $|D_c| > \sigma$: trip phase S (17)

$|D_a| > \sigma$ and $|D_b| > \sigma$ and $|D_c| < \sigma$: trip phase T (18)

Any other combination : three-phase trip (19)

2. Travelling wave based directional detection ; the improved algorithm.

2.1. Fault detection.

After the superimposed quantities have passed through a low pass filter, four detection functions are calculated in this new proposal.

$$D_1^{Fw} = (v_t - v_s) - R_1 (i_t - i_s) \quad (20)$$

$$D_2^{Fw} = (v_r - v_t) - R_1 (i_r - i_t) \quad (21)$$

$$D_1^{Bw} = (v_t - v_s) + R_1 (i_t - i_s) \quad (22)$$

$$D_2^{Bw} = (v_r - v_t) + R_1 (i_r - i_t) \quad (23)$$

No homopolar detection functions (D_0^{Fw} , D_0^{Bw}) have been used. The reasons for this will be given in section 4.10. For the other detection functions other combinations of phases have been used to reduce the number of calculations needed (compare equation (20) through (23) with (3) through (8)).
The following detection algorithm will be applied:

$$\left[|D_1^{Fw}|<\delta \text{ and } |D_2^{Fw}|<\delta \right] \text{ and } \left[|D_1^{Bw}|>\delta \text{ or } |D_2^{Bw}|>\delta \right] \quad : \text{Backward fault} \quad (24)$$

$$|D_1^{Fw}|>\delta \text{ or } |D_2^{Fw}|>\delta \quad : \text{Forward fault} \quad (25)$$

$$\left[|D_1^{Fw}|<\delta \text{ and } |D_2^{Fw}|<\delta \right] \text{ and } \left[|D_1^{Bw}|<\delta \text{ and } |D_2^{Bw}|<\delta \right] \quad : \text{No fault.} \quad (26)$$

A backward fault is concluded if one of the backward detection functions becomes non-zero while both forward detection functions are still zero (Equation 24). In the original algorithm a backward fault was concluded if the above was valid for at least one of the modes. During some forward inter-circuit faults on a double-circuit line the following situation arrises : $|D_1^{Fw}|<\delta$, $|D_2^{Fw}|>\delta$, $|D_1^{Bw}|>\delta$, $|D_2^{Bw}|>\delta$. This leads to an incorrect blocking with the original algorithm, but to a correct tripping with the new one.

After the detection of a backward fault the relay sends a blocking signal to the other line terminal and waits for the end-of-transient to continue its protection task.

$|D_1^{Fw}|>\delta$ or $|D_2^{Fw}|>\delta$ or $|D_1^{Bw}|>\delta$ or $|D_2^{Bw}|>\delta$:

end-of-transient not yet reached (27)

$|D_2^{Fw}|<\delta$ and $|D_2^{Fw}|<\delta$ and $|D_1^{Bw}|<\delta$ and $|D_2^{Bw}|<\delta$:

end-of-transient reached (28)

After the end-of-transient a clearing signal is send to the remote line terminal. Although only a blocking signal is needed, the additional clearing signal will increase the reliability. The end-of-transient will be reached after a few periods of the power frequency.

If the relay is not in the blocking mode a forward fault is concluded if one of the forward detection functions becomes non-zero. After a forward fault has been detected the relay sends a clearing signal to the other line terminal and waits for the reception of a clearing or blocking signal. After receiving a clearing signal a tripping signal is generated by the relay.

If a blocking signal is received no tripping signal will be generated and the relay waits for the end-of-transient.

2.2. Phase selection.

After a forward fault has been detected, the fault type can be selected. Depending on the fault type a single-phase or a three-phase tripping signal will be generated. From the forward detection functions six selection functions are calculated.

$$S_1 = D_1^{Fw} \quad (29)$$

$$S_2 = D_2^{Fw} \quad (30)$$

$$S_3 = D_1^{Fw} + D_2^{Fw} \quad (31)$$

$$S_4 = D_1^{Fw} - D_2^{Fw} \quad (32)$$

$$S_5 = D_1^{Fw} + 2\,D_2^{Fw} \quad (33)$$

$$S_6 = -2\,D_1^{Fw} - D_2^{Fw} \quad (34)$$

In terms of voltages and currents, the following expressions can be derived:

$$S_1 = (v_t - v_s) - R_1(i_t - i_s) \quad (35)$$

$$S_2 = (v_r - v_t) - R_1(i_r - i_t) \quad (36)$$

$$S_3 = (v_r - v_s) - R_1(i_r - i_s) \quad (37)$$

$$S_4 = (2\,v_t - v_r - v_s) - R_1(2\,i_t - i_r - i_s) \quad (38)$$

$$S_5 = (2\,v_r - v_s - v_t) - R_1(2\,i_r - i_s - i_t) \quad (39)$$

$$S_6 = (2\,v_s - v_r - v_t) - R_1(2\,i_s - i_r - i_t) \quad (40)$$

During an R-N fault (phase R to ground) the superimposed voltage in phase S will be almost equal to the one in phase T. The same applies to the current. Because of this the selection function S_1 will be almost zero. The same is valid for S_2 during an S-N fault and for S_3 during a T-N fault.
During an R-S fault the superimposed voltage in phase R is almost opposite to the superimposed voltage in phase S and the superimposed voltage in phase T is almost equal to zero. The selection function S_4 is therefore almost equal to zero during an R-S fault. S_5 corresponds to an S-T fault and S_6 to an R-T fault.
The following algorithm for phase selection has been used in this study.

$|S_1| < \sigma$, all others $> \sigma$: R-N (41)

$|S_2| < \sigma$, all others $> \sigma$: S-N (42)

$|S_3| < \sigma$, all others $> \sigma$: T-N (43)

$|S_4| < \sigma$, all others $> \sigma$: R-S (44)

$|S_5| < \sigma$, all others $> \sigma$: S-T (45)

$|S_6| < \sigma$, all others $> \sigma$: R-T (46)

all selection functions $> \sigma$: three-phase trip (47)

When a single-phase-to-ground fault is detected the faulted phase will be tripped. After a phase-to-phase fault one of the faulted phases will be tripped. It is important in the latter case, to make sure that both relays trip the same phase.

Fault Type	CEGB 400 kV	CEGB 275 kV	Ont. H. 230 kV	Ont. H. 500 kV	Sweden 130 kV
φ-n	69%	50%	70%	93%	45%
φ-φ	22%	45%	10%	-	20%

Table 1 : Relative occurence of single-phase and phase-to-phase faults.

Table 1 gives the relative occurence of single-phase-to-ground and phase-to-phase faults on 5 different networks. The total number of faults on lines is 100 % for every network. Column 1 and 2 give the results of fault registration in the British CEGB 400 kV and 275 kV networks respectively during the period 1968-1974 [17]. Column 3 and 4 are for the Ontario Hydro System based on 13 years of registration [18]. Column 5 gives the results for a Swedish 130 kV line of 120 km length during 2 years of registration [19]. Table 1 shows that it may be suitable to use single-phase tripping not only for single-phase-to-ground but also in case of phase-to-phase faults (during a single-phase trip the transport of electrical energy can be maintained). Therefore three additional selection functions are introduced (S_4,S_5 and S_6). After a single-phase trip (e.g. due to T-N) has been generated, only the corresponding selection function (S_3) will be monitored. If this selection function exceeds the threshold after some time, a three-phase trip will be generated as yet. In that case the fault has evolved to a more complex one. Also some non-evolving complex faults show a delayed three-phase trip after an initial single-phase trip.
To prevent a false three-phase trip due to spikes in the selection functions (see appendix B), the cut-off frequency of the low pass filter needs to be changed to a lower value after a single-phase trip.

After a single-phase trip, not followed by a three-phase trip the faulted phase will be reclosed. The algorithm for directional detection cannot be used to detect whether the fault still exists. A special switch-on-to-fault algorithm will be needed, or a classical relay may be used.

2.4. Protection philosophy; testing of the algorithms.

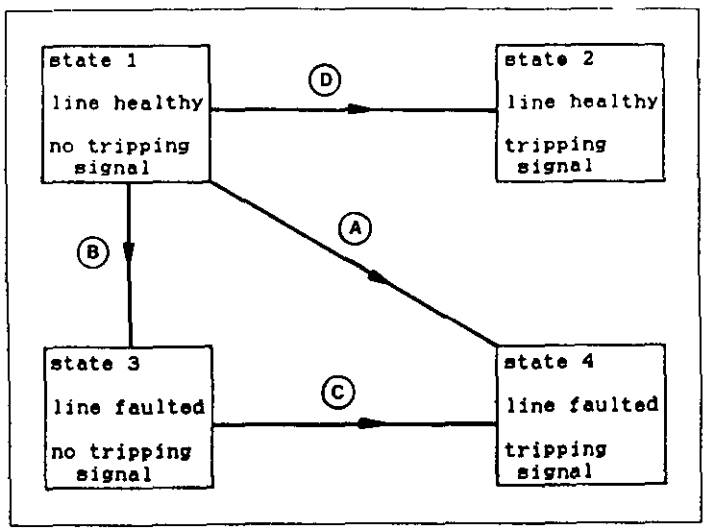

Figure 2: Four possible states for the combination line and relay.

The combination protection and line can be in any of the four states shown in figure 2. State 1 is the normal state. The line is not faulted and the protection does not give a tripping signal. As soon as the line gets faulted, the protection needs to generate a tripping signal. The combination gets into state 4. The transition A is the most preferable. The tripping signal would be generated at the instant of fault initiation.

Because of the causality principle this is not possible (Unless the protection can predict the moment of fault initiation, but in that case the fault can be prevented).

The transition from state 1 to state 4 will always go through state 3. The line is already faulted, but the protection has not yet generated a tripping signal. One of the purposes of the protection is to keep the duration of this state below a certain time. This holds especially for fast protection. The duration of state 3 (the detection time) depends on the fault situation: fault-initiation-angle, combination of faulted phases, network configuration. For a certain algorithm it might be possible that a certain fault situation will not lead to a (fast enough) transition C. For the line protection as a whole, this should not occur, so a back-up algorithm or relay is needed in that case.

State 2 must never be reached. A non-faulted line must never be disconnected. This criterium holds for the fast relay as well as for the back-up relay.

The algorithm is based on equations valid for a balanced three-phase line. Testing will be needed to see if the algorithm is still applicable for realistic situations. For the study described in this report a double-circuit line has been chosen. The same methods can be used for other cases (single-circuit, triple-circuit, teed lines and even more exotic ones).

To test the algorithm the following situations have been studied:

- a fault initiated on the circuit-to-be-protected;
- a fault initiated in the backward direction or on the parallel circuit;
- a lightning stroke leading to a fault;
- a lightning stroke not leading to a fault;
- line energizing leading to fault initiation;
- line energizing not leading to fault initiation.

The network models used to simulate these situations will be described in chapter 3, the relevant results are discussed in chapter 4. A more complete presentation of the results can be found in appendices A, B and C.

3. The network models used.

To study the protection algorithm two network models have been used: a simple one called TWONFIL and a complex one called EMTP. The TWONFIL model has been used to study a large number of situations. The worst cases and other typical situations have been studied by using EMTP.

3.1. The simple model : TWONFIL.

To study the protection algorithms in a large number of situations a relatively simple line model has been used. For the line type as used in the Dutch 380 kV network the modal transformation matrices and the wave impedances have been calculated by using the LINE CONSTANTS routine of the EMTP package [20,21]. All calculations were performed with a ground resistivity of 100 Ωm and a transformation frequency of 5000 Hz.
A lossless frequency independent model has been used in order to simplify the calculation of the transients. The protection algorithms have been studied for the first travelling waves arriving at a line terminal, so damping and frequency dependency will not have too much influence. Therefore the results will be applicable for real lines.
The algorithms have been studied also for two other line types [22]. There were no important differences between the results for the three line types, so the results of the two other line types will not be reproduced here.
The current transformation matrix Q is the matrix of eigenvectors of the matrix product $Y^{(p)}Z^{(p)}$, where $Z^{(p)}$ and $Y^{(p)}$ are the matrices occuring in the multi-phase telegraph equations [23].
The current transformation matrix can be used to introduce modal currents,

$$I^{(p)} = Q\, I^{(c)} \tag{49}$$

where the superscript (p) denotes phase quantities and the superscript (c) modal (component) quantities. In about the same manner a voltage transformation matrix S is introduced [23]. This matrix links phase voltages and modal voltages.

$$V^{(p)} = S\, V^{(c)} \tag{50}$$

The diagonal wave-impedance matrix $Z^{(c)}$ can be used to describe forward and backward travelling waves.

$$F^{(c)} = V^{(c)} + Z^{(c)}\ I^{(c)} \tag{51}$$

$$B^{(c)} = V^{(c)} - Z^{(c)}\ I^{(c)} \tag{52}$$

Where $F^{(c)}$ is the vector of forward travelling (modal) waves and $B^{(c)}$ is the vector of backward travelling waves. Forward means in the positive reference direction of the current.
The matrix S can be derived from Q by using

$$S^{-1} = Q^{T} \tag{53}$$

Where S^{-1} is the inverted voltage transformation matrix and Q^{T} is the transpose of the current transformation matrix [20,23].

To demonstrate the TWONFIL model the calculation of voltages and currents due to a fault on the line-to-be-protected is given below. Only the travelling waves caused by the voltage jump at fault initiation (the so-called superimposed quantities) are calculated.

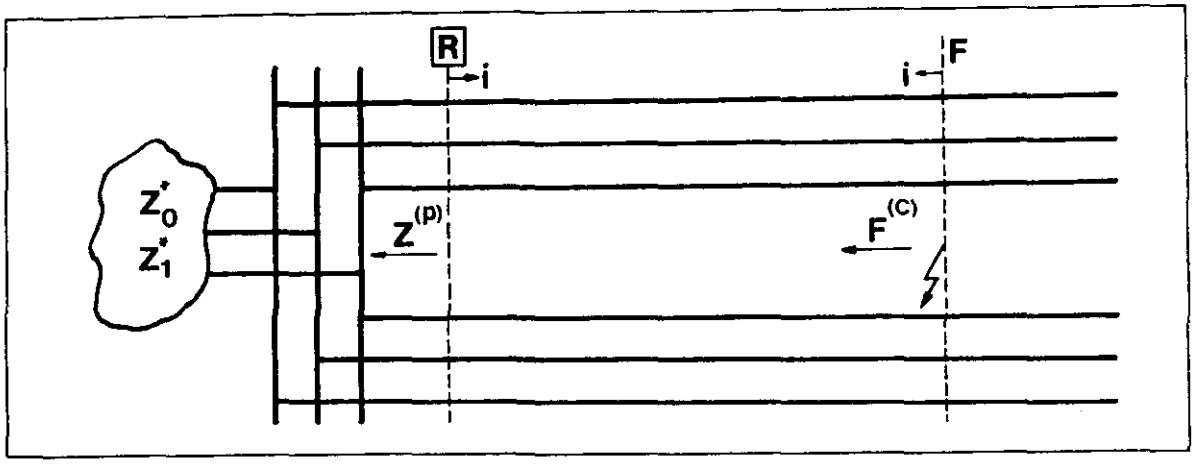

Figure 3 : Fault-initiation on a double-circuit line.

Consider the situation shown in figure 3. A fault is initiated at the fault position F. This will cause waves travelling from the fault position to the relay position R. At the relay position the double-circuit line is terminated by a three-phase busbar. The latter is terminated by a network with homopolar impedance Z_0^* and positive sequence impedance Z_1^*.

The travelling waves that originate at the fault position during a fault with earth connection have to satisfy the next boundary conditions:

$$I_j^{(p)} = 0 \qquad \text{for } j = \text{non faulted phase} \qquad (54)$$

$$V_i^{(p)} = E_i \qquad \text{for } i = \text{faulted phase} \qquad (55)$$

and E_i = voltage jump caused by the fault

During a fault without earth connection the waves have to satisfy the next boundary conditions.

$$I_j^{(p)} = 0 \qquad \text{for } j = \text{non-faulted phase} \qquad (56)$$

$$\sum_k I_k^{(p)} = 0 \qquad \text{for } k = \text{faulted phases;} \qquad (57)$$

$$V_i^{(p)} - V_j^{(p)} = E_{ij} \qquad \text{for } i,j = \text{faulted phases} \qquad (58)$$

and E_{ij} = voltage jump caused by fault.

Because the fault initiation is supposed to be the only source of travelling waves, there are, during a certain time, only waves travelling away from the fault. This introduces the initial condition:

$$V^{(c)} - Z^{(c)} I^{(c)} = 0 \qquad (59)$$

By using (49), (50) and (59) together with (54) and (55) or (56) through (58) voltages $V^{(c)}$ and currents $I^{(c)}$ at the fault location are calculated.
The waves caused by the fault initiation are given by

$$F^{(c)} = V^{(c)} + Z^{(c)} I^{(c)} \qquad (60)$$

These waves originated at the fault location travel to the relay position where they reflect at the terminal impedance. This terminal impedance is a representation of the three phase busbar in combination with the connected network. TWONFIL includes procedures to calculate the terminal impedance $Z^{(p)}$ for the situation shown in figure 3 as well as for another double-circuit line connected to the busbar.

At the relay position the following equations hold.

$$F^{(c)} = V^{(c)} - Z^{(c)} I^{(c)} \qquad (61)$$

Notice the different reference direction of the current leading to the minus sign in equation (61).

$$V^{(p)} = - Z^{(p)} I^{(p)} \qquad (62)$$

By using the above equations in combination with (49) and (50) another TWONFIL-procedure calculates voltages and currents at the relay position. These voltages and currents have been used to study the behaviour of the protection algorithm. Some results of that study are reproduced in chapter 4 and appendix C of this report as well as in reference [22].

Voltages and currents at the relay position have been calculated ,by using the TWONFIL-model, for the following situations.

- All possible single-circuit and inter-circuit faults (a total of 64 fault types) on the line to be protected. Each fault type has been studied for 12 different fault-initiation-angles. Calculations have been performed for a balanced termination as shown in figure 3 as well as for non-balanced situations (other non-transposed lines).
- The same situations for a fault on a backward line, as shown in figure 4, where each line stands for a three-phase circuit.
- The same situations for a fault very close to the relay, in forward as well as in backward direction. In this case the voltage at the relay position is considered to be equal to the voltage at the fault position.
- All possible (19) combinations of switches for the energizing of the parallel circuit, for 12 switch-angles.

More information about the TWONFIL-procedures can be found in reference [24].

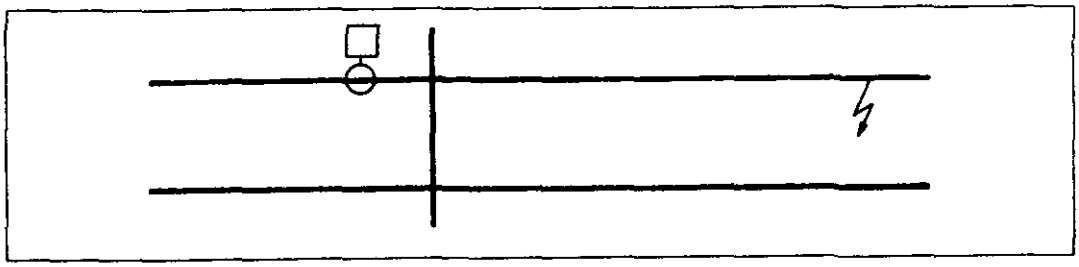

Figure 4 : Fault on a backward line; the square denotes the relay postition.

For a six-phase (double-circuit) line six component-waves are possible: an inter-circuit wave and 4 line waves travelling with almost the speed of light (about 290 m/μs); a ground wave travelling with a lower velocity (about 275 m/μs). In the study described hereafter distinction has been made between the arrival of the (fast) aerial waves and the (slow) ground wave.

The amplitude of the line-to-ground voltage is considered to be 1000 units. A value of 101 units means 10.1 % of that amplitude. The r.m.s. value of the line-to-line voltage would be 1225 units in this case
All losses and frequency dependences have been neglected. But the fact that the line is non-transposed is incorporated in the model.

Although the model is relatively simple it is of value for the study of protection algorithms.

- The simplicity of the model makes it fast and easy to implement for different situations (line type, faulted phase, phase-initiation-angle). It has been possible to simulate thousands of fault situations to study protection algorithms.
- Travelling wave based protection detects a fault from information obtained from the first travelling waves coming from the fault, so losses and frequency dependence have not yet much influence on the voltages and currents.
- The results of the study on the simple model can be a starting point for a study on a more complex model. Only the worst cases need to be studied leading to an enormous reduction of study time.

3.2. The complex model : EMTP.

To study the protection algorithm for more realistic situations the EMTP program [20,21] has been used.
A high-voltage network based on the Dutch 380 kV network has been simulated. Figure 5 shows the configuration used. Squares denote the relay positions.

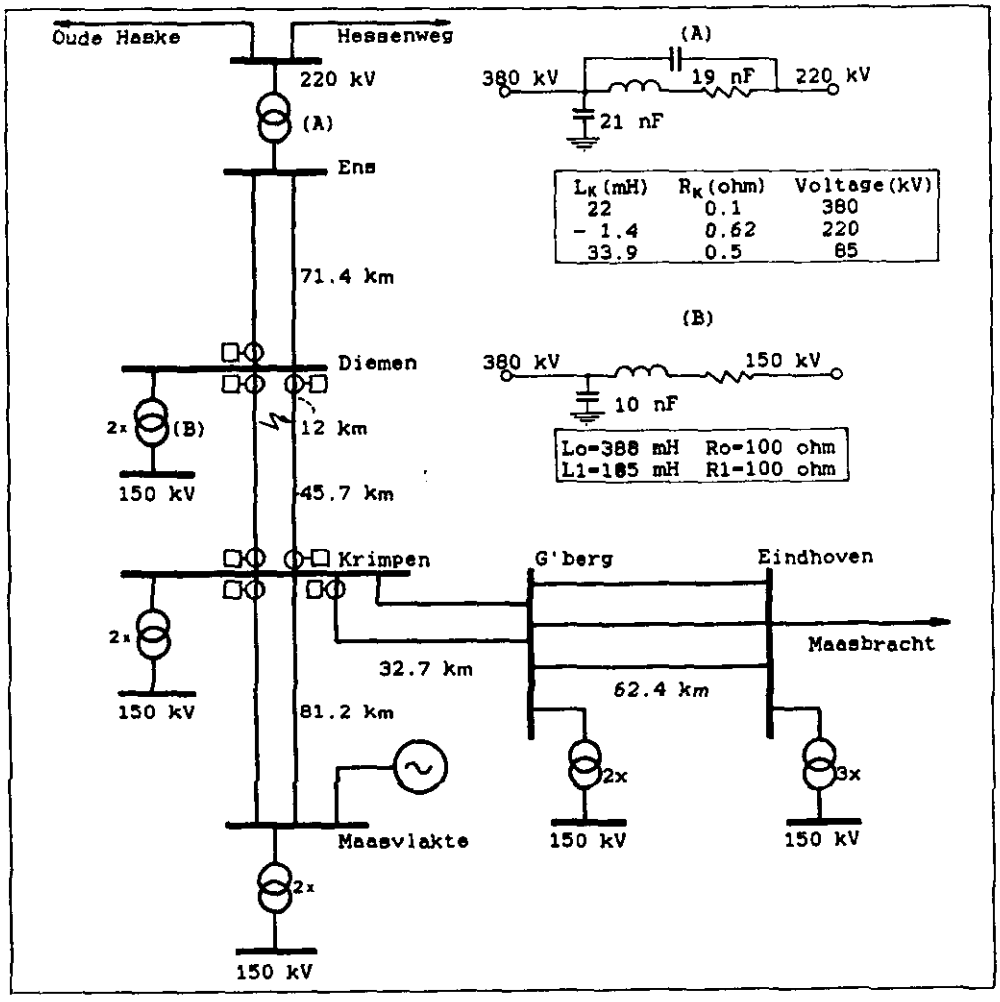

Figure 5: Configuration used for complex-network study.

The line model used is the JMARTI setup. It uses a real frequency independent transformation matrix. Differences between this model and models with a complex frequency-dependent transformation-matrix are small [25].

The line Eindhoven-Geertruidenberg (a triple-circuit line) has been represented in the EMTP-model as a three-phase line. The line Eindhoven-Maasbracht has been represented by the real part of its wave impedance. The same has been done for the 220 kV lines Ens-Oude Haske and Ens-Hessenweg.
All other lines have been represented as six-phase lines in the EMTP-model.
The source files for the JMARTI-setup containing the tower configuration are given in Appendix D.

Substations are of a much smaller extend than lines. Because of this, travel times are much shorter and the whole station can be represented as a single (three-phase) node.
The 380/150 kV transformers have been represented by their short-circuit impedance and the input-capacitance on high voltage side. The resistance representing copper losses has been taken relatively high (100 Ω) to fit the higher losses at higher frequencies. The transformers in Ens are autotransformers with a relatively high capacitance between h.v. and l.v. side. Therefore also this capacitance as well as the capacitance from l.v. side to ground are included in the EMTP model.
These transformer models are fairly good representations up to at least 100 kHz [26]. The complete source file for EMTP including all details of the network is also included in Appendix D.

A comparable model has been used for a simulation of line-energizing. The results showed great conformity with measured voltages [27]. Because the latter measurements were done on the line Diemen-Krimpen the same line has been chosen as the faulted line in the study of protection algorithms.
A time-step of 1 μs has been chosen for the calculations. Voltages and currents derived can be considered as "real" voltages and currents passed through a low-pass-filter with a cut-off frequency of a few hundreds of kHz [20]. A smaller time-step is not realistic because the models used are only valid up to some hundreds of kHz.
An example of the voltage waveform derived with this model is given in appendix F, together with the influence on the waveform of all kinds of reflections.

The algorithm for directional detection has been studied for 7 relay positions. 4 in the substation Krimpen and 3 in the substation Diemen.
In the substation Krimpen 4 relays are situated. The relay on the line to Maasvlakte (denoted shortly as Krimpen to Maasvlakte 1) as well as the relay on the line to Geertruidenberg (Krimpen to Geertruidenberg 1) need to detect a backward fault. Also Diemen to Ens 1 needs to detect a backward fault. For a single-circuit fault Krimpen to Diemen 1 and Diemen to Krimpen 1 need to detect a forward fault while Krimpen to Diemen 2 and Diemen to Krimpen 2 need to detect a backward fault. For an inter-circuit fault all four relays on the line Diemen-Krimpen need to detect a forward fault.
The algorithm for phase selection has been studied for the relays that need to detect a forward fault.
Some of the results of the EMTP-study are reproduced in chapter 4, appendix A (fault detection) and appendix B (phase selection). A list of all the fault situations studied by using the EMTP model is given in appendix E.

3.3. Relay settings.

The algorithms described in chapter 2 make use of just one "impedance". This "impedance" is a "real approximation of the wave impedance for the aerial wave". But a six-phase (= double-circuit) line possesses four different aerial wave impedances. Each of them is also dependent on frequency. Table 2 gives the values of the different wave impedances for some frequencies.

Freq.	R_0	R_d	R_1	R_2	R_3	R_4	$\bar{R}$
50 Hz	748.8	393.5	264.4	267.1	250.6	280.9	265.8
500 Hz	705.4	392.2	262.4	265.8	249.5	278.1	264.0
5 kHz	650.6	390.4	260.7	264.7	248.4	275.7	262.4
50 kHz	594.1	386.9	259.9	264.3	248.1	274.3	261.7
500 kHz	559.6	382.1	259.5	264.1	247.9	273.8	261.3

Table 2: Wave impedances for different frequencies in Ω. R_0 and Rd are homopolar mode and inter-circuit mode impedances respectively. R_1, R_2, R_3 and R_4 are the different single-circuit aerial mode impedances. $\bar{R}$ is the average of the latter four.

These values are the absolute values of the complex impedances for the line type as used in the Dutch 380 kV network, between Krimpen and Diemen. They have been calculated by using the EMTP-package. The last column gives the average of the four preceeding columns.
From table 2 it is clear that there is not just one value for the wave impedance setting. Although a value between 260 Ω and 265 Ω seems to be an acceptable setting according to table 2, a value of 250 Ω has been chosen for the EMTP as well as for the TWONFIL calculations. By choosing a "wrong" value deliberately, an additional error has been introduced. This will make the results more realistic because in most cases it will not be possible to determine the optimum relay setting very exactly.
Because of this no additional threshold needs to be introduced to incorporate errors in wave impedance setting.

4. Results of the study.

The algorithm for travelling-wave-based directional detection as proposed in chapter 2 has been studied for a large number of situations. During this study some situations have been found that endangered the reliability or selectivity of the algorithm. Some problems have been solved by introducing thresholds, time-delays and filters, others remained.
The remaining problems as well as some other relevant situations will be discussed in this chapter. The results for a large number of situations can be found in appendices A, B, and C.
All values of the detection and selection functions are related to the stationary operating-voltage of the line. The amplitude of the phase-to-ground voltage is considered to be 1000 units.

4.1. Derivation of the superimposed quantities.

Directional detection uses superimposed quantities. These will be derived as the difference between the momentary values and the values one power-frequency cycle back in time. Because the power frequency shows small deviations, errors are introduced. The time delay needs to be adjusted to the momentary value of the power frequency; still the time delay will never exactly fit the power frequency.
Suppose the superimposed value d(t) is the value used as a detection function. The undisturbed value is D $\cos(\omega_0 t)$ and the momentary value is M(t).

$$d(t) = M(t) - D\cos(\omega_0 t - \omega_0 T), \text{ where } \omega_0 T = 2\pi \qquad (63)$$

Suppose the error in the delay period is ΔT with $\omega_0 \Delta T \ll 2\pi$, the maximum error in the detection function Δd is then given by

$$\Delta d = D\omega_0 \Delta T \qquad (64)$$

For the detection functions used, D = 1800 units (amplitude of the nominal phase-to-phase voltage). With an error of 0.5 Hz in frequency (ΔT = 0.2 ms) and a standard frequency of 50 Hz, this yields for the error in the detection function:

Δd = 110 units.

The consequences of this additional error are discussed in section 4.6.

4.2. Low pass filter.

Figure 6 gives the forward detection functions D_1^{Fw} and D_2^{Fw} for the relay Diemen to Krimpen 2 after an RSN fault at a fault-initiation-angle of 50^o. The insert in figure 6 gives the fault situation. Because the relay needs to observe a backward fault, the forward detection functions must remain below the threshold for some time. The backward detection functions get a high value within a few microseconds. The forward detection functions show large spikes in the beginning (instant A in figure 6). These spikes are caused by the different travel times for the different modal waves. They may cause a false tripping of the non-faulted circuit. (The threshold level will be about 250 units here.) A low pass filter will be needed to prevent this, as is shown in figure 7 where a cut-off frequency of 50 kHz has been used. The jump in the forward detection functions at the instant B will be discussed in the next section.

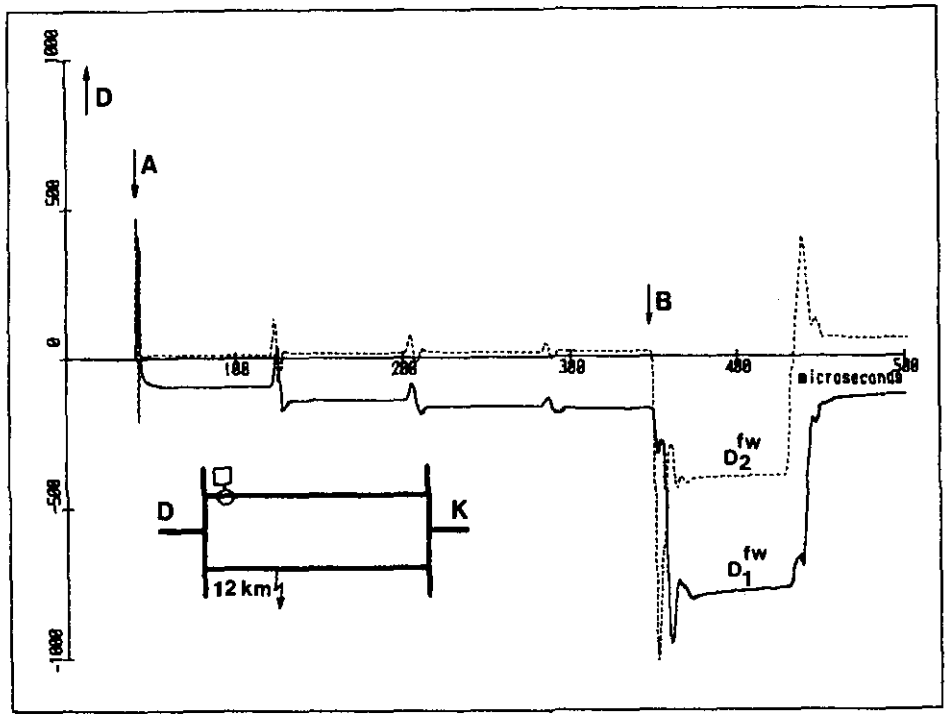

Figure 6 : Forward detection functions in parallel circuit.

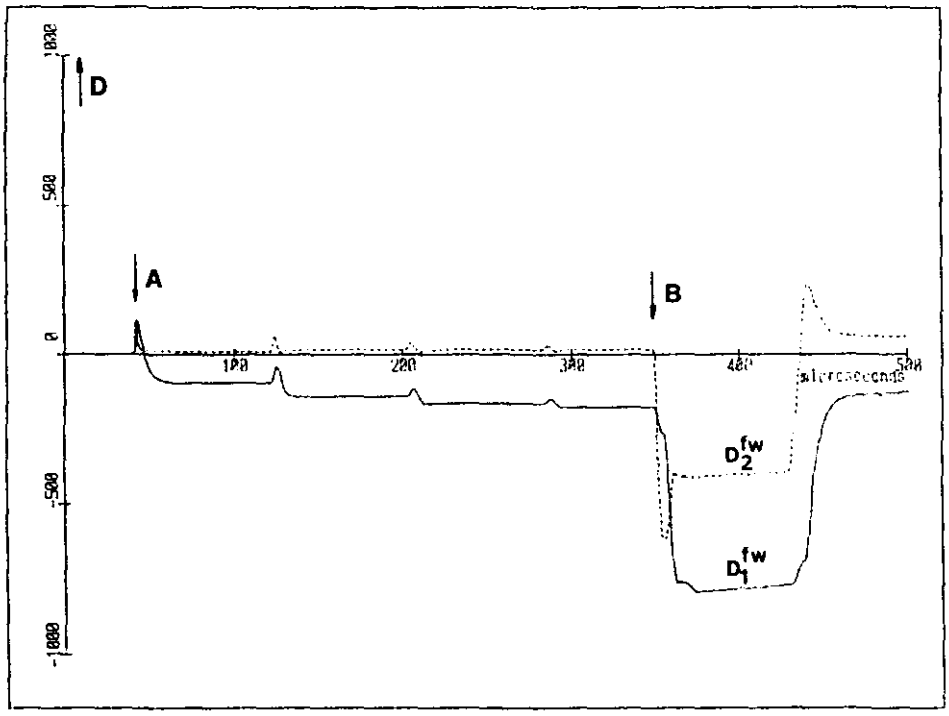

Figure 7 : Detection functions of figure 6 after low pass filtering.

The low pass filter is also needed to suppress all kinds of external disturbances. The lower the cut-off frequency the better the suppression. But too low a cut-off frequency will make the algorithm slower and may even endanger the reliability. As will be shown in the next section a backward fault on a double-circuit line must be detected within the travelling time τ of the line-to-be-protected. Therefore a block function with a duration time τ should not be disturbed too much. From this the criterium shown in figure 8 has been derived. After an input step the output must be within 10% of the final value after 1/2 τ.

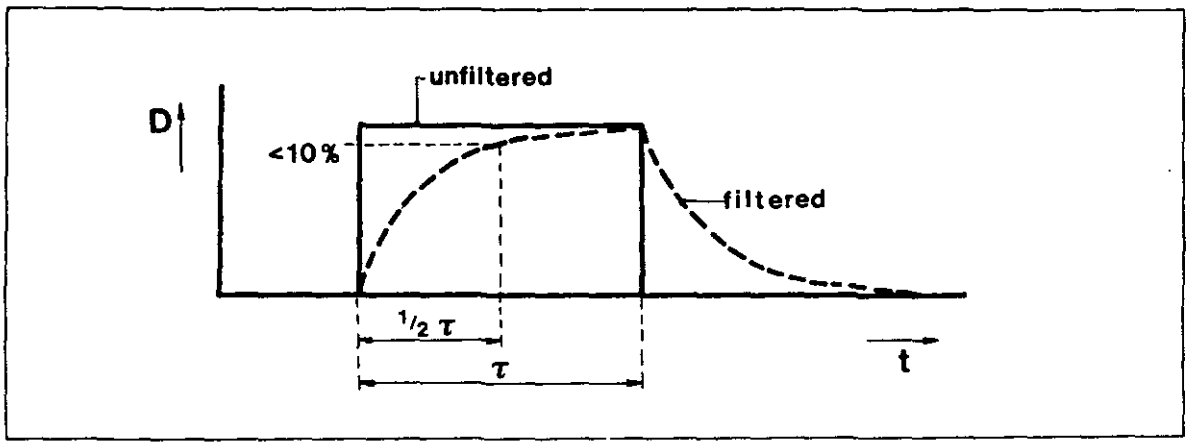

Figure 8: Criterium for low pass filtering.

A first order filter will be used, with a transfer function of the form

$$H(f) = \frac{1}{1 + jf/f_o} \qquad (65)$$

where f_o is the cut-off frequency.
The step response a(t) of this filter is

$$a(t) = 1 - \exp(-2\pi f_o.t) \quad , t > 0 \qquad (66)$$

From the criterium of figure 8 follows

$$1 - \exp(-\pi f_o \tau) > 0.9$$

so

$$f_o > \frac{\ln 10}{\pi.\tau} = \frac{0.73}{\tau} \qquad (67)$$

The minimum cut-off frequencies for the lines used in the complex-network study are given in table 3.

Line	Length	travel-time	Cut-off Freq
Krimpen-Diemen	57.7 km	192 μs	3.8 kHz
Diemen-Ens	71.4 km	238 μs	3.1 kHz
Krimpen-Maasvlakte	81.2 km	271 μs	2.7 kHz
Krimpen-Geertruidenberg	32.7 km	109 μs	6.7 kHz

Table 3: minimum cut-off frequencies.

An acceptable value for the cut-off frequency is $f_c = 1/\tau$, where τ is the travelling time of the line-to-be-protected. For the line Diemen-Krimpen this is 5700 Hz.
The detection functions shown in this chapter are filtered versions of the EMTP output. The cut-off frequency was $1/\tau$ throughout this chapter, except when otherwise noted. The non-filtered detection functions are shown in appendices A and B.
An additional filter needed after a single-phase trip will be discussed in section 4.9.

4.3 Backward faults.

During a fault on a backward line (position 1 in figure 9) or a fault in the parallel circuit (position 3) the relay must observe a backward fault. Therefore the forward detection function must be low in these cases.

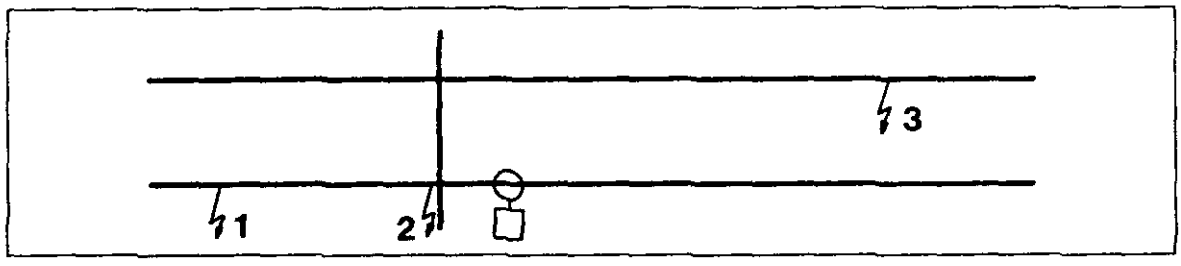

Figure 9 : " Non-forward" faults.

Two phenomena may cause the false detection of a forward fault, they will be discussed here.

1. Although there exist no waves from the forward direction, the forward detection functions possess non-zero values. This is caused by the difference between the real transformation matrices for the (unbalanced double-circuit = six-phase) line and the transformation matrix used in the algorithm (only valid for a balanced three-phase line).
2. After one or more reflections the waves from a backward fault will arrive at the relay position from the forward direction and the forward detection functions will get non-zero values. Before this instant the fault must be recognized as a backward one and the relay must get into the blocking mode.

By using the TWONFIL model, a large number of backward faults have been studied to find out which combination of faulted phases gives the largest value of the forward detection functions. The largest values found, as well as the values for some "normal" fault situations, are given in table 4. Position 1 (see figure 9) is a fault somewhere on a backward line; position 2 is a backward fault close to the relay position, e.g. a fault in the substation.
The highest value found was 215 units, as shown in table 4. The worst cases have been studied by using EMTP. The results for the following situations are reproduced in this chapter:

- RSTUVW-fault at a fault-initiation-angle of 60 degrees,
  fault position : 12 km from Diemen,
  detection functions for Diemen-to-Ens 1 in figure 10;
- RST-fault at a fault-initiation-angle of 60 degrees,
  fault position : 2 km from Diemen,
  detection functions for Diemen-to-Ens 1 in figure 11;
- RS-fault at a fault-initiation-angle of 30 degrees,
  fault-position : 12 km from Diemen,
  detection functions for Diemen-to-Ens 1 in figure 12.

Fault	Phase angle	D_1^{Fw}	D_2^{Fw}	
RN	0°	41	13	Position 1
SN	60°	49	21	
TN	120°	39	22	
RS	30°	101	10	
RT	150°	2	13	
ST	90°	98	1	
RSTUV	45°	200	17	
RSTUVN	45°	200	23	
RSTUVW	15°	155	23	
RSTUVW	60°	215	9	
RN	0°	69	21	position 2
SN	60°	86	38	
TN	120°	71	41	
RS	30°	196	19	
RT	150°	3	25	
ST	90°	191	3	
RST	60°	215	26	
RST	15°	155	24	

Table 4 Absolute values of forward detection functions during a backward fault; according to TWONFIL calculations

All detection functions have passed through a low pass filter with a cut-off frequency of 4200 Hz ($1/\tau$ for Diemen to Ens) The backward detection functions rise to a high value within a few microseconds. The forward detection functions remain much lower. As these are the highest values found during a backward fault a minimum value for the threshold will be determined by these situations.

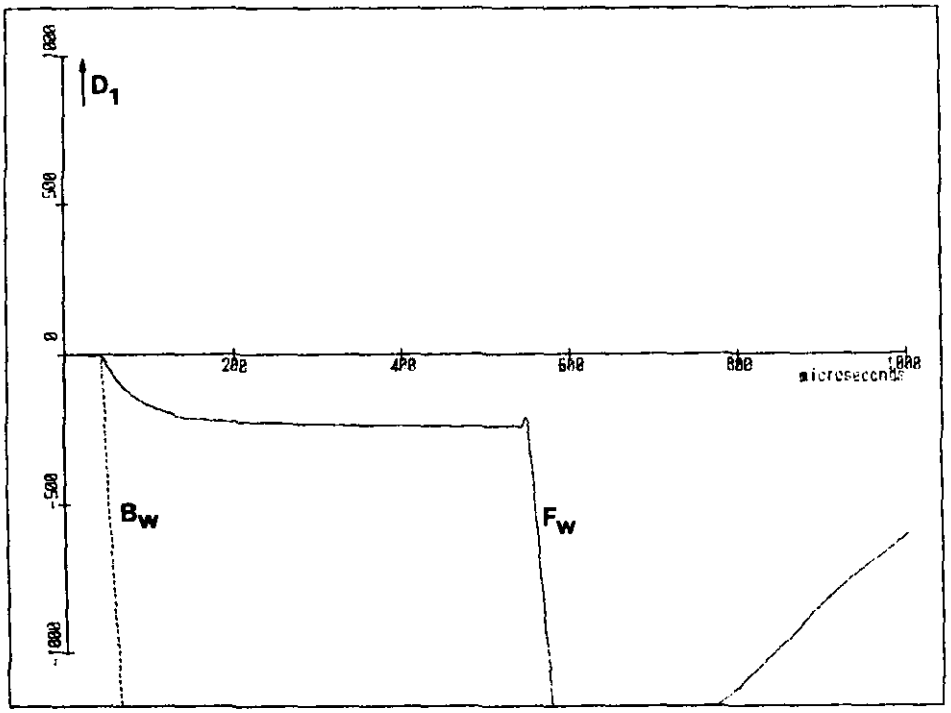

Figure 10 : RSTUVW, $\varphi = 60^{\circ}$, fault at 12 km from Diemen.

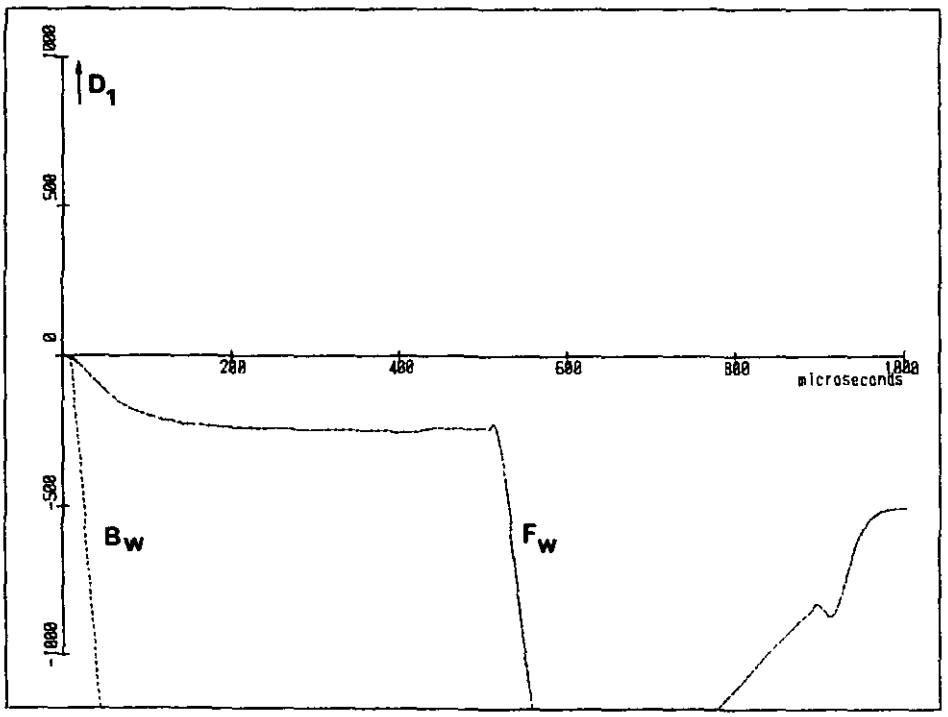

Figure 11 : RST, $\varphi = 60^{\circ}$, fault at 2 km from Diemen.

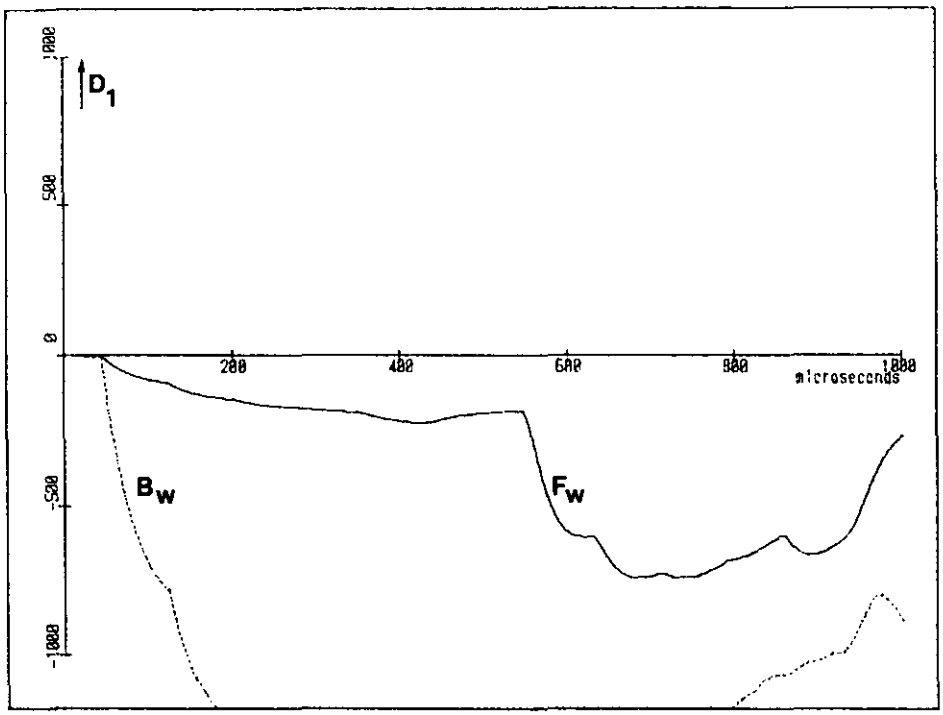

Figure 12 : RS, φ = 30°, fault at 12 km from Diemen.

Figure 10 (RSTUVW at 12 km) gives for D_1^{Fw} a value of -221 units after 200 μs and -229 units after 300 μs. For the RST-fault at 2 km (figure 11) these values are -231 and -238 units respectively. It will be shown below that the backward fault must be detected within 1 travelling time of the line-to-be-protected, so 238 units can be registered as the highest value of the forward detection functions shortly after a backward fault.
Besides it can be concluded that the TWONFIL value of 215 units gives an acceptable indication.

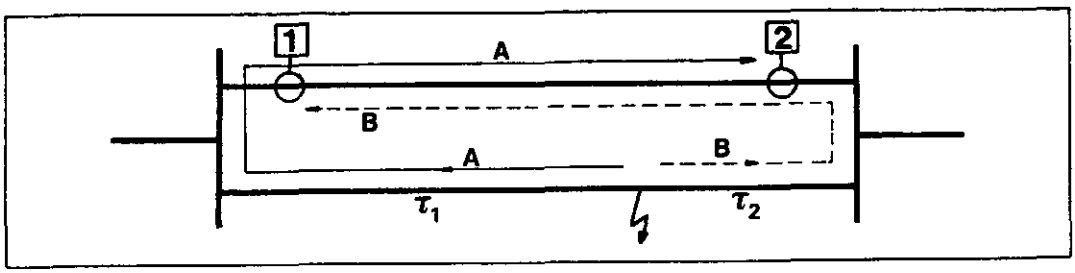

Figure 13 : Fault on parallel circuit;
τ_1 = travel time fault - relay 1 ;
τ_2 = travel time fault - relay 2.

In figure 10 through 12 it can be seen that the forward detection functions get a high value after about twice the travelling time of the line. An even worse situation occurs for a fault on a parallel circuit (figure 13). As soon as the waves following path A arrive at relay 1 (after a time τ_1) the backward detection functions will become non-zero. The forward detection functions become non-zero as soon as the waves following path B arrive ($\tau_1+2\tau_2$ after fault initiation). If the fault is close to relay 2 the time difference ($2\tau_2$) is very short and relay 1 will probably (incorrectly ?) detect a forward fault. Fortunately relay 2 will have almost twice the travelling time of the line ($2\tau_1$) to detect the backward fault. The communication between the relays will prevent the disconnection of the non-faulted circuit.

The worst situation is a fault midway on the parallel circuit. In that case both relays have only one travelling time available. So after a backward fault the relay must go into the blocking mode within one travelling time of the line-to-be-protected.

As an example figures 14 and 15 give the detection functions for the parallel circuit caused by an RN-fault at voltage maximum. The fault is situated at 12 km from Diemen. A cut-off frequency of 5700 Hz has been used. Only D_2^{Fw} and D_2^{Bw} are given, D_1^{Fw} and D_1^{Bw} possess only small values.

Figure 14 gives the situation for the relay Diemen-to-Krimpen 2. A relatively large "detection-window" is visible, but the relay Krimpen-to-Diemen 2 (figure 15) has a much shorter window available.

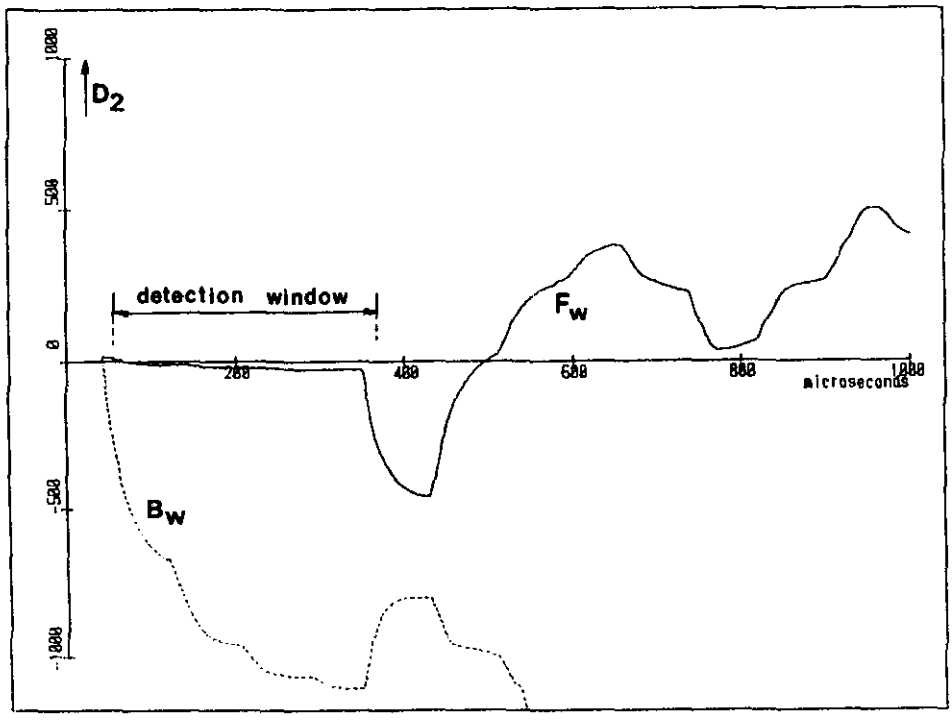

Figure 14 : RN, $\varphi = 0^o$, fault at 12 km from Diemen.

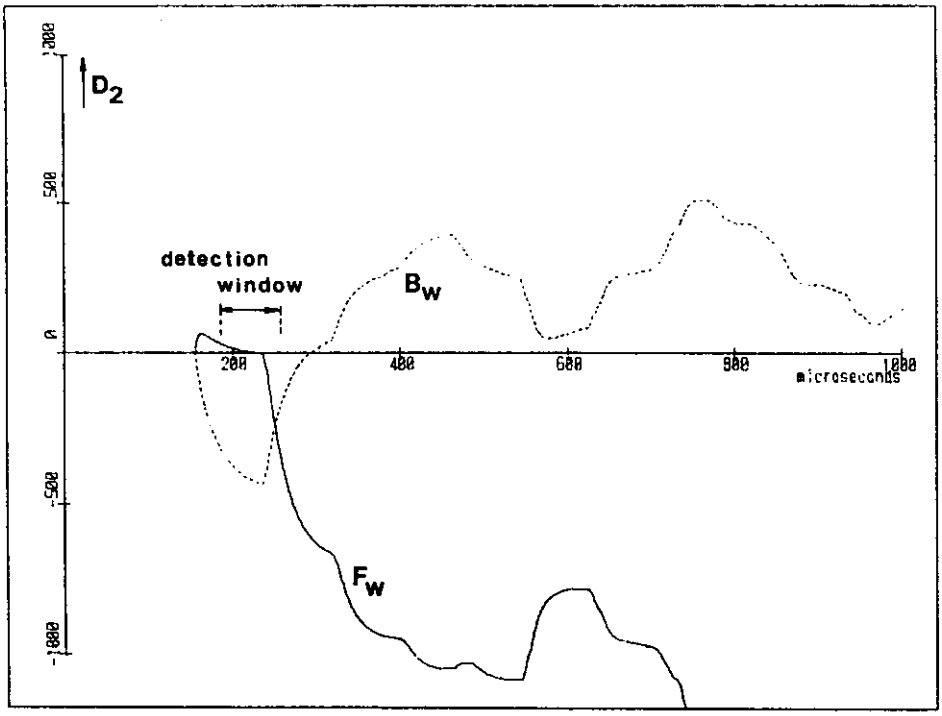

Figure 15 : RN, $\varphi=0^{o}$, fault at 45.7 km from Krimpen.

4.4. Line energizing.

During line energizing travelling waves are initiated at the breaker position, as shown in figure 16. Relay 1 and 3 will detect a backward fault, relay 2 and 4 a forward fault. Both circuits will not be disconnected.

Table 5 : Absolute values of the forward detection functions during line energizing, according to TWONFIL- calculations.

Switches		Switch	relay 3		relay 1	
closed	closing	angle	D_1 Fw	D_2 Fw	D_1 Fw	D_2 Fw
-	R	0^{o}	36	60	77	67
S	R	0^{o}	33	58	83	68
T	R	0^{o}	34	62	71	79
ST	R	0^{o}	32	60	76	79
-	RS	15^{o}	21	45	103	69
T	RS	15^{o}	20	47	100	75
-	RT	165^{o}	27	65	52	108
S	RT	165^{o}	26	65	53	108
-	RST	150^{o}	22	60	41	107

The values shown in table 5 (the highest values that can occur during line energizing) are far below the highest value that can occur during a backward fault (215 units according to table 4). So line energizing will not cause the forward detection functions to exceed the threshold.

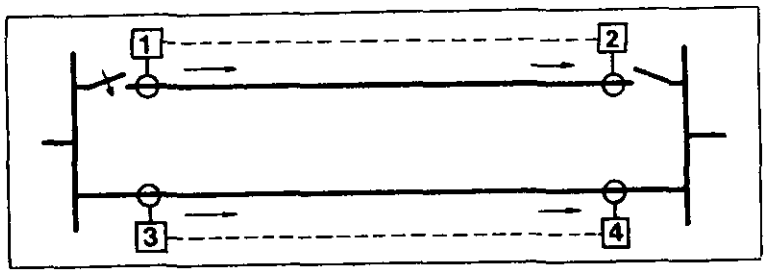

Figure 16 : Travelling waves because of line energizing

As shown in figure 16, voltage and current measurements must be performed on the line side of the circuit breaker. If this is done on the station side, relay 1 will observe a forward fault and the energized line will be disconnected again. In that case the relay must be blocked (manually or automatically) prior to line energizing.

For both measurement positions all four relays will be blocked. But the blocking period is longer for the measurement on the station side of the circuit breaker and the blocking will not be automatically in that case.
A fault shortly after (due to) line energizing will not be detected by the relay. A back-up relay will be needed to protect the line in this situation.
A travelling-wave-based switch-on-to-fault algorithm will be discussed in a seperate report [30].

4.5 Lightning strokes.

A lightning stroke close to a h.v. line will cause intense travelling waves on the line. These waves may be detected by the travelling-wave-based protection leading to a false tripping signal. The influence of the lightning strokes is reduced in two ways.

- A lightning stroke not direct to a phase conductor, causes intense homopolar waves. These are not detected by the relay. The aerial mode waves are, in general, relatively small.
- Voltages and currents caused by a lightning stroke may be very high, their duration is relatively short (50-100 μs). Therefore the low pass filter will remove a substantial part of the spikes.

The most serious threat will be a direct stroke on a phase conductor not leading to a flash-over. In that case the forward detection functions will almost certainly get a value above the threshold. A verification time between the threshold crossing and the generation of the tripping signal will solve the lightning problem. But a too long delay time may endanger the reliability. A compromise will be a verification time about equal to the travelling time of the line-to-be-protected.

A fault initiated because of a lightning stroke will, in general be no problem. The voltage jump is high enough to cause a fast threshold crossing of the foreward detection functions. The only difficult situation is a lightning stroke on another line leading to the detection of a backward fault (the relay will get into the blocking mode), followed by a lightning stroke on the line-to-be-protected. If both strokes are too close together the second one will not be detected by the travelling-wave-based relay. A back-up relay will be needed for this situation.

4.6. Thresholds

4.6.1. Fault detection.

The forward detection functions must remain below the threshold for some time, after a disturbance in the backward direction. To put it the other way around: the threshold value must be higher than the highest possible value for the forward detection functions.

Four mechanisms can be distinguished to create an undesirable non-zero value for the forward detection functions.

1. The incorrect modal transformation used. The worst situation leads to a value of about 225 units for the forward detection functions, as shown in section 4.3.
2. An incorrect delay during the derivation of the superimposed quantities may lead to an additional increase of about 100 units. Although the values of all detection functions will be affected, this is only of concern for the forward detection functions during a backward disturbance.
3. An incorrect value of the wave-impedance setting may also introduce an error in the detection functions. This error is already deliberately introduced by chosing a value of 250 Ω instead of 260 Ω. The latter would give lower absolute values of the forward detection functions (see section 3.3).
4. All kinds of noise picked up from the outside world, or created inside of the protection system (e.g measurement errors and quantisation errors). A substantial part of the external noise will be suppressed by the low pass filter while false trips due to short duration spikes are, in general, not possible because of the verification period introduced in section 4.5.

From all of this a threshold level of 400 units has been chosen. This is considered to be a safe value.

4.6.2. Phase selection.

The phase selection algorithm needs to recognise the six single-phase and phase-to-phase faults. Therefore six phase-selection functions have been introduced in section 2.2. Each phase-selection function must be below the threshold during the corresponding fault. Table 6 gives the initial value of these selection functions, according to TWONFIL calculations. Case 1 is the situation when all modal waves arrive at the relay position together. For case 2 the ground waves arrive later. These values are for the time interval between the arrival of the aerial waves and the arrival of the ground wave. Case 3 is a fault very close to the relay position.

Table 6 : Absolute values of the selection functions for single-phase and phase-to-phase faults; according to TWONFIL-calculations.

Fault type	Sel.Func.	Case 1	Case 2	Case 3
RN	S_1	37	139	69
SN	S_2	21	17	38
TN	S_3	58	117	112
RS	S_4	106	49	215
ST	S_5	95	39	179
RT	S_6	10	26	16

The maximum value is 215 units, the same as for fault detection (table 4). The other three error sources mentioned before are also present, so for phase selection the same threshold value can be used (400 units) as for fault detection.

After a few reflections the detection functions sometimes exceed the thresholds. This can be prevented by introducing an additional low pass filter as will be discussed in section 4.9.

4.7 Faults around voltage zero.

Consider a single-phase line as shown in figure 17. At time-zero a fault is initiated, somewhere on the line.

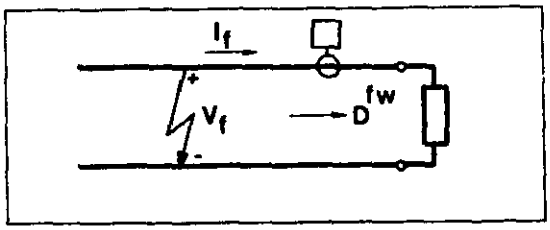

Figure 17: Single-phase situation.

The superimposed quantities (see chapter 1) are caused by a harmonic source on the fault position, switched on at time-zero.

$$V_f(t) = -\hat{V}\cos(\omega_o t + \Phi).U(t) \qquad (68)$$

Where $\hat{V}$ is the amplitude of the undisturbed voltage, ω_o the power frequency and Φ the fault-initiation-angle. U(t) is Heavyside's step function being zero for negative times and unity for positive times.

The forward detection function measured at the relay location is given as:

$$D^{Fw}(t) = -2\hat{V}\cos(\omega_o t + \Phi)U(t) \qquad (69)$$

During a fault with a considerable voltage jump, the value of $D^{Fw}(t)$ does not change much before reflections disturb the sine form. But a fault somewhere around voltage-zero gives a detection function as shown in figure 18, where the fault is considered to be initiated slightly before voltage-zero.

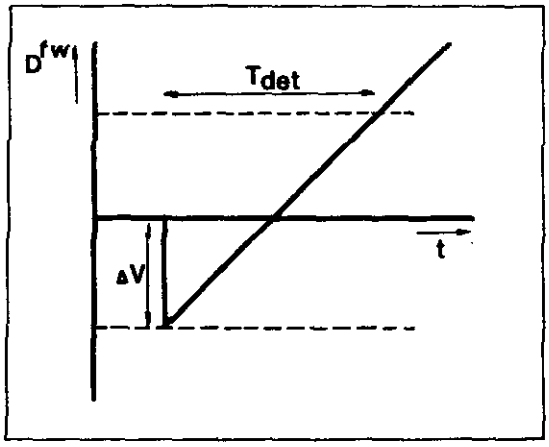

Figure 18: Detection functions around voltage-zero.

At the first arrival of travelling waves, the detection function shows a small negative jump followed by a steady increase.

The time needed to cross the threshold is maximal if the initial jump ΔV is equal to the threshold value. This time will be called the *maximum-detection-time* for a certain fault type.

The single-phase situation is only valid for single-phase-to-ground and phase-to-phase faults. The zero-crossings coincide for all detection functions in those cases. During a more complex fault the zero-crossings do not coincide. Always at least one of the detections functions possesses a "large" value, so these complex faults will be detected very fast (i.e. within some tens of microseconds, depending on cut-off frequency and sampling rate).

Table 7 gives the maximum-detection-time for single-phase-to-ground and phase-to-phase faults, as well as the time needed for fault detection plus phase selection. Both are determined for a threshold value of 400 units. the fault is situated 12 km from Diemen and 45.7 km from Krimpen.

Table 7 : Maximum time needed for fault detection and phase selection for faults around voltage-zero.

	Fault detection		Fault det. + phase sel.	
	Diemen	Krimpen	Diemen	Krimpen
R-N	1120 μs	1460μs	1160μs	1460μs
S-N	1050	1400	1080	1400
T-N	1010	1440	1150	1440
R-S	860	1220	920	1220
R-T	500	660	850	1160
S-T	520	730	940	1240

All faults are detected within 1.5 millisecond. Most fault situations lead to a much faster fault detection. During a single-phase-to-ground fault at voltage maximum one of the detection functions crosses the threshold within 10 microseconds for both relays.

4.8 Inter-circuit faults.

An inter-circuit fault is a rarely occuring situation when one or more conductors in one circuit make electrical contact with one or more conductors of the second circuit. Causes for inter-circuit faults are gallopping conductors and lightning strokes to a tower. According to fault registrations in the British CEGB networks about 3 % of all faults concern inter-circuit faults [17]. The next sections discuss a non-detectable situation (4.8.1) and the failure of phase selection during inter-circuit faults (4.8.2).

4.8.1. Non-detectable inter-circuit faults.

With some inter-circuit faults the zero crossings of the forward detection functions (i.e. of the waves generated at fault-initiation) do not coincide for both circuits. Figure 19 shows the travelling waves for an inter-circuit fault that occurred close to a zero crossing in circuit 1.

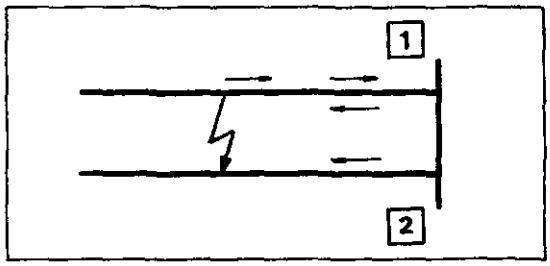

Figure 19: Inter-circuit fault.

Travelling waves are initiated in circuit 2, but not in circuit 1. At the busbar behind the relay position both circuits are connected. A forward wave in one circuit will cause a backward wave in both circuits. In circuit 2 forward and backward detection functions exceed the thresholds leading to the detection of a forward fault. In circuit 1 only the backward detection functions exceed the threshold. This will cause the relay to make a wrong decision (backward fault instead of forward fault).

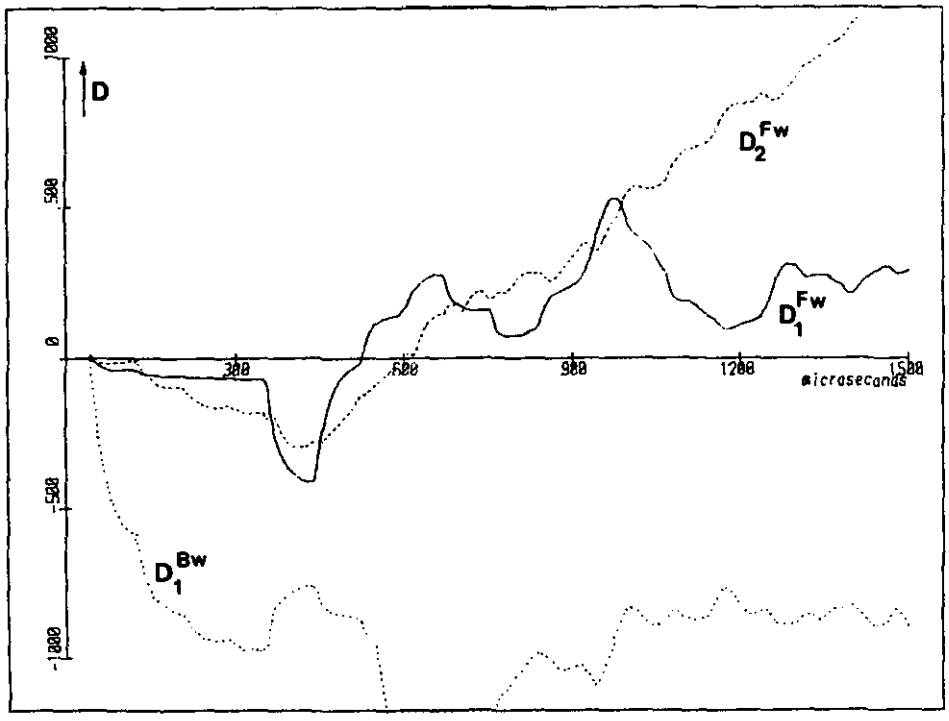

Figure 20 : RVN, $\varphi = 96^{o}$, fault at 12 km from Diemen.

Figure 20 shows an example of such a non-detectable situation. An RVN fault at a fault-initiation-angle of 96° causes travelling waves in circuit 2 but not in circuit 1. The figure shows the situation for the relay Diemen to Krimpen 1. The forward detection functions remain below the threshold (300-400 units) for some hundreds of microseconds, while D_1^{Bw} exceeds the threshold soon after the waves arrive at the relay position. Therefore a backward fault is detected instead of a forward fault. Although the relay Krimpen to Diemen 1 may detect a forward fault, the relay at Diemen will block both relays and the (faulted) circuit will not be disconnected. The other circuit shows no problems during this fault situation.
Although this is an extremely rare situation a back-up relay will be necessary for this. According to [17] about 130 faults occur each year in the British CEGB network. Three percent of them are inter-circuit faults. There are 53 types of inter-circuit faults, 15 of them show the behaviour discussed above. Suppose all inter-circuit faults and all fault-initiation angles are of equal probability. Further suppose that those 15 fault-situations are non-detectable during 10 % of the power frequency cycle. In that case 1 non-detectable inter-circuit fault is expected each 10 years on the CEGB network.

4.8.2. Failure of phase selection during inter-circuit faults.

When one conductor of the first circuit gets into contact with one conductor of the other circuit both relays might detect a single-phase fault, leading to two single-phase trips. In that case the double-circuit line will not be lost, considered the fault will extinguish.
Unfortunately phase selection does not show a correct behaviour for inter-circuit faults. Figure 21 and 22 give the selection functions for an R-V fault at a fault-initiation angle of 30° (maximum voltage jump). Figure 21 shows S_1 (see e.g. equation (35) and (41)) for the relay Diemen to Krimpen 1. Only phase R of circuit 1 is faulted, therefore S_1 should remain below the threshold. This is indeed true for the first 300 μs after fault-initiation, and it will lead to a single-phase trip of phase R. But after some time S_1 exceeds the threshold as yet, leading to a delayed three-phase trip. The introduction of a 250 Hz filter (see section 4.9) might solve the problem for this side of the line, but not for the other side as visible in figure 22. It shows S_2 for the relay Krimpen to Diemen 2. A three-phase trip will be given almost immediately after fault-initiation. The same holds for the other circuit.
It can be concluded that the algorithm for phase selection dicussed here, fails for inter-circuit faults.

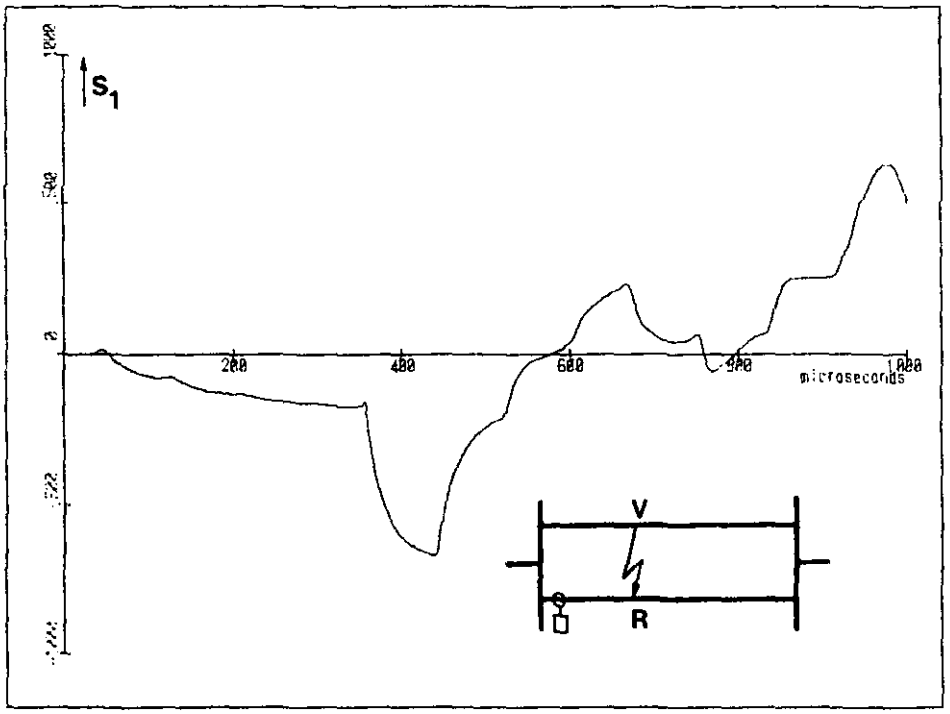

Figure 21 : RV, $\varphi = 30^{o}$, fault at 12 km from Diemen.

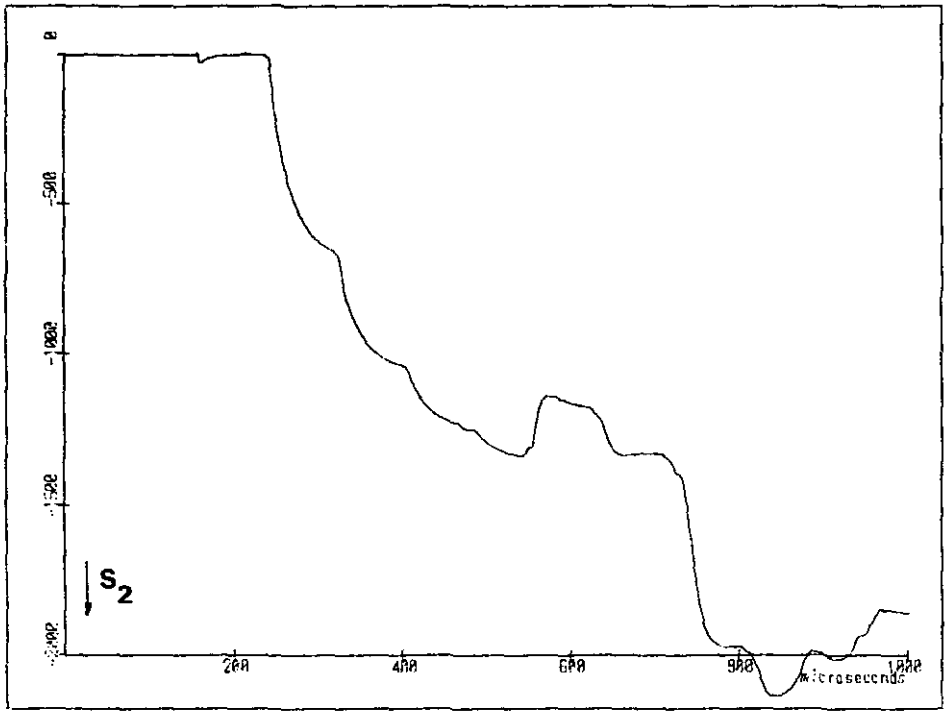

Figure 22 : RV, $\varphi = 30^{o}$, fault at 45.7 km from Krimpen.

4.9 Delayed phase selection.

During a complex fault (not single-phase-to-earth or phase-to-phase) all selection functions are in general non-zero. But for certain fault-initiation-angles one of the selection functions is zero. This may lead to an incorrect single-phase trip. There are three possible methods to reduce the risk of an incorrect single-phase trip.

1. A single-phase trip will only be given when the corresponding selection function is below the threshold for a certain period. With this method there is a chance of an incorrect three-phase trip during a single-phase-to-ground or phase-to-phase fault. The selection time is much longer because the relay has to wait a long time to distinguish between a simple fault and a complex fault.

   The extra selection time needed will be about 2.5 milliseconds for phase-to phase faults, if a threshold of 400 units is used. The total tripping time (time between fault initiation and generation of tripping signal) will amount to 4 milliseconds for some fault situations. This is considered far too long for "normal" fault situations, so this method will not be used.
2. A single-phase trip will be given as soon as all but one selection functions are above the threshold. A back-up relay will eventually give tripping signals for the other phases. The back-up relay will be needed anyway (chapter 4.4 and 4.8) so this method will not make the protection more complicated. Because the back-up relay is not the purpose of this study, this method will not be discussed further.
3. A single-phase trip will be given as soon as all but one selection functions are above the threshold.

   The selection function below the threshold will be monitored longer to see if no threshold-crossing occurs. If a threshold crossing occurs the other two phases will also be tripped. To prevent false tripping the detection functions will be filtered with an additional low pass filter. The cut-off frequency can be lower than the limit given in section 4.2. The only discrimination that has to be made is between a noisy signal around zero and a noisy signal with a small drift.

The last method has been studied in more detail. A possible implementation is given in chapter 5.

The continued monitoring must not lead to a delayed three-phase trip during single-phase-to-ground or phase-to-phase faults. During inter-circuit faults this cannot be prevented as shown in section 4.8.2, but for faults confined to one circuit it can. A low pass filter with a cut-off frequency of about $^{1}/_{10}\ \tau$ will be needed for this (250-500 Hz for the 57.7 km line between Krimpen and Diemen). This low cut-off frequency is mainly needed to suppress spikes during phase-to-phase faults.
The longest delay for non-evolving faults is about 2 ms for faults confined to one circuit and about 3 ms for inter-circuit faults.
Evolving faults will also lead to a delayed three-phase trip.

4.10. What happened to the homopolar detection functions ?

The algorithm makes no use of homopolar mode quantities. Three reasons for this can be given.

- Homopolar detection functions show large spikes of short duration comparable to the ones shown in figure 6 of section 4.2. They cannot be removed sufficiently by the $1/\tau$ filter as will be shown below. These spikes may cause false tripping of a circuit parallel to the faulted circuit.
- Homopolar mode quantities are strongly dependent on frequency as well as on the composition of the ground. It is therefore difficult to choose a wave impedance setting for the relay. This would cause an additional error source.
- A lightning stroke close to the line will induce all conductors in about the same extend, leading to a large homopolar wave, but almost none aerial waves.

Figure 23 shows D_o^{Fw} according to equation (3) of section 1.3.2. for the relay Diemen to Krimpen 2 with different cut-off frequencies used. An R-N fault occured at maximum voltage on the parallel circuit, halfway between Diemen and Krimpen. Even a cut-off frequency of 3800 Hz ($^{0.7}/\tau$) is not enough for sufficient reduction of the spike.

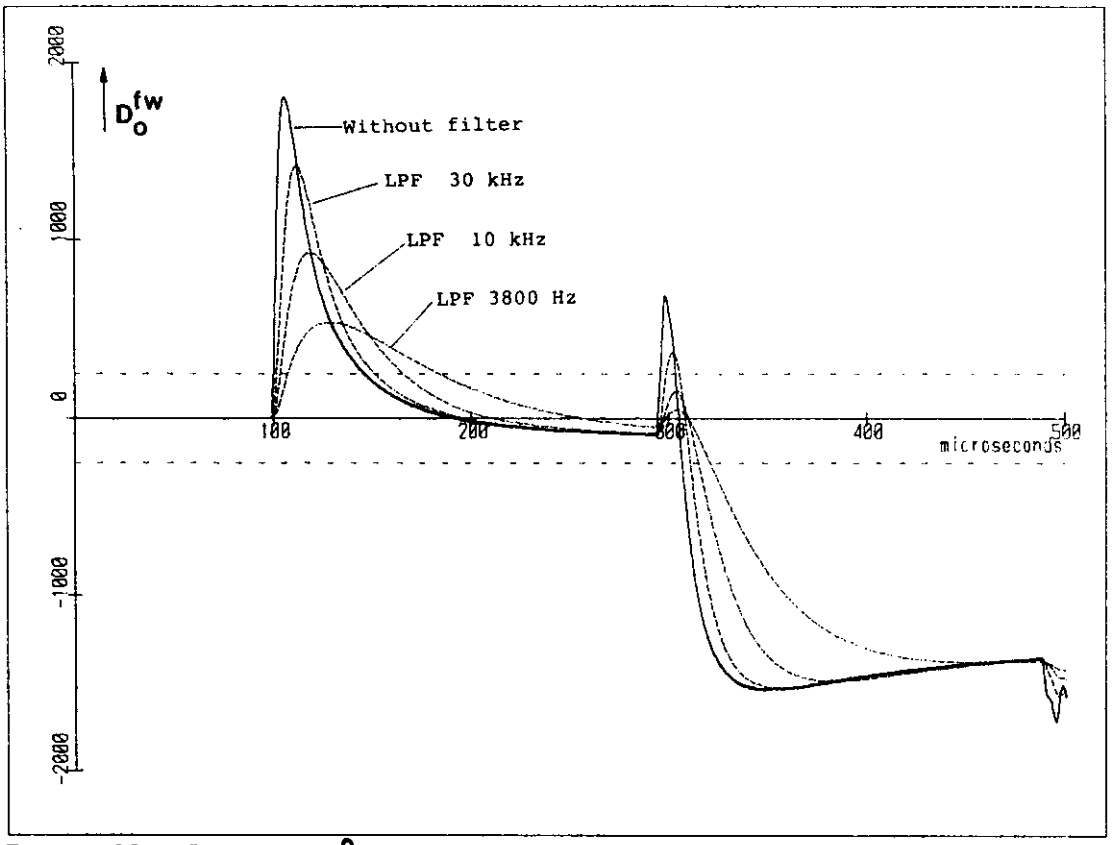

Figure 23 : R-N, $\varphi = 0^o$, fault midway between Diemen and Krimpen.

4.11. A summary of the results.

The above sections described some situations where the algorithm does not perform as needed. Non-detectable situations (problems with reliability) as well as false trips (problems with selectivity) have been found. They will be summarised in this section.

Problems with reliability.

The following situations showed not to be detectable:
1. a fault during (due to) line energizing;
2. a single-circuit fault evolving to an inter-circuit fault;
3. a fault within a few cycles after a lightning stroke to another line;
4. a fault within a few cycles after a fault on another line;
5. a few rarely occuring inter-circuit faults.

Problems with selectivity.

The following situations might lead to false trips:
6. a lightning stroke to a phase conductor not leading to a flash-over;
7. an inter-circuit fault with only one phase of a circuit involved
   (three-phase trip instead of single-phase trip).

Problem 1 and problem 7 seem to be the most serious problems. The first one because during line-energizing there is an increased risk of insulation failure due to the high overvoltages that occur. The second one because the availability of the double-circuit line is reduced. Each inter-circuit fault (also the extinghuishing faults) will lead to a loss of connection. Fast (six-phase) reclosure will not be possible in general, due to loss of synchronisation between both ends of the line.

5. Conclusions

In the preceeding chapters an algorithm for directional detection has been presented and discussed. After the study of a large number of situations on two different network models, it can be concluded that the principle is able to detect all "normal" fault situations within one and a half millisecond. The detection time for a fault with a considerable voltage jump (the most frequent situation) will be some tens of microseconds, if not limited by the speed of the A/D-convertor.
During the simulation study, some problems have been found concerning the reliability and the selectivity of the algorithms. The most serious ones are a fault during line energizing (this will not be detected by the algorithm) and a lightning stroke to a phase conductor not leading to a fault (this will sometimes cause a false trip).

An algorithm for phase selection also has been studied. For most fault situations the additional time needed for phase selection is just a few tens of microseconds. A few situations showed an initial single-phase trip followed by the necessary three-phase trip after about 1 ms.
During inter-circuit faults the algorithm for phase selection failes. Both circuits are always disconnected, also when only two single-phase trips are needed.

A possible implementation of the algorithms will be given in a seperate report [30] showing that there are no great technical problems.

The TWONFIL-model used to simulate a large number of fault situations and switching operations in a short time, has shown to be suitable for a fast first testing of algorithms for travelling-wave-based protection.

REFERENCES

[1] Hicks, K.L. and W.H. Butt
FEASIBILITY AND ECONOMICS OF ULTRA-HIGH-SPEED FAULT CLEARING.
IEEE Trans. Power Appar. & Syst., Vol. PAS-99(1980), p. 2138-2145.

[2] Thuries, E. and Pham Van Doan
INTERRELATION BETWEEN THE 1-CYCLE BREAKER AND THE CURRENT-LIMITING DEVICE.
In: Proc. Joint Power Generation Conf., Charlotte, N.C., 7-11 Oct. 1979.
New York: IEEE, 1979. Paper A 79 827-7

[3] Thorp, J.S. and A.G. Phadke, S.H. Horowitz, J.E. Beehler
LIMITS TO IMPEDANCE RELAYING.
IEEE Trans. Power Appar. & Syst., Vol. PAS-98(1979), p. 246-260.

[4] Crossley, P.A. and P.G. McLaren
DISTANCE PROTECTION BASED ON TRAVELLING WAVES.
IEEE Trans. Power Appar. & Syst., Vol. PAS-102(1983), p. 2971-2983.

[5] Johns, A.T. and A. Barker, M.A. Mahmoud
Discussion after [4].
Ibid., p. 2980.

[6] Koglin, H.-J. and Biao Zhang
A NEW ALGORITHM FOR DIGITAL DISTANCE PROTECTION BASED ON THE TRAVELLING WAVE PRINCIPLE.
In: Proc. 9th Power Systems Computation Conf. (PSCC), Cascais, Portugal, 30 Aug.-4 Sept. 1987.
London: Butterworth, 1987. P. 746-750.

[7] Shehab-Eldin, E.H. and P.G. McLaren
TRAVELLING WAVE DISTANCE PROTECTION: Problem areas and solutions.
IEEE Trans. Power Delivery, Vol. PWRD-3(1988), p. 894-902.

[8] Kohlas, J.
ESTIMATION OF FAULT LOCATIONS ON POWER LINES.
In: Identification and System Parameter Estimation, Proc. 3rd IFAC Symp., The Hague/Delft, 12-15 June 1973. Ed. by P. Eykhoff.
Amsterdam: North-Holland, 1973. P. 393-402.

[9] Ibe, A.O. and B.J. Cory
A TRAVELLING WAVE-BASED FAULT LOCATOR FOR TWO AND THREE-TERMINAL NETWORKS.
IEEE Trans. Power Delivery, Vol. PWRD-1(April 1986), No. 2, p. 283-288.

[10] Dongen, A.W.A. van
EEN DISTANTIEBEVEILIGINGSALGORITHME VOOR HOOGSPANNINGSLIJNEN.
M.Sc. thesis. Electrical Energy Systems, Faculty of Electrical Engineering, Eindhoven University of Technology, 1988.
EO.88.A.49

[11] Takagi, T. and J. Baba, K. Uemura, T. Sakaguchi
FAULT PROTECTION BASED ON TRAVELLING WAVE THEORY.
Part 1: Theory.
In: IEEE/PES Summer Meeting, Mexico City, 17-22 July 1977.
New York: IEEE, 1977. Paper A 77 750-3

[12] Dommel, H.W. and J.M. Michels
HIGH SPEED RELAYING USING TRAVELLING WAVE TRANSIENT ANALYSIS.
In: IEEE/PES Winter Meeting, New York, 29 Jan.-3 Febr. 1978.
New York: IEEE, 1978. Paper A 78 214-9

[13] Mansour, M.M. and G.W. Swift
A MULTI-MICROPROCESSOR BASED TRAVELLING WAVE RELAY:
Theory and realization.
IEEE Trans. Power Delivery, Vol. PWRD-1(Jan. 1986), No. 1,
p. 272-279.

[14] Chamia, M. and S. Liberman
ULTRA HIGH SPEED RELAY FOR EHV/UHV TRANSMISSION LINES:
Development, design and application.
IEEE Trans. Power Appar. & Syst., Vol. PAS-97(1978),
p. 2104-2116.

[15] Johns, A.T.
NEW ULTRA-HIGH-SPEED DIRECTIONAL COMPARISON TECHNIQUE
FOR THE PROTECTION OF E.H.V. TRANSMISSION LINES.
IEE Proc. C, Vol. 127(1980), p. 228-239.

[16] Johns, A.T. and M.M. El-Din Mahmoud
NEW APPROACH TO ULTRA-HIGH-SPEED PHASE SELECTION IN
SINGLE-POLE AUTORECLOSURE SCHEMES.
IEE Proc. C, Vol. 133(1986), p. 188-200.

[17] Light, B.R.
TRANSIT STABILITY ASPECTS OF POWER SYSTEM RELIABILITY
(CEGB SYSTEM).
In: Proc. Int. Conf. on Reliability of Power Supply
Systems, London, 21-23 Febr. 1977.
London: Institution of Electrical Engineers, 1977.
IEE Conference Publication, No. 148. P. 101-104.

[18] Anders, G.J. and P.L. Dandeno, E.E. Neudorf
COMPUTATION OF FREQUENCY OF SEVERE POWER SYSTEM FAULTS.
IEEE Trans. Power Appar. & Syst., Vol. PAS-103(1984),
p. 2369-2374.

[19] Engqvist, A. and L. Eriksson
NUMERICAL DISTANCE PROTECTION FOR SUB-TRANSMISSION LINES.
In: Proc. 31st Int. Conf. on Large High Voltage Electric
Systems (CIGRE), Paris, 28 Aug.-3 Sept. 1988.
Paris: CIGRE, 1988. Paper 34-04.

[20] Dommel, H.W. et al.
ELECTROMAGNETIC TRANSIENTS PROGRAM REFERENCE MANUAL
(EMTP theory book).
Portland, Oregon 97208 (P.O. Box 3621): Bonneville
Power Administration, August 1986.

[21] ELECTROMAGNETIC TRANSIENTS PROGRAM [EMTP]. Rule Book.
Rev. version June 1984.
Portland, Oregon 97208 (P.O. Box 3621): Bonneville Power Administration.

[22] Bollen, M.H.J.
THRESHOLDS AND TIME DELAYS FOR TRAVELLING-WAVE-BASED PROTECTION OF HIGH-VOLTAGE LINES.
IEE Proc. C, submitted for publication in 1989.

[23] Wedepohl, L.M.
APPLICATION OF MATRIX METHODS TO THE SOLUTION OF TRAVELLING-WAVE PHENOMENA IN POLYPHASE SYSTEMS.
Proc. Inst. Electr. Eng., Vol. 110(1963), p. 2200-2212.

[24] Vijver, R.E. van de
TWONFIL, HET SNELLE EMTP ALTERNATIEF.
Student report. Electrical Energy Systems, Faculty of Electrical Engineering, Eindhoven University of Technology, 1988.
EO.88.S.46

[25] Marti, J.R. and H.W. Dommel, L. Marti, V. Brandwajn
APPROXIMATE TRANSFORMATION MATRICES FOR UNBALANCED TRANSMISSION LINES.
In: Proc. 9th Power Systems Computation Conf. (PSCC), Cascais, Portugal, 30 Aug.-4 Sept. 1987.
London: Butterworth, 1987. P. 416-422.

[26] Bollen, M.H.J. and P.T.M. Vaessen
FREQUENCY SPECTRA FOR ADMITTANCE AND VOLTAGE TRANSFERS MEASURED ON A THREE-PHASE POWER TRANSFORMER.
Faculty of Electrical Engineering, Eindhoven University of Technology, 1987.
EUT Report 87-E-181

[27] Kersten, W.F.J. and G.A.P. Jacobs
ANALOG AND DIGITAL SIMULATION OF LINE-ENERGIZING OVERVOLTAGES AND COMPARISON WITH MEASUREMENTS IN A 400 kV NETWORK.
Faculty of Electrical Engineering, Eindhoven University of Technology, 1988.
EUT Report 88-E-193

[28] Blackburn, J.L.
PROTECTIVE RELAYING: Principles and applications.
New York: Marcel Dekker, 1987.
Electrical engineering and electronics, Vol. 37.

[29] Christopoulos, C. and D.W.P. Thomas, A. Wright
SCHEME, BASED ON TRAVELLING-WAVES, FOR THE PROTECTION OF MAJOR TRANSMISSION LINES.
IEE Proc. C, Vol. 135(1988), p. 63-73.

[30] Bollen, M.H.J. and G.A.P. Jacobs
IMPLEMENTATION OF AN ALGORITHM FOR TRAVELLING-WAVE-BASED DIRECTIONAL DETECTION.
Faculty of Electrical Engineering, Eindhoven University of Technology, in preparation for 1989.
EUT Report

Appendix A: EMTP results of fault detection

In this appendix some normal fault cases like the single-phase-to-ground fault will be discussed in detail, but also a few faults of less frequent occurence like inter-circuit faults.
The calculations have been made with the Electromagnetic Transient Program (EMTP) version M39 from the Bonneville Power Administration (Portland, Oregon). It was implemented on a Apollo Domain DN3000 personal workstation. The program was obtained through Leuven EMTP Center, Leuven, Belgium.*
For a description of the simulated network, see section 3.2.
The detection functions shown in this appendix are calculated from superimposed voltages and currents by using the following equations (see section 2.1.):

$$D_o^{Fw} = (v_r + v_s + v_t) - R_o\,(i_r + i_s + i_t)$$
$$D_1^{Fw} = (v_t - v_s) - R_1\,(i_t - i_s)$$
$$D_2^{Fw} = (v_r - v_t) - R_1\,(i_r - i_t)$$
$$D_o^{Bw} = (v_r + v_s + v_t) + R_o\,(i_r + i_s + i_t)$$
$$D_1^{Bw} = (v_t - v_s) + R_1\,(i_t - i_s)$$
$$D_2^{Bw} = (v_r - v_t) + R_1\,(i_r - i_t).$$

Although homopolar detection functions are not used anymore in the new algorithm, they are still reproduced in this appendix because they were used during the testing period.
The following fault-detection algorithm has been used.

$(|D_1^{Fw}|<\sigma$ and $|D_2^{Fw}|<\sigma)$ and $(|D_1^{Bw}|>\sigma$ or $|D_2^{Bw}|>\sigma)$: backward fault

$|D_1^{Fw}|>\sigma$ or $|D_2^{Fw}|>\sigma$: forward fault

$(|D_1^{Fw}|<\sigma$ and $|D_2^{Fw}|<\sigma)$ and $(|D_1^{Bw}|<\sigma$ and $|D_2^{Bw}|<\sigma)$: no fault

In all figures of this appendix, two dotted horizontal lines indicate a threshold value of 250 units (25% of the amplitude of the phase-to-ground voltage). This value has been used as a first choice. All time values, related to threshold crossings are (in this appendix) based on a threshold value of 250 units.

* K.U. Leuven EMTP Center
Kard. Mercierlaan 94
B-3030 Heverlee - Belgium

First single-phase-to-ground faults will be discussed and after that phase-to-phase faults, a two-phase-to-ground fault, a phase-to-phase inter-circuit fault and some special cases will follow.

A.1. single phase-to-ground fault

This is the most common fault occuring in high voltage grid (See table 1, chapter 2.2.). For each fault two fault-initiation-angles have been chosen to illustrate the differences in detection at voltage maximum and at voltage minimum*.

A.1.1. R-N fault at fault-initiation-angle of 0 degrees

This case is a single-phase-to-ground fault at a fault-initiation-angle of zero degrees (at voltage maximum which causes a maximum voltage jump).

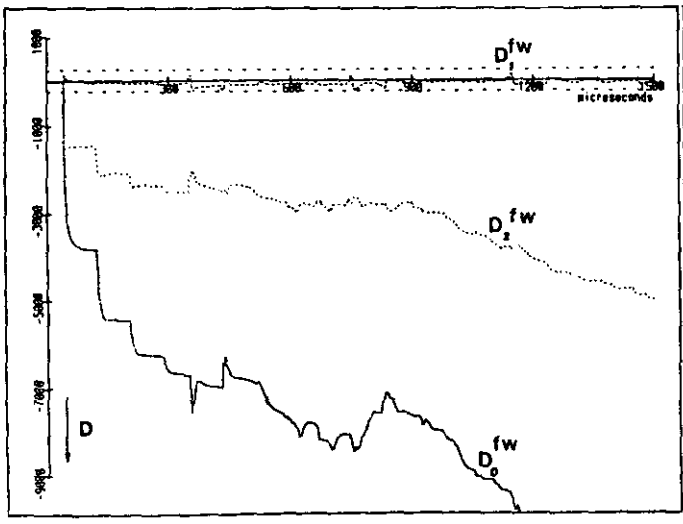

Fig. 24 R-N Φ=0°: Diemen to Krimpen 1

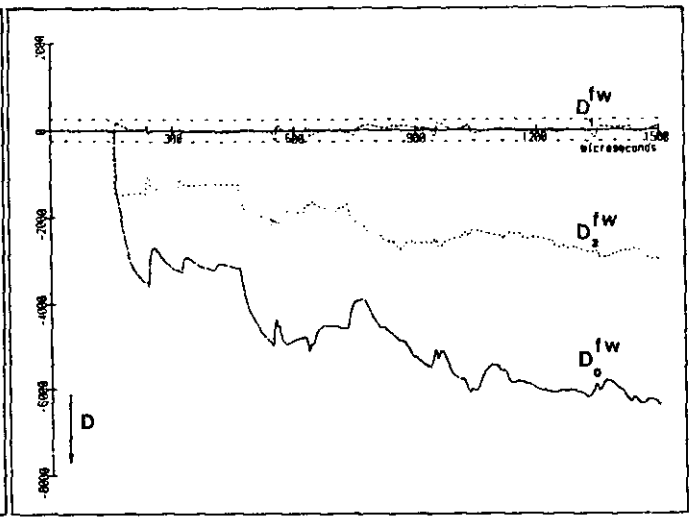

Fig.25 R-N Φ=0° Krimpen to Diemen 1.

Figure 24 shows the forward detection functions for the relay Diemen to Krimpen 1 on the faulted circuit. D_2^{Fw} rises above the threshold value (250 units) immediately. D_1^{Fw} stays below the threshold value but this has no influence on fault detection.

* In this EMTP calculations we used cosine-sources which means that voltage maximum is at zero degrees. The fault-initiation-angle is always refered to the R-phase.

Figure 25 gives the same detection functions for Krimpen to Diemen 1.

Again D_1^{Fw} remains below the threshold value and D_2^{Fw} rises above it immediately. The conclusion from figures 24 and 25 is that the relays in station Diemen as well as in station Krimpen determine a forward fault on the faulted circuit. In figure 26 and 27 the two backward detection functions and the two forward functions respectively are shown for Diemen to Krimpen 2. D_2^{Bw} rises above the threshold value immediately.

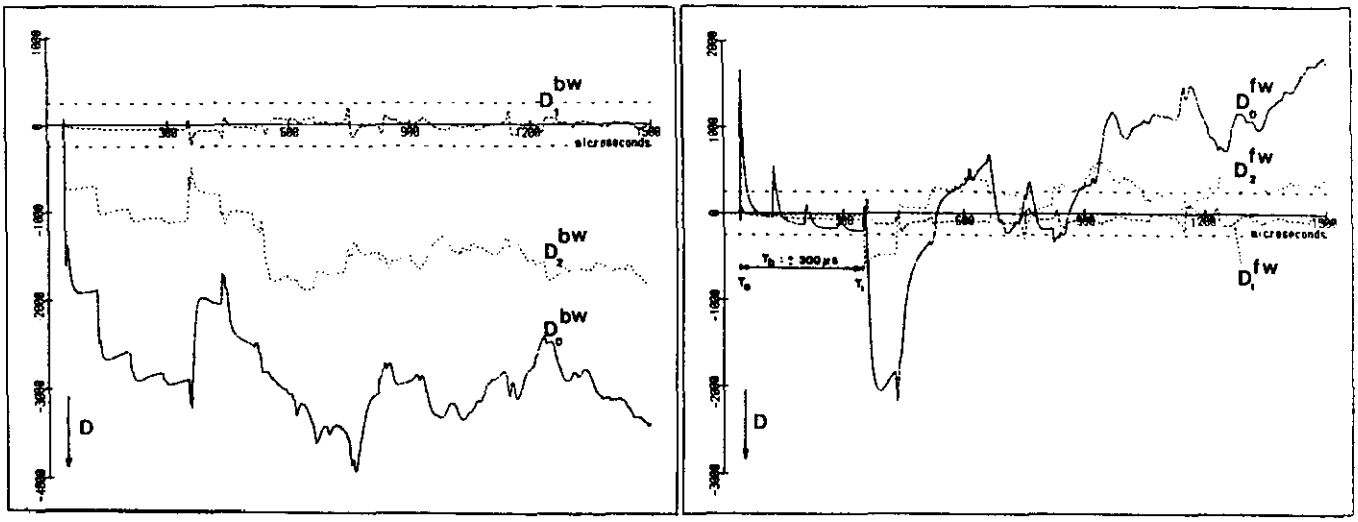

Fig. 26 R-N Φ=0°: Diemen to Krimpen 2 *Fig. 27 R-N Φ=0°: Diemen to Krimpen 2.*

There is about 300 microseconds left before D_2^{Fw} rises above the threshold. Figure 27 clearly shows the maximum time available to determine a backward fault. As shown in figures 27 and 13 (chapter 4.3, page 32) wave A arrives at the relay Diemen to Krimpen 2 at time τ_0 as a backward wave (which has to be detected) but wave B from the same fault arrives at time τ_1 as a forward wave. The time difference is relatively large because the fault is close to the relay position. Figures 28 and 29 show the detection functions for the relay on the remote terminal: Krimpen to Diemen 2. Because for the latter relay the fault is close to the other line terminal, only little time is left to determine a backward fault. Looking at D_2^{Fw} (figure 29) shows an available time of about 80 μs.

Looking at the homopolar detection functions one can see that in station Diemen (figure 26) a correct backward fault is concluded but in station Krimpen a false forward fault is seen because the backward as well as the forward detection functions arise both at the same time above the threshold value. In this case it is impossible to use a low pass filter because suppressing the peak in D_o^{Fw} will also suppress the peak in D_o^{Fw}. Only a communication link between the relays in Diemen 2 and Krimpen 2 will prevent a

false tripping. One of the reasons why the homopolar functions are not used anymore is because of the trouble in detecting a simple fault in the parallel circuit (see section 4.10).

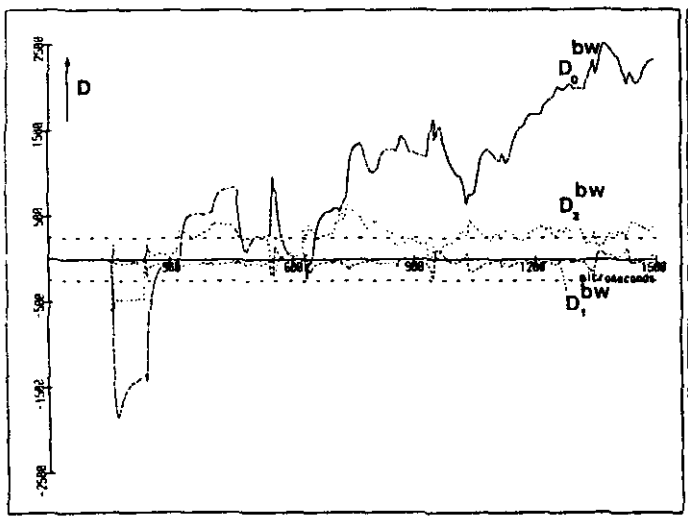

Fig. 28 R-N Φ=0°: Krimpen to Diemen 2

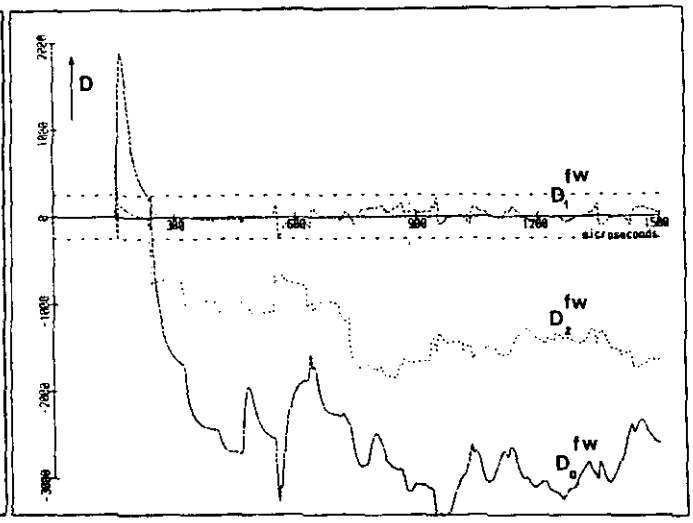

Fig. 29 R-N Φ=0°: Krimpen to Diemen 2.

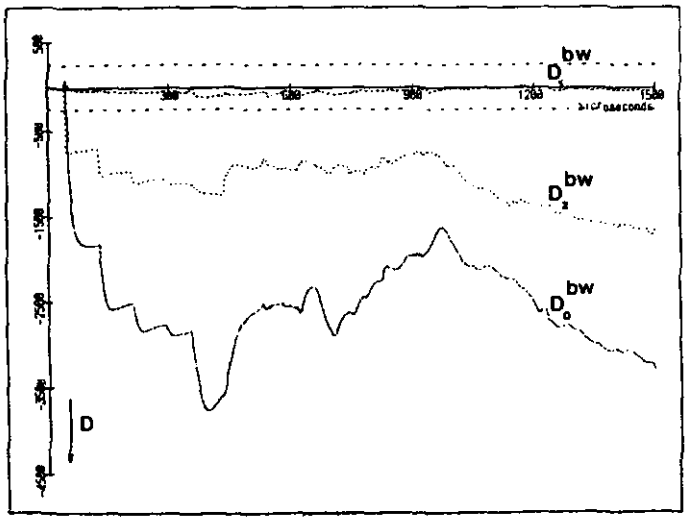

Figure 30 R-N φ=0° Diemen to Ens 1

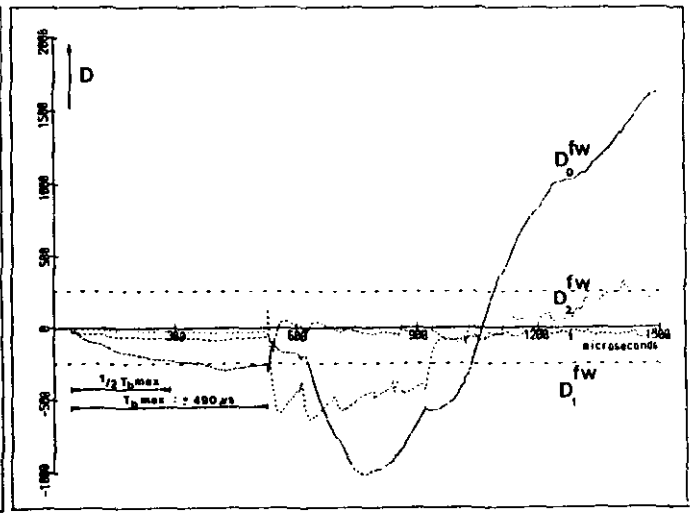

Figure 31 R-N φ=0° Diemen to Ens 1

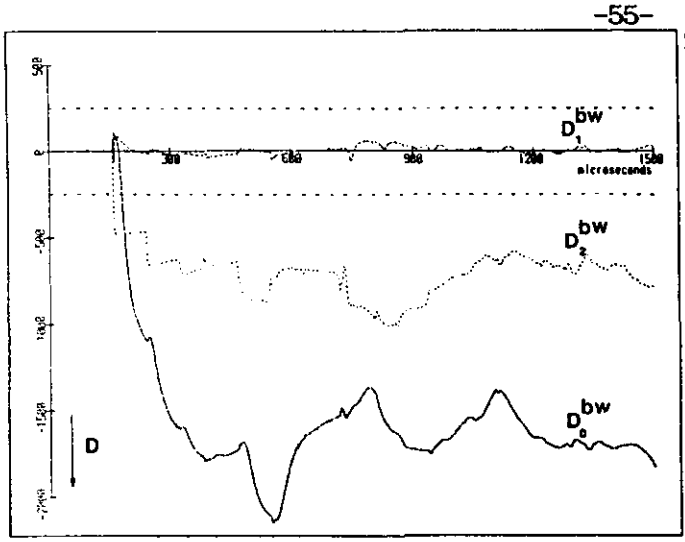

Figure 32 R-N φ=0° Krimpen to Maasvlakte 1

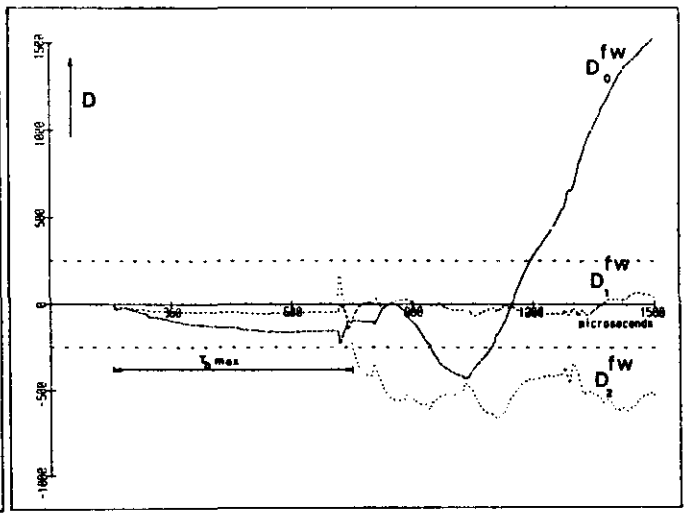

Figure 33 idem

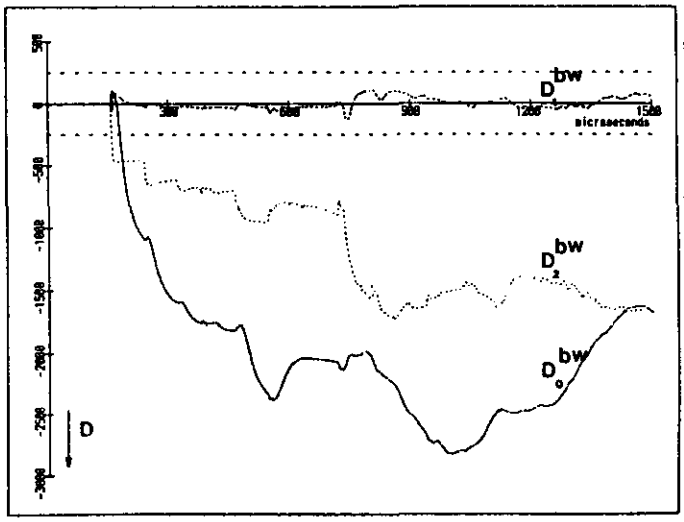

Figure 34 R-N φ=0° Krimpen to Geertruidenberg 1

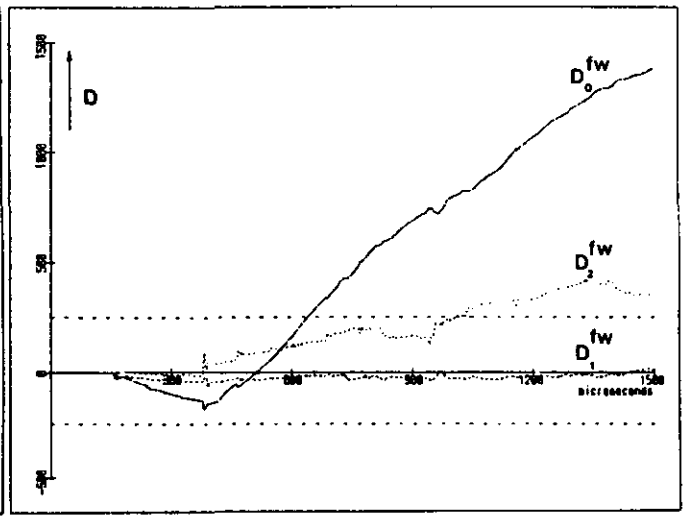

Figure 35 idem

The relays Diemen to Ens 1 (figures 30, 31), Krimpen to Maasvlakte 1 (figures 32, 33) and Krimpen to Geertruidenberg (figures 34, 35) give no problems.

D_2^{Bw} rises above the threshold value immediately and the forward waves rise above the threshold value after two times the travel time of the related lines. This time is available for the relay to ascertain a backward fault.

A.1.2. R-N fault at initiation-angle of 90 degrees

This case is a single-phase-to-ground fault at an fault-initiation-angle of 90 degrees (voltage zero). It will cause a minimum voltage jump.
Because of the very low voltage jump it takes more time to reach the threshold value as can be seen in figure 36 (Diemen to Krimpen 1) where it takes 440 μs for D_2^{Fw}. In figure 37 (Krimpen to Diemen 1) it takes 590 μs for D_2^{Fw} to exceed the threshold value of 250 units.

In the remaining circuits the relays can ascertain backward faults without any problems. The time delay will cause no problems here as long as the backward detection functions exceed the threshold before the forward detection functions.

It can be concluded that in case of the single-phase-to-ground fault at voltage-zero there is a correct detection of a forward fault in the faulted circuit and a backward fault in the other circuits, but the detection times become much longer than during a fault at voltage maximum.

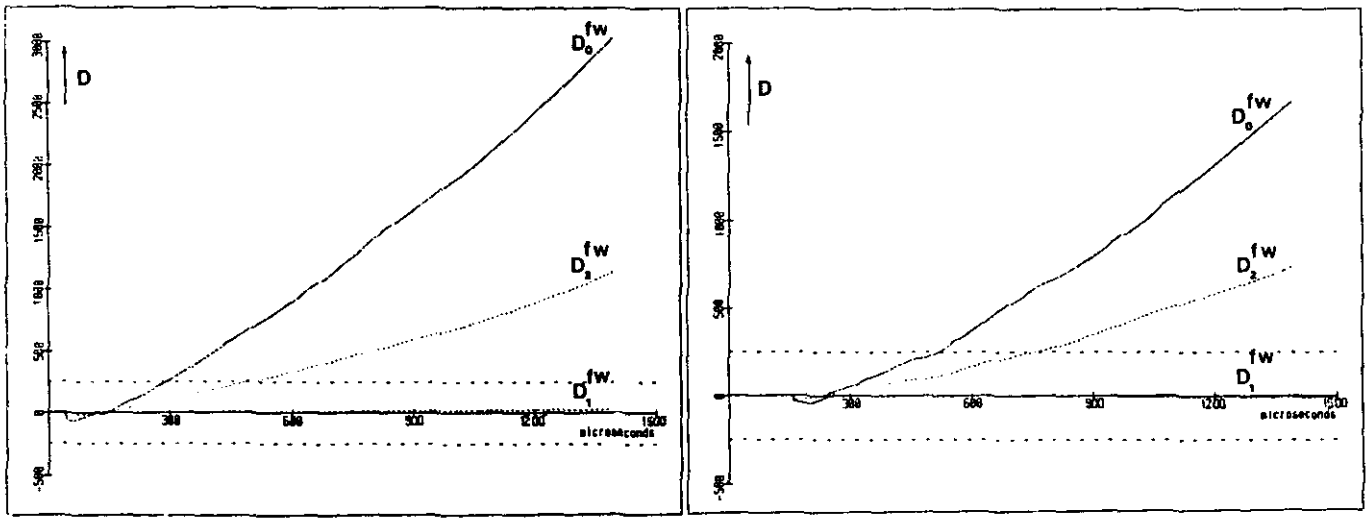

Fig. 36 R-N $\Phi=90_0$:Diemen to Krimpen 1. Fig. 37 R-N $\Phi=90^0$:Krimpen to Diemen 1.

A.2. Phase-to-phase faults

The most common fault but one is the phase-to-phase fault. The EMTP-model has been used to study the R-S fault at a fault-initiation-angle of 30^0 (maximum voltage jump) and at a fault-initiation-angle of 120^0 (zero voltage jump). The other phase-to-phase faults have also been studied, but the results are not reproduced here.

A.2.1. R-S fault at fault-initiation-angle of 30^0

This case is a phase-to-phase fault at a fault-initiation-angle of 30^0 and will show a maximum voltage jump. Some results are shown in figure 38 for Diemen to Krimpen 1, a relay on the faulted circuit. D_1^{Fw} and D_2^{Fw} rise above the threshold immediately. About the same behaviour has been found for Krimpen to Diemen 1. Fast fault detection is possible in the faulted circuit for this case.

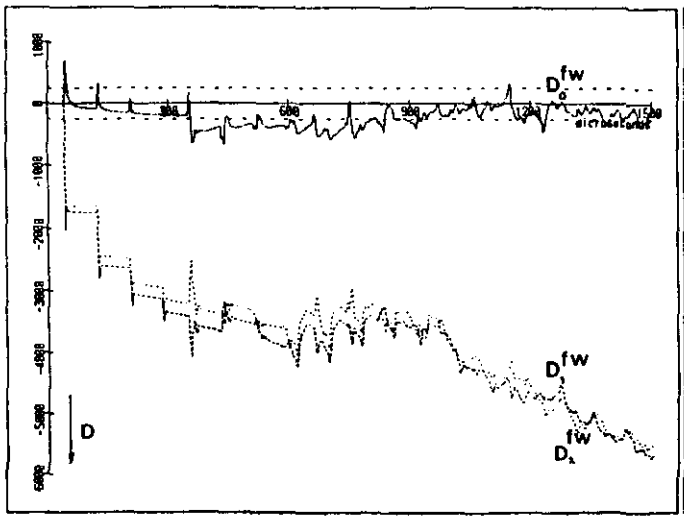

Fig. 38 R-S Φ=30°:Diemen to Krimpen 1

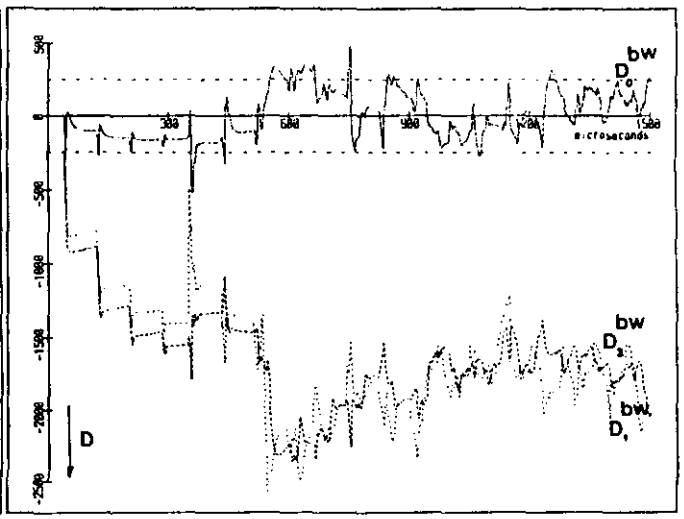

Fig. 39 R-S Φ=30°:Diemen to Krimpen 2.

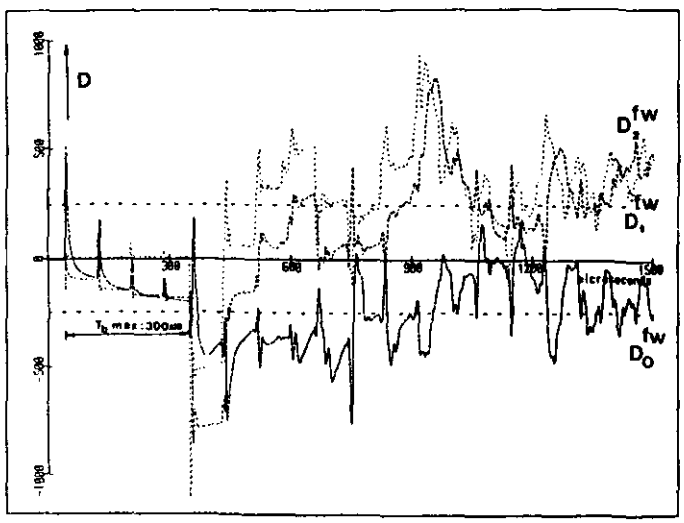

Fig. 40 R-S Φ=30°:Diemen to Krimpen 2

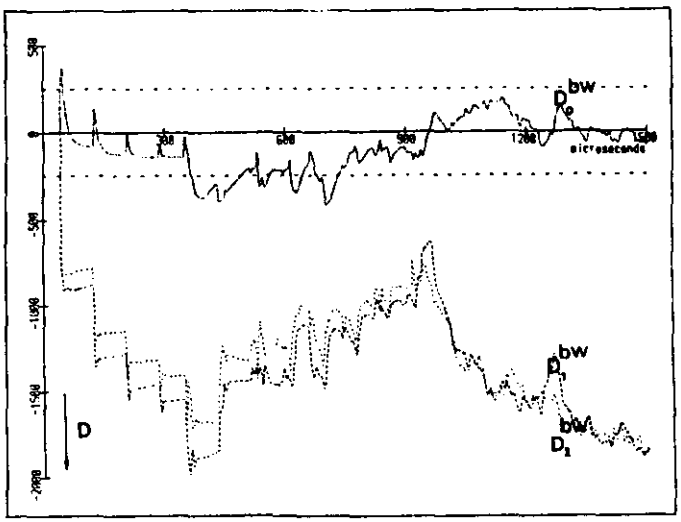

Fig. 41 R-S Φ=30°:Diemen to Ens 1

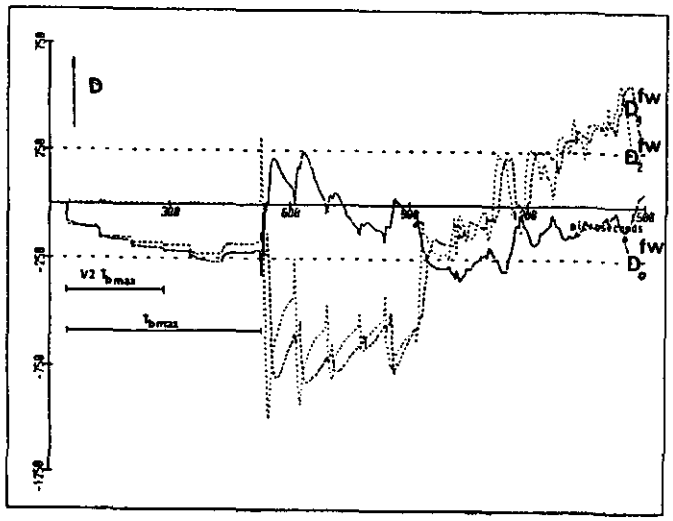

Fig. 42 R-S Φ=30°:Diemen to Ens 1

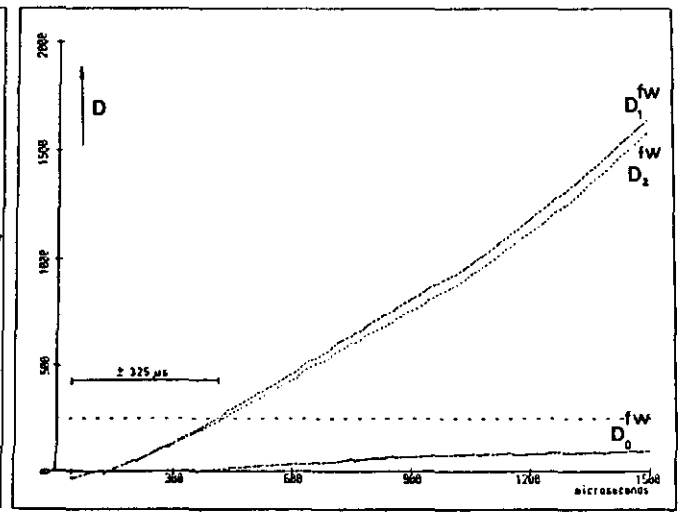

Fig. 43 R-S Φ=120°:Diemen to Krimpen 1.

As shown in figure 39 (Diemen to Krimpen 2) D_1^{Bw} and D_2^{Bw} rise above the threshold value quickly and after only 300 µs D_1^{Fw} and D_2^{Fw} (figure 40) do the same. In the faulted circuit the relay can determine a forward fault without any problems. In the parallel circuit a backward fault is detected if this can be done within 300 µs. In the other circuits no problems occur during the detection of a backward fault as shown in figure 41 and 42 for Diemen to Ens 1. D_1^{Bw} and D_2^{Bw} rise above the threshold immediately. D_1^{Fw} and D_2^{Fw} rise above it just after 485 µs. This fault type gives at maximum voltage jump no problems with directional detection.

A.2.2. R-S fault at a fault-initiation-angle of 120°

This case describes a phase-to-phase fault at a fault-initiation-angle of 120° leading to a zero voltage jump. The only difference with the previous case is the time needed for the detection functions to exceed the threshold. This detection time is much longer for the case near voltage-zero. As an example one can see in figure 43 that both aerial forward detection functions (D_1^{Fw} and D_2^{Fw}) exceed the threshold for Diemen to Krimpen 1 after 325 µs. The maximum detection-time for an R-S fault is 570 µs for Diemen and 800 µs for Krimpen.

In the other circuits there are no problems for backward directional detection, except that it takes more time because of the low voltage jump when the fault occurs.

As we concluded in the previous case there are no problems for directional detection in this case with a minimum voltage jump. Further explanation of phenomena around voltage-zero has been given in chapter 4.7.

A.3. The two-phase-to-ground fault

A two-phase-to-ground fault is a more complex fault than a single-phase-to-ground or phase-to-phase fault. The superimposed quantities cannot be explained by the introduction of one source at the fault position. For a two-phase-to-ground fault two sources are needed. Because the sources have different phase angle there is no situation with zero detection functions.

A.3.1. R-S-N fault at fault-initiation-angle of 24 degrees

This case describes a two-phase-to-ground fault at a fault-initiation-angle of 24^{o}. This angle has been chosen because it shows a high value of D_1^{Fw} and D_2^{Fw} on a relay with a backward fault. R-S-N faults at other fault-initiation angles showed an uncomplicated detection. On the faulted circuit a forward fault is detected almost immediately, because D_1^{Fw} and D_2^{Fw} exceed the threshold. The parallel circuit shows no serious problems. The results for Diemen to Ens 1 are reproduced in figure 44 (backward detection functions) and figure 45 (forward detection functions). In figure 45 D_1^{Bw} and D_2^{Bw} exceed the threshold almost instantaneously while D_1^{Fw} and D_2^{Fw} remain below the threshold for more than the travel time of the line to be protected (230 μs). For a fault more closer to Diemen the reflections will arrive with smaller intervals. This may lead to a faster crossing of the threshold causing the false detection of a forward fault. A small increase of the threshold will reduce this risk.

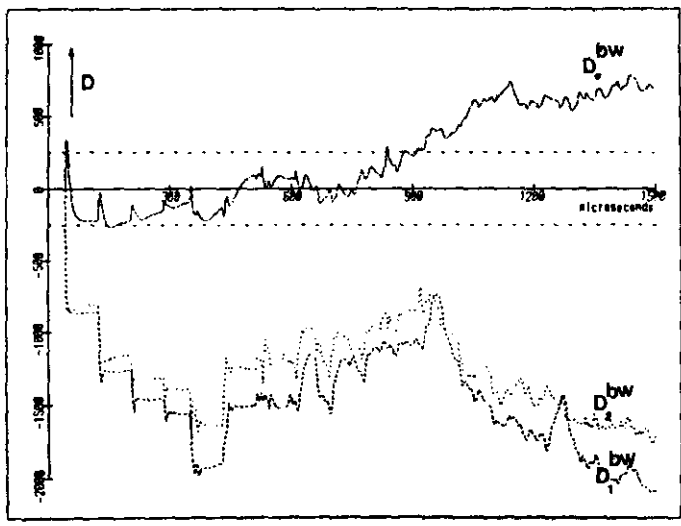

Fig. 44 R-S-N Φ=24°:Diemen to Ens 1

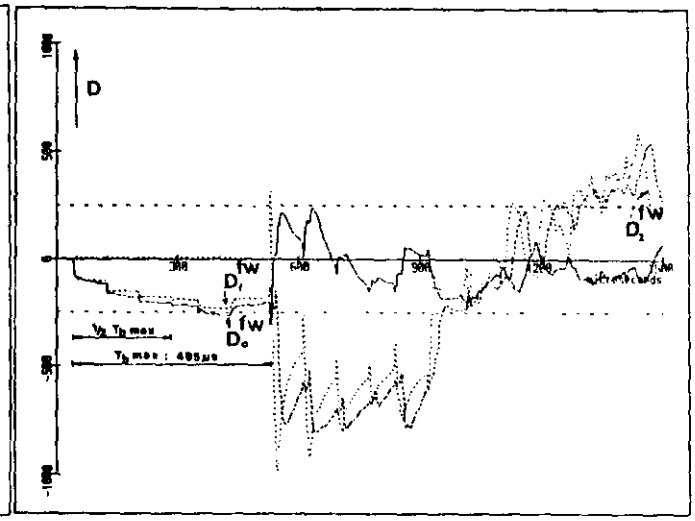

Fig. 45 R-S-N Φ=24°:Diemen to Ens 1.

A.4. Phase to phase inter-circuit faults

The cases described in the preceeding chapters were all situations in which the fault was limited to one circuit. These fault situations are by far the most common in practice. Fault situations concerning two phases of different circuits may be extremely rare but they are not impossible. A protection algorithm must show a correct behaviour for all possible situations, also for extremely rare ones. Therefore also some inter-circuit faults have been studied.

By using the complex EMTP-network model two phase-to-phase inter-circuit faults have been studied in more detail:

- R-V, Φ = 30°, maximum detection functions;
- R-V, Φ = 120°, minimum detection functions.

Only the first situation will be described below.

A.4.1. R-V fault at fault-initiation-angle of 30 degrees

This case describes a fault between two phases of different circuits at the fault-initiation-angle causing a maximum voltage jump. All 4 relays on the faulted line will detect a forward fault. As an example figure 46 gives the forward detection function for the relay Diemen to Krimpen 1. D_0^{Fw} and D_2^{Fw} exceed the threshold instantaneously. In Diemen to Krimpen 2 (figure 47) D_1^{Fw} causes the detection of a forward fault. All relays outside the faulted line detect a backward fault without any problems.

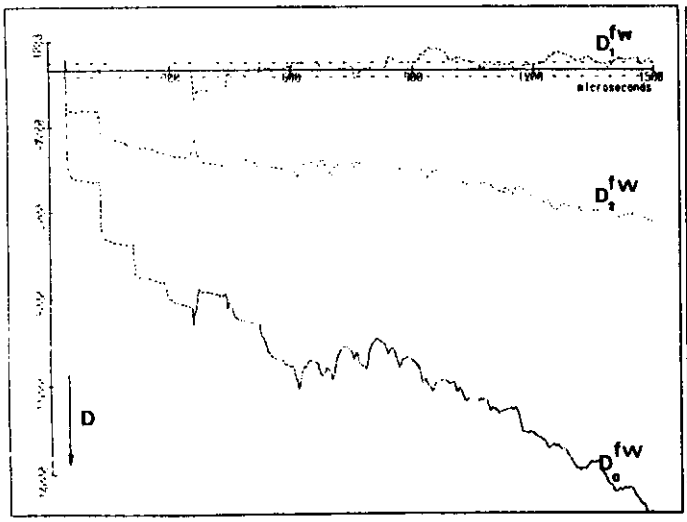

Fig. 46 R-V Φ=30°:Diemen to Krimpen 1

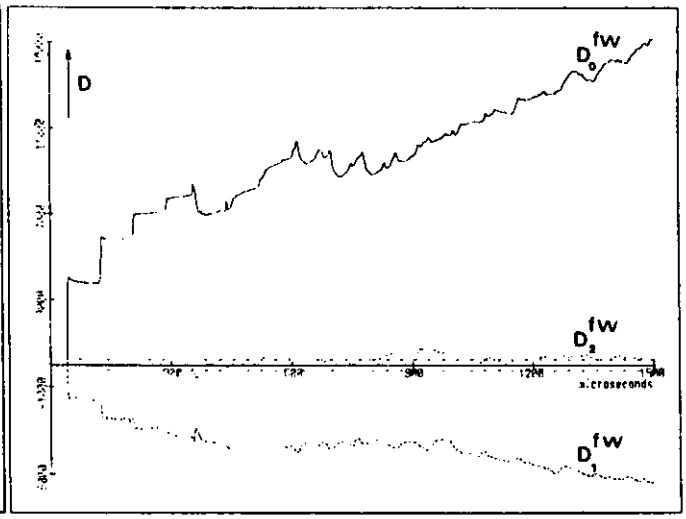

Fig. 47 R-V Φ=30°:Diemen to Krimpen 1.

A.5. Worst cases

The preceeding chapters described some "normal" fault situations. Except for the inter-circuit-faults, the situations are likely to occur on a high-voltage line. This chapter will discuss some situations that are less likely to occur. They were found as worst cases during the study on the simple network model. The following situations will be discussed:

1. R-S-T fault at a fault-initiation-angle of 35°. This situation is characterised by a large value of D_1^{Fw} and D_0^{Fw} in the parallel circuit;
2. R-S-T-U-V-W fault at a fault-initiation-angle of 35°. This six-phase-fault shows the largest values of D_1^{Fw} and D_0^{Fw} for a relay with a backward fault;
3. R-V-N fault at a fault-initiation-angle of 96°. This inter-circuit fault is initiated during the zero-crossing of the detection functions in circuit 1. This may cause problems as described in chapter 4.8.1.

A.5.1. R-S-T fault at fault-initiation-angle of 35 degrees

This case describes a three-phase fault at a fault-initiation-angle of 35 degrees. This causes a high value for the forward detection function in the parallel circuit. The relay Diemen to Krimpen 1 (in the faulted circuit) detects a forward fault instantaneously. The same holds for Krimpen to Diemen 1. Figure 48 shows the backward detection functions for Diemen to Krimpen 2. Figure 49 shows the forward detection functions. D_1^{Bw} and D_2^{Bw} immediately exceed the threshold. D_1^{Fw} and D_2^{Fw} do so after about 300 μs. The relay will detect a backward fault. The situation for Krimpen to Diemen 2 is

given in figure 50 (backward detection functions) and figure 51 (forward detection functions). The time-span between the threshold crossing of the backward detection functions and that of the forward detection functions, is about 75 μs. This short period will not give any problems because the communication with the other side will prevent false tripping. In Diemen to Ens 1 figure 52), D_1^{Bw} and D_2^{Bw} exceed the threshold value immediately. D_1^{Fw} and D_2^{Fw} (figure 53) remain below the threshold value for more than the travel time of the line (230 μs). So Diemen to Ens 1 detects a backward fault, just like Krimpen to Maasvlakte 1 and Krimpen to Geertruidenberg 1. Although problems were expected for this case, directional detection works reliable for an R-S-T fault.

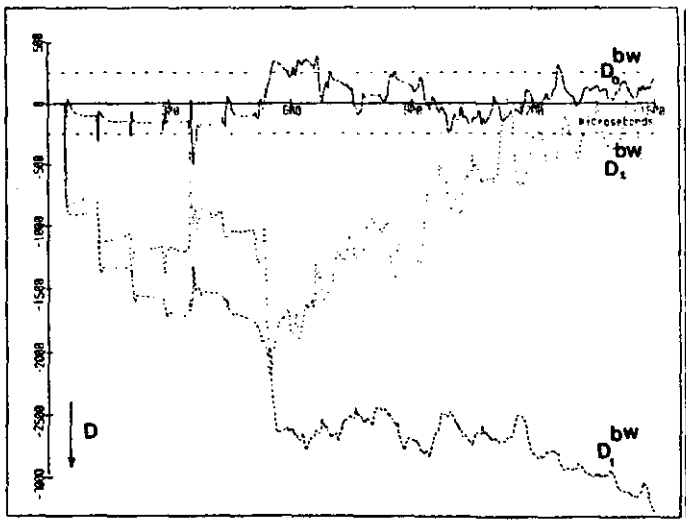

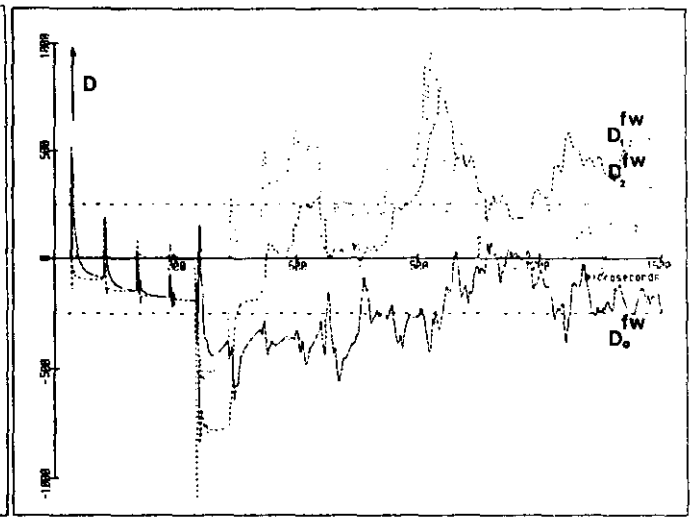

Fig. 48 R-S-T Φ=35°:Diemen to Krimpen 2 *Fig. 49 R-S-T Φ=35°:Diemen to Kr. 2.*

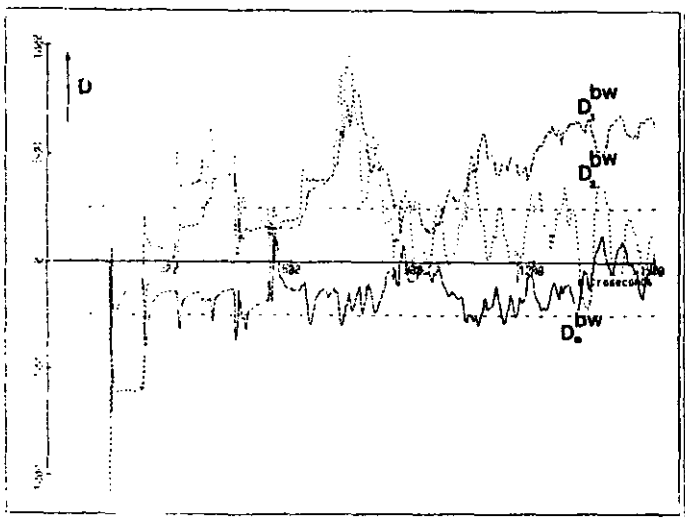

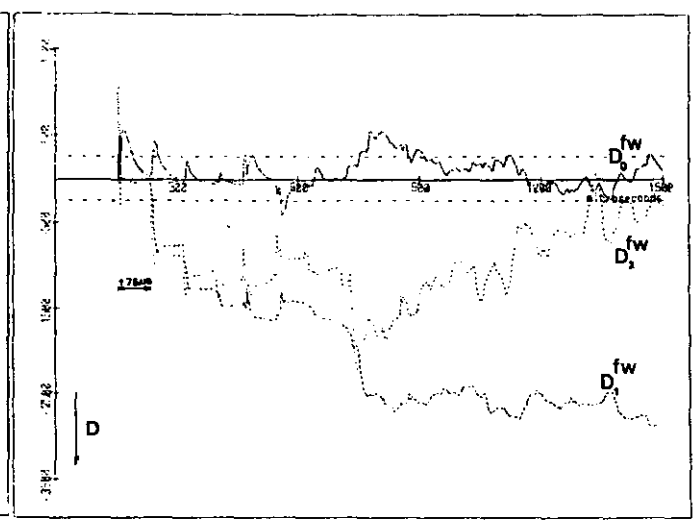

Fig. 50 R-S-T Φ=35°:Krimpen to Diemen 2 *Fig. 51 R-S-T Φ=35°:Krimpen to Die.2*

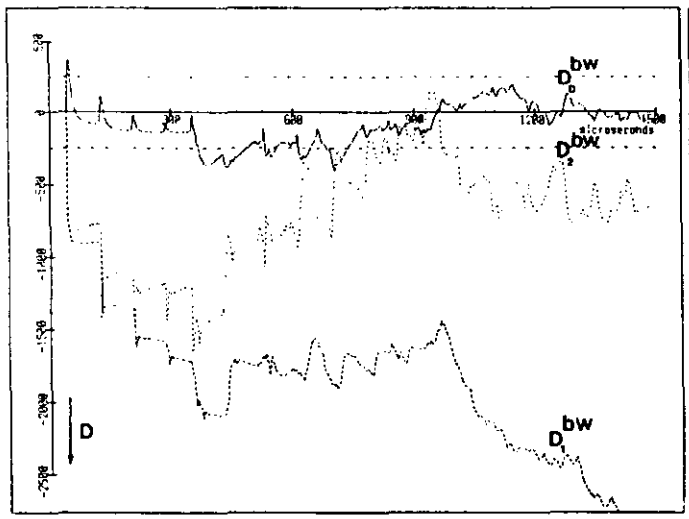

Fig. 52 R-S-T Φ=35°:Diemen to Ens 1

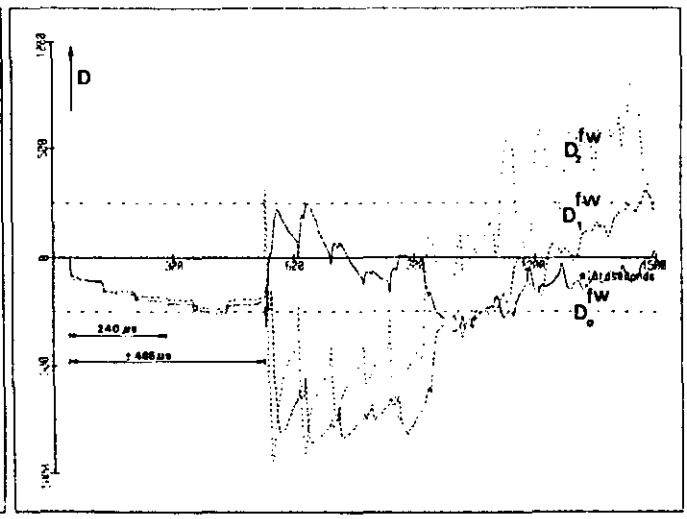

Fig. 53 R-S-T Φ=35z°:Diemen to Ens 1.

A.5.2. R-S-T-U-V-W fault at fault-initiation-angle of 35 degrees

This case concerns a fault between all six phases of both circuits. From the simple-network study it was concluded that his situation showed largest values of the forward detection functions in the backward circuit.
The faulted line showed no problems according to the complex-network study. All four relays determine a forward fault immediately. The highest value of the forward detection during a backward fault was found at the relay Diemen to Ens 1. Figure 54 shows that D_1^{Bw} and D_2^{Bw} exceed the threshold immediately.

Figure 55 (forward detection functions) shows that D_1^{Fw} reaches a value of about 200 units very soon after fault initiation but the value of 250 units is not reached till about 300 μs after fault initiation. Just before the arrival of the reflected wave D_1^{Fw} reaches a value a little below 250 units. About the same maximum value is reached during the R-S-T fault (figure 53), the R-S-N fault (figure 45), the R-S fault (figure 42) and during the R-N fault (figure 31).
From this it can be concluded that a threshold value of 300 units for the forward detection functions will succesfully discrimitate between a forward fault and a backward fault.

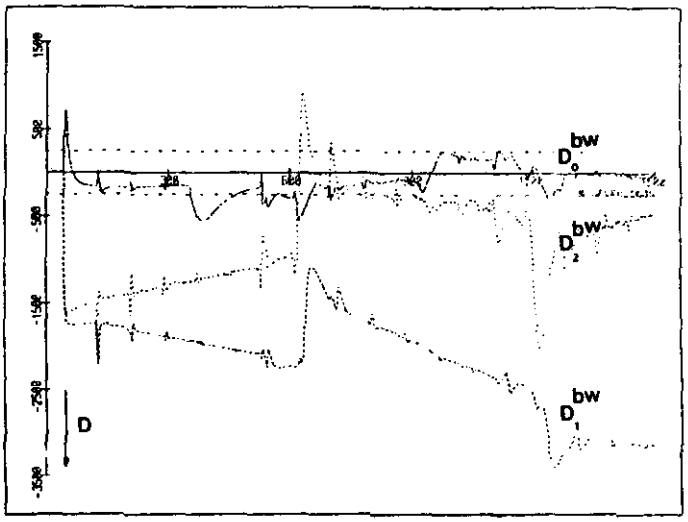

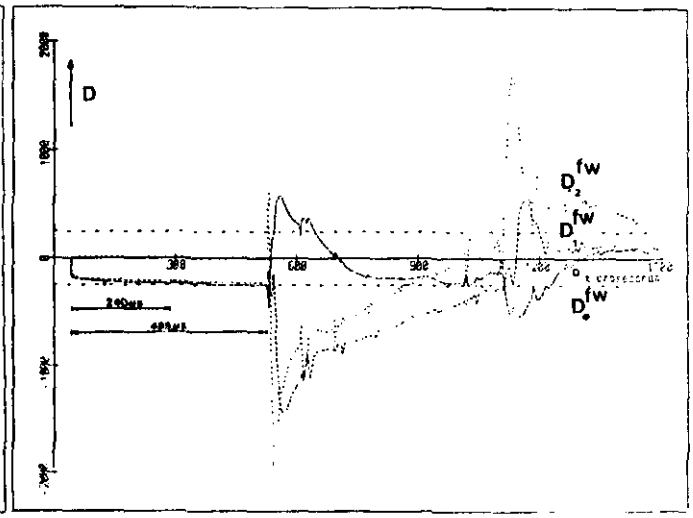

Figure. 54 RSTUVW Φ=35°:Diemen to Ens 1. Figure 55: idem

A.5.3. R-V-N fault at fault-initiation-angle of 96 degrees

This case is one of the "non-detectable-faults" as described in chapter 4.8.1. The detection functions in circuit 1 show a zero-crossing for this fault-initiation-angle. Figure 56 shows the forward detection functions for the relay Diemen to Krimpen 1.
Without using the homopolar detection functions the forward detection functions for Diemen to Krimpen 1 will get high after the backward detection functions. So a backward fault is detected. The same holds for Krimpen to Diemen 1, though not as worse. Therefore the fault on circuit 1 will not be detected and a back-up relay will be neccessary.

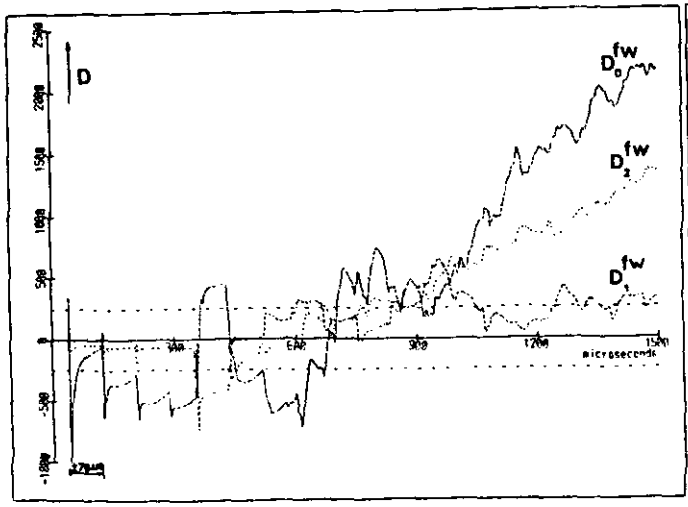

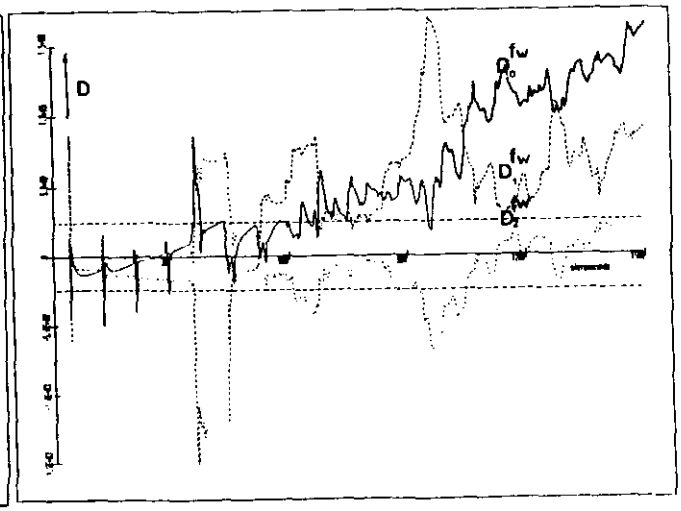

Fig. 56 RVN Φ=96°:Diemen to Krimpen 1 Fig. 57 RSTUN Φ=90°:Diemen to Krimpen 2.

A.5.4. R-S-T-U-N fault at fault-initiation-angle of 90 degrees

Another fault situation with a zero-crossing in one circuit is the R-S-T-U-N fault at a fault-initiation-angle of 90 degrees. The forward detection functions for Diemen to Krimpen 2 for this case are given in figure 57.
Apart from some small peaks the three detection functions are below the threshold of 250 units. The backward detection functions are above the threshold, so a backward fault will be detected by the relay.
The conclusion is that the second circuit is not protected by the algorithm for directional detection for an R-S-T-U-N fault at a fault-initiation-angle of 90 degrees. This is a very rare fault situation and this problem may not seem of much concern. But the fault situation is not impossible and the line protection must be able to detect all possible fault situations. A back-up relay will be needed to detect this fault situation and the other situations given in chapter 4.8.1.

Appendix B: EMTP results of phase selection.

After a forward fault is ascertained the algorithm for phase selection starts. This means that the algorithm only needs to be tested for a faulted circuit. That will be, in most cases, for the relays Krimpen to Diemen 1 as well as Diemen to Krimpen 1.
The following chapter will discuss the calculated selection functions for the three single-phase-to-ground faults and the three phase-to-phase faults, at maximum voltage jump as well as near voltage-zero.
Beside these "normal faults" some special cases will be discussed further on. These special cases were found from the simple-network study.
As with directional detection a first choice for the threshold (250 units) is shown in the figures as two dotted horizontal lines.
The selection functions have been calculated from the superimposed quantities by using the following equations (see section 2.2)

$$S_1 = (v_t - v_s) - R_1(i_t - i_s)$$
$$S_2 = (v_r - v_t) - R_1(i_r - i_t)$$
$$S_3 = (v_r - v_s) - R_1(i_r - i_s)$$
$$S_4 = (2v_t - v_r - v_s) - R_1(2i_t - i_r - i_s)$$
$$S_5 = (2v_r - v_s - v_t) - R_1(2i_r - i_s - i_t)$$
$$S_6 = (2v_s - v_r - v_t) - R_1(2i_s - i_r - i_t)$$

The following phase selection algorithm has been used.

$|S_1| < \sigma$, all others $> \sigma$: R-N
$|S_2| < \sigma$, all others $> \sigma$: S-N
$|S_3| < \sigma$, all others $> \sigma$: T-N
$|S_4| < \sigma$, all others $> \sigma$: R-S
$|S_5| < \sigma$, all others $> \sigma$: S-T
$|S_6| < \sigma$, all others $> \sigma$: R-T
all selection functions $> \sigma$: three phase trip

B.1. Single-phase-to-ground faults

B.1.1. R-N fault at fault initiation-angle of 0 degrees

For this case a fault-initiation-angle of zero degrees has been chosen. This will cause a maximum voltage jump. During an R-N fault the selection function S_1 should be below the threshold value. All other selection functions should be above.

The results for Diemen to Krimpen 1 are shown in figure 58. Only the single-phase-to-ground selection functions (S_1, S_2 and S_3) are shown here. The phase-to-phase selection functions exceed the threshold instantaneously. Also S_2 and S_3 exceed the threshold, whereas S_1, remains below the threshold of 250 units.

The relay will select an R-N fault and a single-phase tripping signal can be given immediately. The small swings in S_1, are caused by differences in travel time between the different waves.

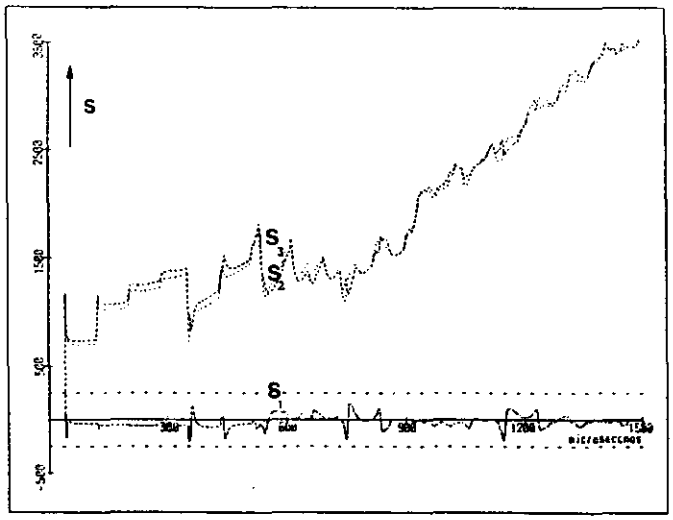

Figure 58 RN φ=0°: Diemen to Krimpen 1

B.1.2. R-N fault at fault-initiation-angle of 90 degrees

For this case a fault-initiation-angle of 90 degrees has been chosen.This is at a zero crossing and will cause a minimum voltage jump leading to slow detection. Also the phase selection is slow around voltage-zero, as is clearly visible in figure 59 and 60.

A single-phase trip will be given when all but one selection function are above the threshold. According to figures 59 and 60 this is 460 μs after the arrival of the first wave front.

The maximum-selection-time will be defined as twice the time-span from the zero-crossing of the selection functions to the generation of the single-phase trip (comparable with the definition of maximum-detection-time in chapter 4.7.).

This maximum-selection-time is 770 μs for the R-N fault as seen from Diemen and 1050 μs as seen from Krimpen.

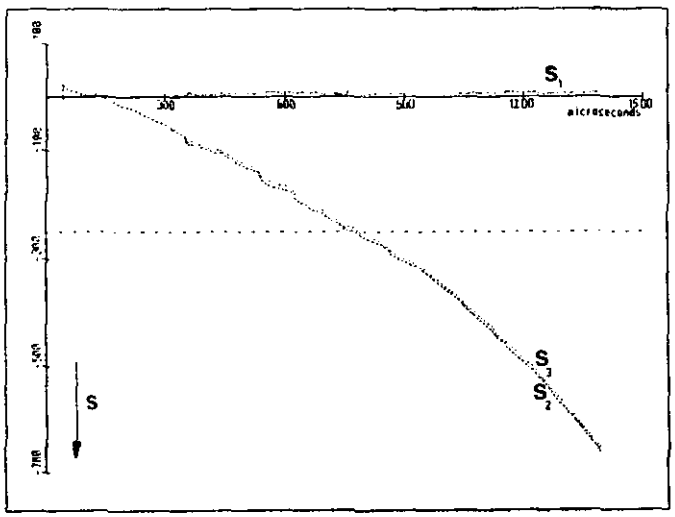

Figure 59 RN φ=90° Diemen to Krimpen 1

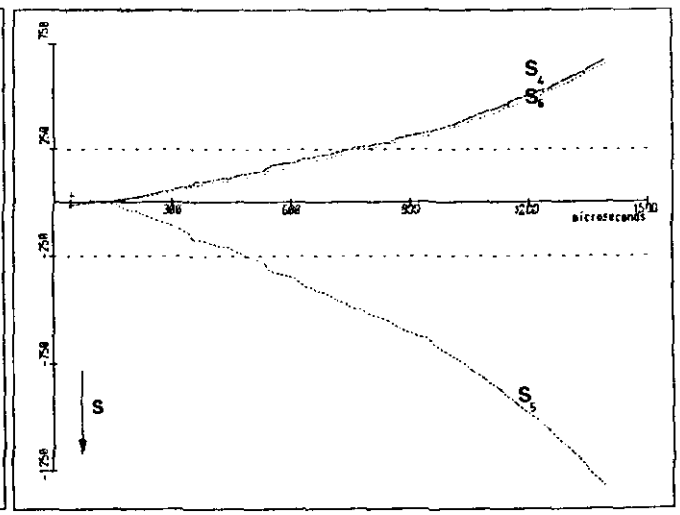

Figure 60 RN φ=90° Diemen to Krimpen 1

B.1.3. S-N fault-initiation-angle of 60 degrees

This case is a situation with maximum voltage jump. As shown in figure 61 and figure 62 all but one selection function rise above the threshold immediately. While S_2 remains below the threshold a single-phase trip for phase S can be given soon after the first travelling waves have arrived at the relay position. How soon depends on a delay time that may be needed. If the time-delay is longer than 300 μs problems might occur for S_2. After 300 μs it reaches a value of about 400 units. A low pass filter might remove the spikes that exceed the threshold. More about low pass filtering and time delay in chapter 4.9.

Figures 63 and 64 show the selection functions for the relay Krimpen to Diemen 1. Except for the spikes in S_2 there are no problems with phase selection. The first spike arrives less than 100 μs after the first travelling waves. This means the time-delay must be very short or a low pass filter is needed.

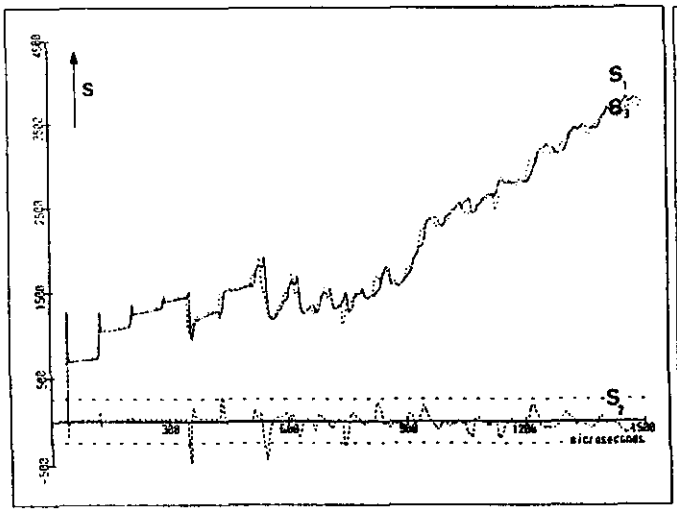

Figure 61 SN φ=60° Diemen to Krimpen 1

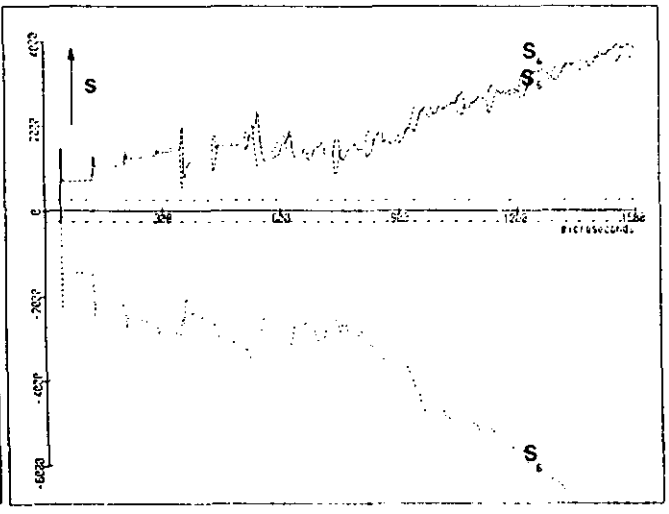

Figure 62 SN φ=60° Diemen to Krimpen 1

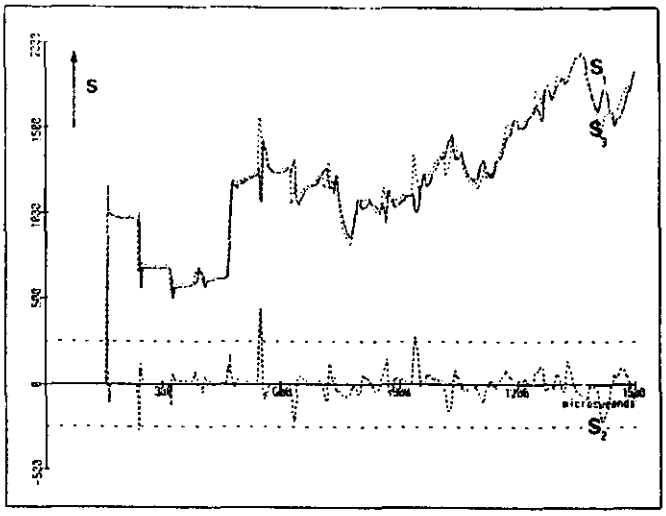

Figure 63 SN φ=60° Diemen to Krimpen 1

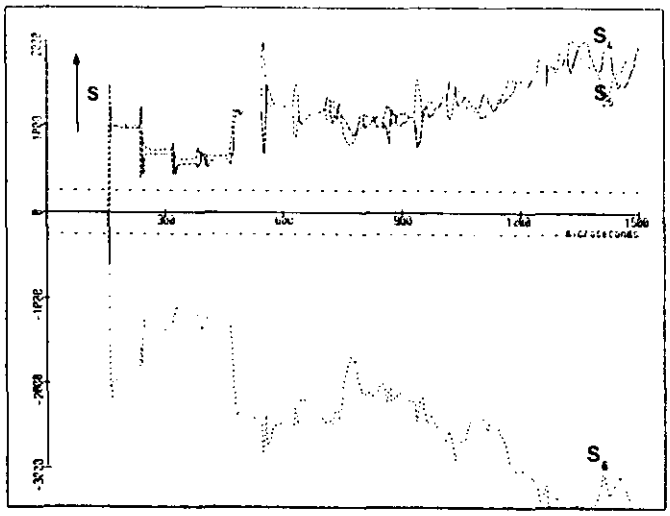

Figure 64 SN φ=60° Diemen to Krimpen 1

B.1.4. S-N fault at fault-initiation-angle of 150 degrees

This case is a single-phase-to-ground fault close to voltage-zero. The selection functions show a slow increase as shown in figure 65 and 66 for Diemen to Krimpen 1. After 425 μs all but one selection function have exceeded the threshold and the faulted phase has been selected.
Figures 67 and 68 give the situation for Krimpen to Diemen 1. The last-but-one threshold crossing takes place after 550 μs. The maximum selection time is 750 μs for Diemen to Krimpen 1 and 950 μs for Krimpen to Diemen 1.

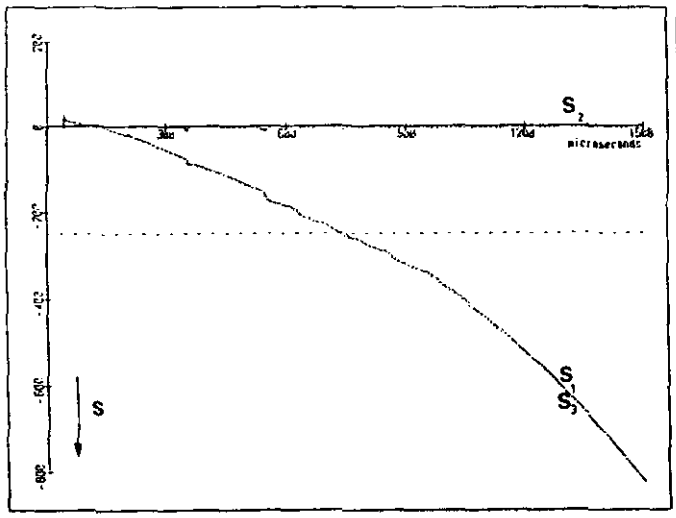

Figure 65: SN φ=150°, Diemen to Krimpen 1

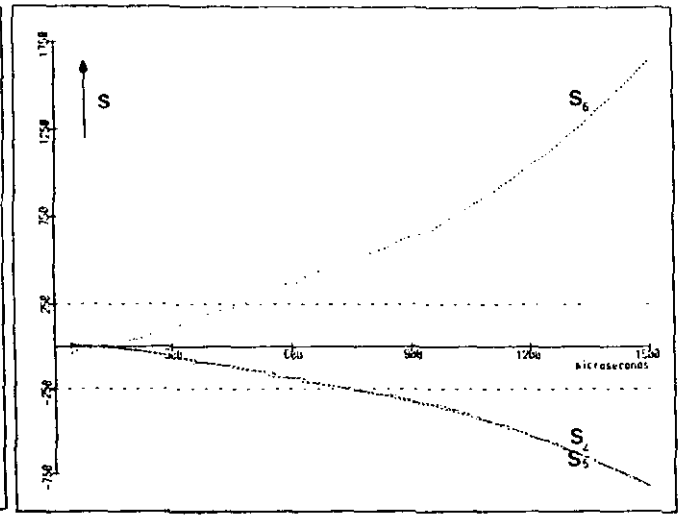

Figure 66 : idem

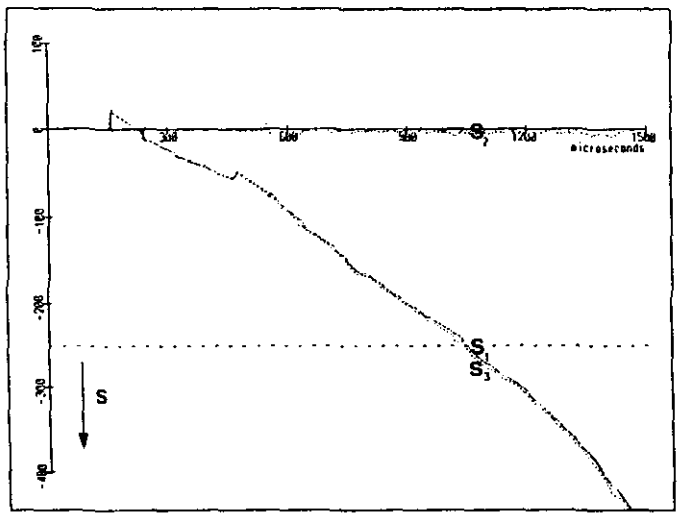

Figure 67: SN φ=150° Krimpen to Diemen 1

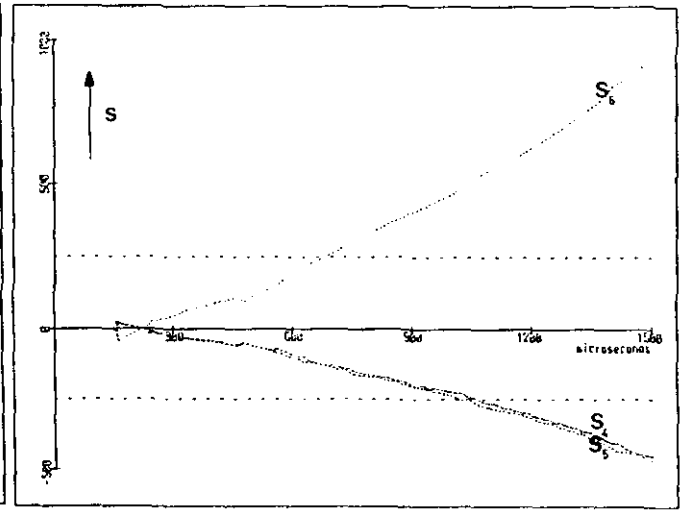

Figure 68: idem

B.1.5. T-N fault at fault-initiation-angle of 120 degrees

Figure 69 shows the single-phase selection functions for a T-N fault at voltage maximum. All selection functions are above the threshold (also S_4, S_5 and S_6, not reproduced here) so a single-phase trip will be generated for phase T.

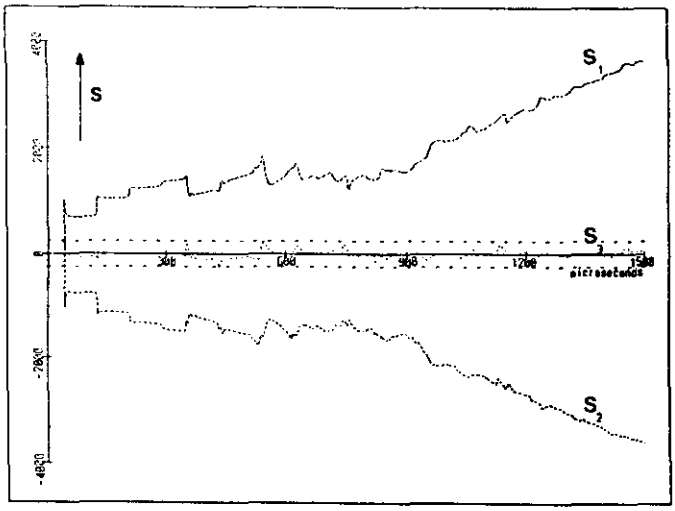

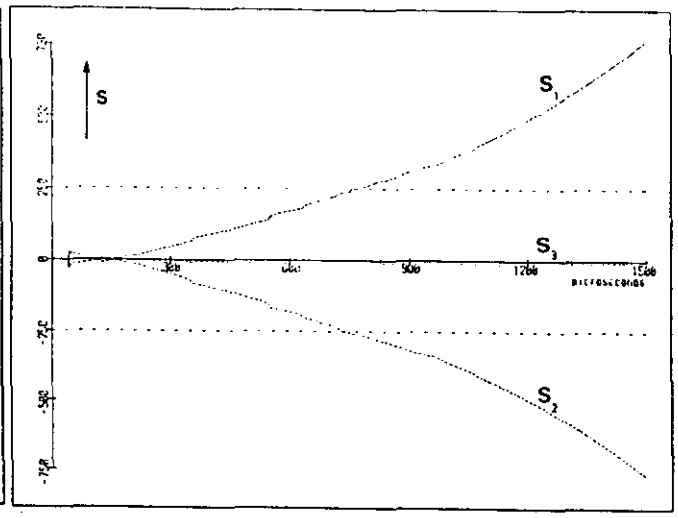

Figure 69: TN φ=120° Diemen to Krimpen 1 *Figure 70: idem φ=30°*

B.1.6. T-N fault at fault-initiation-angle of 30 degrees

This is the same case as the previous one but now near a voltage-zero. Figure 70 above shows the single-phase selection functions. S_3 remains low and all others have exceeded the threshold after 410 μs.
The maximum selection time is 720 μs for Diemen to Krimpen 1 and 1030 μs for Krimpen to Diemen 1.

B.2. Phase-to-phase faults

B.2.1. R-S fault at fault-initiation-angle of 30 degrees

This case describes a phase-to-phase fault with a maximum voltage jump. As shown in figure 71, S_5 and S_6 exceed the threshold immediately while S_4 remains below the threshold. Also S_1, S_2 and S_3 (not reproduced here) exceed the threshold. S_4 shows a lot of spikes exceeding the threshold for a short time. This will give problems if a delay time will be introduced as discussed in section 4.9.

B.2.2. R-S fault at fault-initiation-angle of 120 degrees

This again is a fault near voltage zero leading to relatively long selection times. Figure 72 shows the phase-to-phase selection functions of which S_4 remains below the threshold. The maximum selection time for an R-S fault is 1030 μs for Diemen to Krimpen 1 and 1550 μs for Krimpen to Diemen 1.

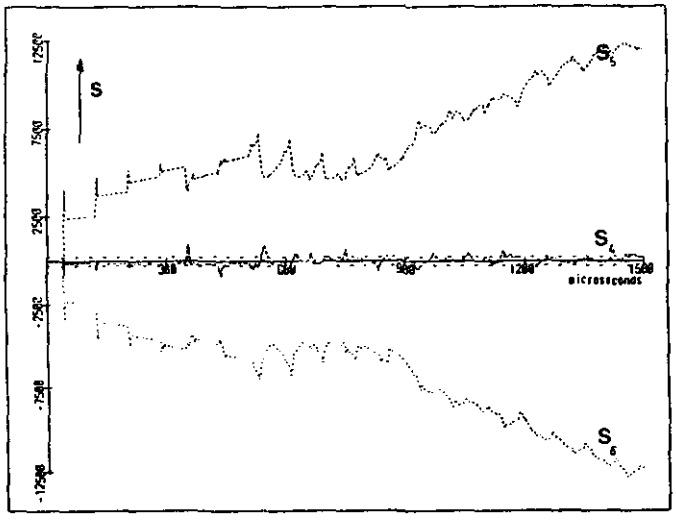

Figure 71: RS φ=30° Diemen to Krimpen 1

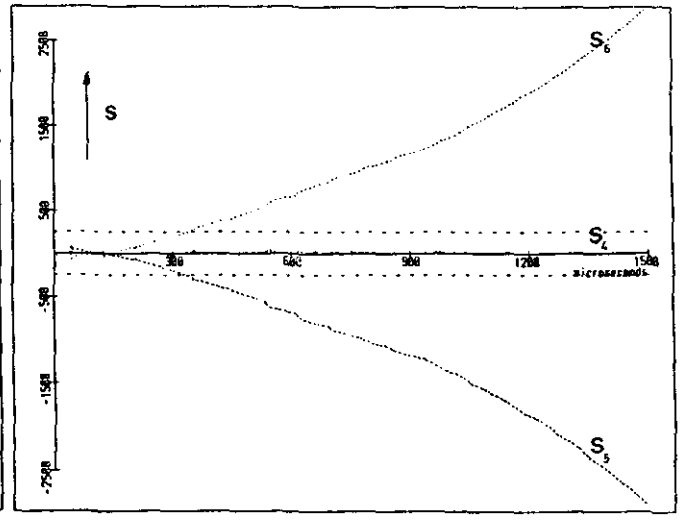

Figure 72: idem φ=120°

B.2.3. R-T fault at fault-initiation-angle of 150 degrees

Figure 73 shows the phase-to-phase selection functions for an R-T fault with maximum voltage jump for the relay Diemen to Krimpen 1. All selection functions, except for S_6, exceed the threshold instantaneously, so a correct phase selection can be made very soon. After a few hundreds of microseconds problems might arise because of large spikes in S_6.

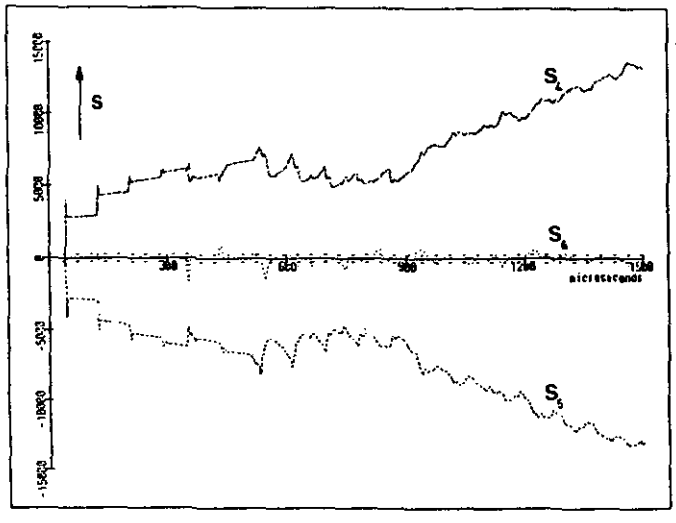

Figure 73: RT φ=150° Diemen to Krimpen 1

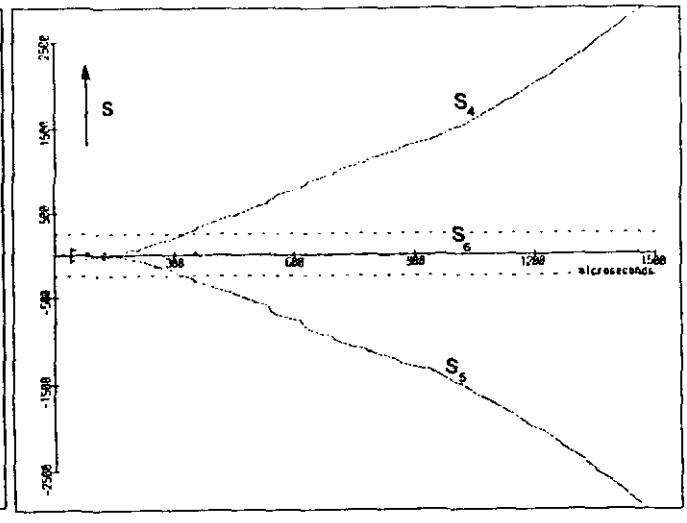

Figure 74: idem φ=60°.

B.2.4. R-T fault at fault-initiation-angle of 30 degrees

This is a case with zero voltage jump. Figure 74 above shows the selection functions for Diemen to Krimpen 1. The maximum selection time is 530 μs for Diemen to Krimpen 1 and 800 μs for Krimpen to Diemen 1.

B.2.5. S-T fault at fault-initiation-angle of 90 degrees

Figure 75 describes the selection functions for Diemen to Krimpen 1. S_4 and S_6 rise above the threshold. S_6 remains below, except for some spikes. The relay correctly detects an S-T fault.

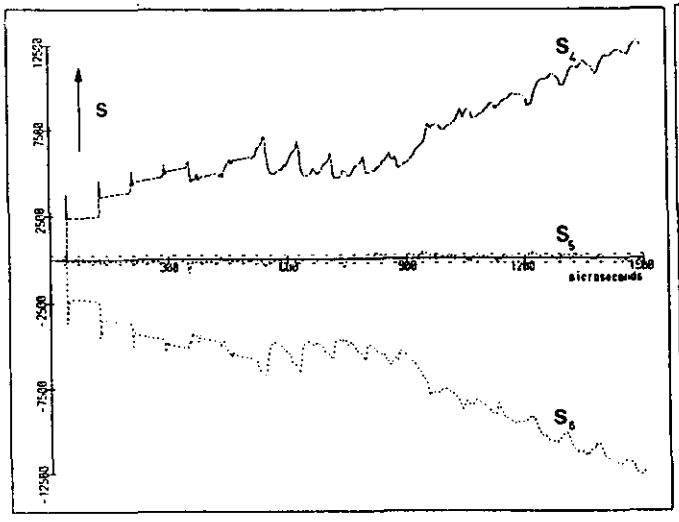

Figure 75: ST φ=90° Diemen to Krimpen 1

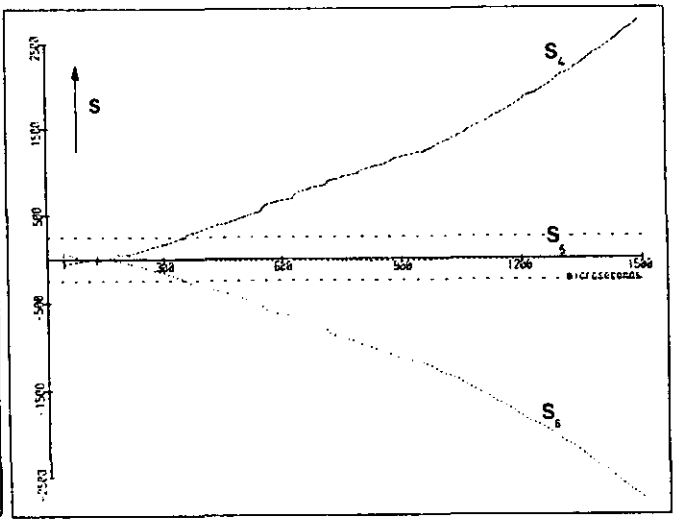

Figure 76: idem φ=0°.

B.2.6. S-T fault at initiation-angle of 0 degrees

Figure 76 shows the selection functions rising above the threshold. Only S_5 remains below the threshold. Also the single-phase selection functions S_1, S_2 and S_3 exceed the threshold after some time. The maximum selection time for the S-T fault is 640 μs for Diemen to Krimpen 1 and 880 μs for Krimpen to Diemen 1.

B.3. Two-phase-to-ground faults

During a two-phase-to-ground fault all the phase selection functions must exceed the threshold. In chapter 4.9 it was shown that this does not hold for some fault-initiation-angles. Two such cases will be discussed below.

B.3.1. R-T-N fault at fault-initiation-angle of 150 degrees

The selection functions for Diemen to Krimpen 1 are plotted in figure 77. The selection functions are almost the same as during an R-T fault at the same fault-initiation-angle (figure 73). To discriminate between these two cases, a low pass filtering will be needed. Even then it will take more than 1000 μs to make a decision. Such a long delay time will make the protection too slow (The delay would be needed for all frequent cases). In chapter 4.9 some possible solutions are discussed.

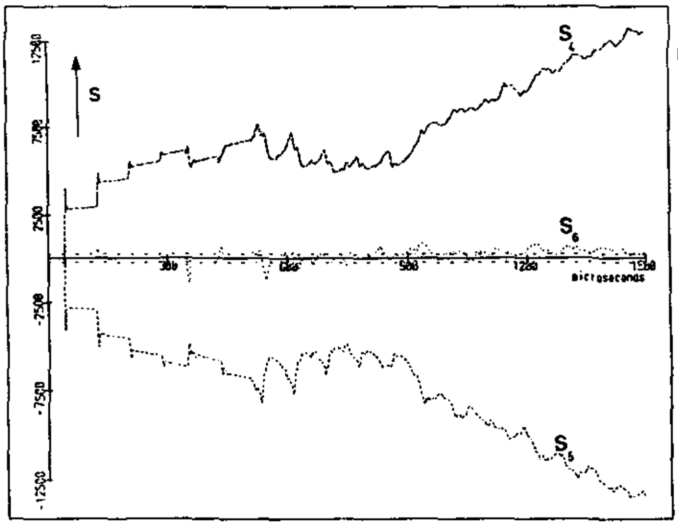

Figure 77: RTN φ=150°
Diemen to Krimpen 1

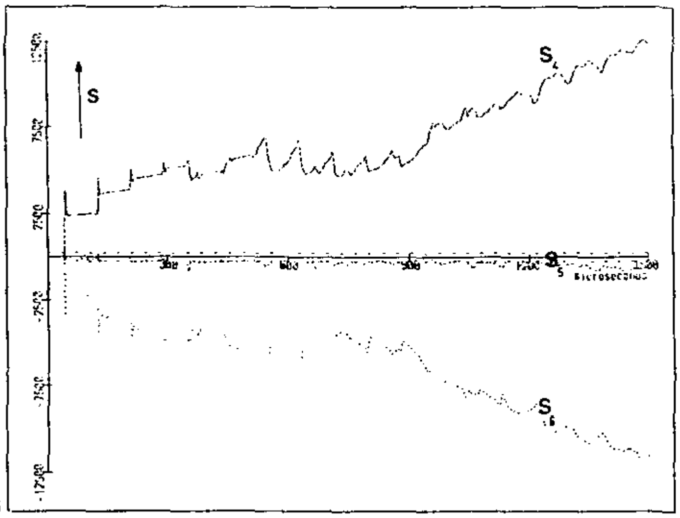

Figure 78: STN φ=96°
Diemen to Krimpen 1

B.3.2. S-T-N fault at fault-initiation-angle of 96 degrees

As shown in figure 78 (Diemen to Krimpen 1) S_6 is close to zero and a delayed phase selection will result.

Appendix C. TWONFIL-results.

By using the TWONFIL-package described in section 3.1., a large number of fault and non-fault situations have been studied. Table 8 gives the 64 fault types studied. These fault types have been studied for 12 fault-initiation-angles and different fault positions.

Table 8: Fault types studied by using TWONFIL.

Single-circuit faults:	
Single-phase-to-ground	: RN, SN, TN
Phase-to-phase	: RS, RT, ST
Two-phase-to-ground	: RSN, RTN, STN
Three-phase	: RST
Three-phase-to-ground	: RSTN
Inter-circuit faults:	
Phase-to-phase	: RV, RW, SW
Two-phase-to-ground	: RUN, RVN, RWN, SVN, SWN, TWN
Three-phase	: RSU, RSV, RSW, RTU, RTV, RTW, RVW, STV, STW
Three-phase-to-ground	: RSUN, RSVN, RSWN, RTUN, RTVN, RTWN, RVWN, STVN, STWN
Four-phase	: RSTU, RSTV, RSTW, RSUV, RSUW, RSVW, RTUW, RTVW, STVW
Four-phase-to-ground	: RSTUN, RSTVN, RSTWN, RSUVN, RSUWN, RSVWN, RTUWN, RTVWN, STVWN
Five-phase	: RSTUV, RSTVW, RSUVW
Five-phase-to-ground	: RSTUVN, RSTVWN, RTUVWN
Six-phase	: RSTUVW
Six-phase-to-ground	: RSTUVWN

C.1. Single-phase-to-ground faults.

Table 9 gives the results of the TWONFIL-calculations for the three single-phase-to-ground faults at voltage maximum. In all cases a value of 1000 units is equal to the amplitude of the stationary phase-to-ground voltage.

Table 9: Detection functions for single-phase-to-ground faults according to TWONFIL-calculations.

		relay 1			relay 2			relay 3		
		sit.1	sit.2	sit.3	sit.1	sit.2	sit.3	sit.1	sit.2	sit.3
R N ϕ= 0°	D_0^{Fw}	-3755	-1733	-6378	- 69	1954	- 122	- 72	- 38	- 122
	D_1^{Fw}	- 37	139	- 69	- 37	139	- 69	- 41	- 17	- 69
	D_2^{Fw}	-1428	-1422	-2425	- 12	- 5	- 21	- 13	7	- 21
	D_0^{Bw}	1859	1842	3006	-1827	-1844	-3250	-1915	111	-3250
	D_1^{BW}	- 1	3	- 69	- 1	3	- 69	- 41	138	- 69
	D_2^{Bw}	694	694	1181	- 722	- 722	-1223	- 721	- 714	-1223
S N ϕ= 60°	D_0^{Fw}	3697	2266	6519	- 16	-1448	- 29	- 17	- 40	- 29
	D_1^{Fw}	-1474	-1599	-2602	- 47	- 172	- 86	- 49	- 66	- 86
	D_2^{Fw}	21	17	38	21	17	38	21	7	38
	D_0^{Bw}	-1872	-1860	-3304	1842	1853	3245	1840	406	3245
	D_1^{Bw}	699	696	1172	- 728	- 731	-1344	- 762	- 889	-1344
	D_2^{Bw}	0	0	38	0	0	38	21	17	38
T N ϕ= 120°	D_0^{Fw}	-3671	-1733	-6680	- 12	1927	- 28	- 16	17	- 28
	D_1^{Fw}	-1442	-1273	-2627	- 36	133	- 71	- 39	- 16	- 71
	D_2^{Fw}	1384	1390	2515	- 22	- 16	- 41	- 22	- 3	- 41
	D_0^{Bw}	1845	1829	3297	-1815	-1831	-3354	-1846	93	-3354
	D_1^{Bw}	689	692	1206	- 718	- 714	-1349	- 743	- 552	-1349
	D_2^{Bw}	- 690	- 690	-1318	717	717	1237	681	664	1237

For situation 1, travel times are considered equal for all modes. The detection functions have been calculated for the instant of arrival of the first wavefront coming from the fault. In the TWONFIL-model all losses and frequency dependences are neglected. Due to this the detection functions jump to their new value immediately at the moment the waves arrive.

For situation 2 a distinction is made between the ground wave having a low velocity and the aerial waves, having a high velocity. The detection functions have been calculated for the moment the aerial mode waves arrive at the relay position.

Situation 3 is a very close fault. It is considered here that the voltage at the relay position drops to zero immediately.

Relay 1 is situated in the faulted circuit and must detect a forward fault. Relay 2 is situated in the parallel circuit. Relay 3 is situated in a backward line. Figure 79 summarises relay and fault position.

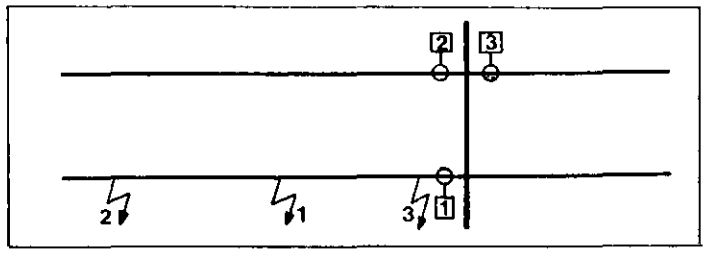

Figure 79: Relay and fault positions used for TWONFIL-study

Figure 80 relates the three situations of figure 86 to the EMTP results of appendix A and B.

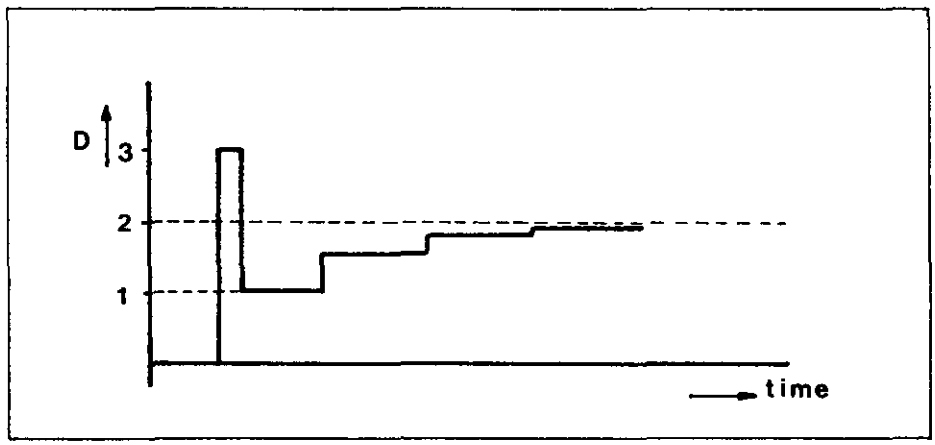

Figure 80: Relation between situations studied in TWONFIL-study and EMTP-results.

Situation 1 shows an almost perfect resemblance between EMTP and TWONFIL. Situations 2 and 3 show some deviation. Situation 2 due to damping (TWONFIL-spikes are higher than EMTP-spikes) and situation 3 because the assumption made within TWONFIL (equal voltages at relay and fault location) is not met during the EMTP-calculation. Still the TWONFIL-results can be used for a first-round testing.
From table 9 it can be concluded that relay 1 always detects a forward fault and relay 3 a backward fault. Apart from the spikes in D_o^{Fw}, relay 2 also detects a backward fault.

C.2. Phase-to-phase faults.

Table 10 shows the detection functions calculated by using TWONFIL for the three single-circuit phase-to-phase faults at maximum voltage jump. Relay positions and situations are as in figure 79.

Table 10 : Detection functions for phase-to-phase faults according to TWONFIL-calculations

		relay 1			relay 2			relay 3		
		sit.1	sit.2	sit.3	sit.1	sit.2	sit.3	sit.1	sit.2	sit.3
R S Ø= 30°	D_0^{Fw}	- 96	584	- 194	- 96	584	- 194	- 100	- 89	- 194
	D_1^{Fw}	-1696	-1637	-3306	- 95	- 36	- 196	- 101	- 93	- 196
	D_2^{Fw}	-1590	-1588	-3092	11	13	19	10	16	19
	D_0^{Bw}	1	- 5	- 194	1	- 5	- 194	- 100	581	- 194
	D_1^{Bw}	783	784	1359	- 818	- 817	-1751	- 901	- 841	-1751
	D_2^{Bw}	785	785	1574	- 816	- 816	-1536	- 791	- 788	-1536
R T Ø=150°	D_0^{Fw}	72	- 16	140	72	- 16	140	71	70	140
	D_0^{Fw}	-1787	-1794	-3510	2	- 6	3	2	1	3
	D_2^{Fw}	3563	3563	7002	- 14	- 14	- 25	- 13	- 13	- 25
	D_0^{Bw}	- 1	0	140	- 1	0	140	71	- 900	140
	D_1^{Bw}	877	876	1760	- 912	- 912	-1754	- 893	1775	-1754
	D_2^{Bw}	1753	-1754	-3538	1823	1823	3489	1776	70	3489
S T Ø= 90°	D_0^{Fw}	- 31	559	- 70	- 31	559	- 70	- 36	- 26	- 70
	D_1^{Fw}	-3238	-3186	-6354	- 92	- 40	- 191	- 98	- 91	- 191
	D_2^{Fw}	1571	1573	3079	- 1	1	- 3	- 1	4	- 3
	D_0^{Bw}	0	- 5	- 70	0	- 5	- 70	- 36	555	- 70
	D_1^{Bw}	1540	1541	2890	-1606	-1605	-3273	-1671	-1618	-3273
	D_2^{Bw}	- 771	- 771	-1543	802	802	1538	785	787	1538

It can be seen that D_0^{Fw} for relay 2 still shows spikes, although not as high as with the single-phase-to-ground faults. Also visible are the relatively high values of D_0^{Fw} and D_1^{Fw} for relay 2 and 3, after a few reflections (compare figures 40 and 42).

C.3. Two-phase-to-ground faults.

A two-phase-to-ground fault is a more complex fault than a single-phase-to-ground or phase-to-phase fault. The superimposed quantities cannot be explained by the introduction of one source at the fault position.

For a two-phase-to-ground fault two sources are needed. Because the sources have different phase angles, there is no situation with zero detection functions. The forward detection functions calculated by using the TWONFIL-model are given in table 11 for some two-phase-to-ground faults. Relay positions and situations are the same as with table 9.

Table 11 : Detection functions for two-phase-to-ground faults according to TWONFIL-calculations.

		relay 1			relay 2			relay 3		
		sit.1	sit.2	sit.3	sit.1	sit.2	sit.3	sit.1	sit.2	sit.3
RSN ϕ=45°	D_0^{Fw}	715	997	1355	- 87	195	- 177	- 91	- 86	- 177
	D_1^{Fw}	-1794	-1769	-3500	- 93	- 68	- 191	- 98	- 95	- 191
	D_2^{Fw}	-1379	-1378	-2695	14	15	26	13	16	26
RSN ϕ=120°	D_0^{Fw}	3027	1624	4902	21	-1381	35	22	- 1	35
	D_1^{Fw}	- 584	- 706	- 973	- 4	- 126	- 7	- 3	20	- 7
	D_2^{Fw}	588	584	926	14	9	23	14	0	23
RTN ϕ=150°	D_0^{Fw}	98	- 4	- 269	73	- 30	135	71	70	135
	D_1^{Fw}	-1782	-1790	-3596	2	- 7	- 1	2	1	1
	D_1^{Fw}	3563	3563	7008	- 14	- 14	- 27	- 12	- 13	27
RTN ϕ=60°	D_0^{Fw}	-2821	-1316	-4699	- 31	1474	- 53	- 33	- 8	- 53
	D_1^{Fw}	- 561	- 430	- 988	- 28	103	- 51	- 30	- 13	- 51
	D_2^{Fw}	- 19	- 14	67	- 13	- 8	- 22	- 13	2	- 22
STN ϕ=90°	D_0^{Fw}	18	586	- 167	- 31	537	- 70	- 36	- 26	- 70
	D_1^{Fw}	-3238	-3188	-6355	- 92	- 42	- 191	- 98	- 91	- 191
	D_2^{Fw}	1562	1564	3097	- 1	1	- 3	- 1	4	- 3
STN ϕ=180°	D_0^{Fw}	-3020	-1639	-5127	2	1383	0	0	23	0
	D_1^{Fw}	15	136	- 16	5	125	5	4	20	5
	D_2^{Fw}	557	562	963	- 18	- 13	- 30	- 18	- 4	- 30

Again spikes are visible in D_0^{Fw} for relay 2. Notice also the relatively high values of the forward detection functions for relay 2 and relay 3 and situation 3.

C.4. Phase-to-phase inter-circuit faults.

Table 12 gives the detection functions for three phase-to-phase inter-circuit faults. Relay positions and situations are again as in figure 79.

Table 12 : Detection functions for phase-to-phase inter-circuit faults according to TWONFIL-calculations.

		relay 1			relay 2			relay 3		
		sit.1	sit.2	sit.3	sit.1	sit.2	sit.3	sit.1	sit.2	sit.3
R V Ø = 30°	D_0^{Fw}	-3785	-3181	-8289	3614	4218	7901	- 89	- 79	- 194
	D_1^{Fw}	- 84	- 32	- 196	-1506	-1453	-3306	- 89	- 82	- 196
	D_2^{Fw}	-1412	-1420	-3092	10	12	19	9	15	19
	D_0^{Bw}	3700	3695	7901	-3699	-3703	-8289	- 89	516	
	D_1^{Bw}	- 726	- 725	-1751	695	696	1359	- 800	- 747	
	D_2^{Bw}	697	697	1574	- 724	- 724	-1536	- 702	- 700	
R W Ø = 150°	D_0^{Fw}	3700	3631	9283	-3587	-3656	-9004	56	54	140
	D_1^{Fw}	1	- 5	- 3	-1399	-1405	-3510	1	0	3
	D_2^{Fw}	1389	1389	3489	1389	1389	3489	- 10	- 10	- 25
	D_0^{Bw}	-3644	-3644	-9004	3643	3644	9283	56	- 14	
	D_1^{Bw}	- 714	- 714	-1754	686	686	1760	- 699	- 705	
	D_2^{Bw}	27	27	- 25	27	- 27	- 25	1390	1390	
S W Ø = 30°	D_0^{Fw}	3524	4036	7949	-3578	-3066	-8089	- 31	- 23	70
	D_1^{Fw}	-1444	-1400	-3273	-1444	-1400	-3273	- 85	- 79	- 191
	D_2^{Fw}	- 1	0	- 3	1363	1365	3079	- 1	4	- 3
	D_0^{Bw}	-3551	-3555	-8089	3551	3547	7949	- 31	482	
	D_1^{Bw}	- 28	- 27	- 191	- 28	- 27	- 191	-1449	-1404	
	D_2^{Bw}	696	696	1538	- 669	- 669	-1543	681	683	

Relay 1 and relay 2 both detect a forward fault, relay 3 detects a backward fault, supposed the threshold value is sufficiently high (above 196 units in this case).

Appendix D: EMTP input files

The tower configuration used for the lines Diemen-Ens, Diemen-Krimpen and Krimpen-Geertruidenberg is given in the file listed below. This is the input file for the JMARTI SETUP for the 45.7 km line between Krimpen and the fault position.

```
BEGIN NEW DATA CASE
JMARTI SETUP
C ANCH  BUS1B-BUS1E-BUS2B-BUS2E-BUS3B-BUS3E-BUS4B-BUS4E-BUS5B-BUS5E-BUS6B-BUS6E-
BRANCH  KIJ-1 FLT-1 KIJ-2 FLT-2 KIJ-3 FLT-3 KIJ-4 FLT-4 KIJ-5 FLT-5 KIJ-6 FLT-6
LINE CONSTANTS
METRIC
C -SKIN-RESIS---T-REACT---DIAM----HORIZ---VTOWER--VMID----SEPAR---ALPHA-NAME--B-
  3.3575  .06650 4        2.785000-15.7   28.      12.      40.      -90.  LIBU   3
  2.3575  .06650 4        2.785000-12.2   39.7     23.7     40.      -90.  LIBO   3
  1.3575  .06650 4        2.785000 -8.7   28.      12.      40.      -90.  LIBI   3
  4.3575  .06650 4        2.785000  8.7   28.      12.      40.      -90.  REBI   3
  5.3575  .06650 4        2.785000 12.2   39.7     23.7     40.      -90.  REBO   3
  6.3575  .06650 4        2.785000 15.7   28.      12.      40.      -90.  REBU   3
  0.3128  .11334 4        2.175    16.2   44.3     31.3                    ARRE
  0.3128  .11334 4        2.175   -16.2   44.3     31.3                    ARLI
BLANK
C +RHO--FREQ------FCAR------ iesces zesies cDIST---- yszssmD--PN-PU-M-T-
  100.0 5000.      0.00000001                1 45.70                    6-2
  100.0   50.0              1                1 45.70                    6
  100.0   0.01              1                  45.70           9 10     6
BLANK
BLANK
C        IDEBUG--IPUNCH--KOUTPR--GMODE---
               2       0       2       0
C +NEXM-EPSTOL--NORMAX--IECODE--IFWTA---IFPLOT--IFDAT---INELIM--
          1.00        30       0       1       1       0       0
C +NEXM-EPSTOL--NORMAX--IECODE--IFWTA---IFPLOT--IFDAT---INELIM--AMINA1--
          1.00        30       0       1       1       0       0     .05
BLANK
```

The transmission line Krimpen - Maasvlakte shows a different tower configuration. The corresponding input file for the JMARTI SETUP is given below.

```
BEGIN NEW DATA CASE
JMARTI SETUP
C ANCH  BUS1B-BUS1E-BUS2B-BUS2E-BUS3B-BUS3E-BUS4B-BUS4E-BUS5B-BUS5E-BUS6B-BUS6E-
BRANCH  KIJ-1 MVL-1 KIJ-2 MVL-2 KIJ-3 MVL-3 KIJ-4 MVL-4 KIJ-5 MVL-5 KIJ-6 MVL-6
LINE CONSTANTS
METRIC
C -SKIN-RESIS---T-REACT---DIAM----HORIZ---VTOWER--VMID----SEPAR---ALPHA-NAME--B-
  3.3578   .04693 4        2.290000    .750 29.      13.      40.       45.  LIBU   4
  2.3578   .04693 4        2.290000   4.000 40.5     24.5     40.       45.  LIBO   4
  1.3578   .04693 4        2.290000   7.250 29.      13.      40.       45.  LIBI   4
  4.3578   .04693 4        2.290000  25.750 29.      13.      40.       45.  REBI   4
  5.3578   .04693 4        2.290000  29.000 40.5     24.5     40.       45.  REBO   4
  6.3578   .04693 4        2.290000  32.250 29.      13.      40.       45.  REBU   4
  0.3328   .11334 4        2.175       .000 46.5     33.5                    ARRE
  0.3328   .11334 4        2.175     33.000 46.5     33.5                    ARLI
BLANK
C +RHO--FREQ------FCAR------ iesces zesies cDIST---- yszssmD--PN-PU-M-T-
  100.0 5000.     0.00000001               1 81.20                    6-2
  100.0   50.0             1               1 81.20                    6
  100.0   0.01             1                 81.20           9 10     6
BLANK
BLANK
C        IDEBUG--IPUNCH--KOUTPR--GMODE---
               2       0       2       0
C +NEXM-EPSTOL--NORMAX--IECODE--IFWTA---IFPLOT--IFDAT---INELIM--
          1.00        30       0       1       1       0       0
C +NEXM-EPSTOL--NORMAX--IECODE--IFWTA---IFPLOT--IFDAT---INELIM--AMINA1--
          1.00        30       0       1       1       0       0      .05
BLANK
```

The transmission line between Geertruidenberg and Eindhoven consists of three circuits (nine bundled conductors). It has been modelled as a three-phase line. The input file for the JMARTI SETUP is given below.

```
BEGIN NEW DATA CASE
JMARTI SETUP
BRANCH  GTB-1 EHV-1 GTB-2 EHV-2 GTB-3 EHV-3
LINE CONSTANTS
METRIC
C I SKIN     RES X   REACT     DIAM   HORIZ  VTOWER    VMID    SEPAR PHASENAME
  1.3575  .06550 4          2.78500   4.000  49.900  33.90040.00000-90.00LIBO    3
  2.3575  .06550 4          2.78500    .500  38.800  22.80040.00000-90.00LIMI    3
  3.3575  .06550 4          2.78500   4.000  27.700  11.70040.00000-90.00LIBE    3
  1.3575  .06550 4          2.78500  18.700  50.850  34.85040.00000-90.00MIBO    3
  2.3575  .06550 4          2.78500  18.700  39.550  23.55040.00000-90.00MIMI    3
  3.3575  .06550 4          2.78500  18.700  28.250  12.25040.00000-90.00MIBE    3
  1.3575  .06550 4          2.78500  33.400  49.900  33.90040.00000-90.00REBO    3
  2.3575  .06550 4          2.78500  36.900  38.800  22.80040.00000-90.00REMI    3
  3.3575  .06550 4          2.78500  33.400  27.700  11.70040.00000-90.00REBE    3
  0.3128  .11334 4          2.17500    .000  57.600  44.600                ARLI
  0.3128  .11334 4          2.17500  37.400  57.600  44.600                ARRE
BLANK CARD TERMINATING CONDUCTOR CARDS
C    RHO       FREQ       FCAR *ICPR* *IZPR* *    DIST PIPR++DECPNTPUN N
  100.0    5000.00          1                 1 64.24                    0-2
  100.0      50.00          1                 1 64.24                    0
  100.0       0.10          1                   64.24          10  5     0
BLANK CARD TERMINATING FREQUENCY CARDS
BLANK CARD TERMINATING LINE CONSTANTS
C          IDEBUG  IPUNCH  KOUTPR   GMODE
               2       0       2       0
C NEXMIS  EPSTOL  NORMAX  IECODE   IFWTA  IFPLOT   IFDAT  INELIM
            5.00      30       0       1       1       0       0
C NEXMIS  EPSTOL  NORMAX  IECODE   IFWTA  IFPLOT   IFDAT  INELIM  AMINA1
            8.00      25       0       1       1       0       0    .05
BLANK CARD TERMINATING JMARTI SETUP
BEGIN NEW DATA CASE
BLANK CARD TERMINATING EMTP RUN
```

As an example the EMTP source file for one of the cases is reproduced below. The case shown is an R-S fault at a fault-initiation-angle of 30 degrees. The fault is situated at 12 km from the station Diemen.

```
BEGIN NEW DATA CASE
C
C Fault on the line Krimpen Diemen
C Distance between Krimpen and fault place : 45.7 km
C R-S fault at a a fault-initiation-angle of 30 degrees
C Output for the stations DIEMEN,  KRIMPEN,  ENS, GEERTRUIDENBERG
C and  MAASVLAKTE
C A total of 15 voltages and 30 currents
C MATH BOLLEN / GERARD JACOBS,  FEBRUARY 29, 1988   Version 2.8
C
C ************************************************************************
C
C WER FREQUENCY                    STATFR--
POWER FREQUENCY                      50.00
C +DELT-TMAX----XOPT----COPT----EPSILN--TOLMAT--TSTART--
   1.E-6 300.E-6
C +IOUT-IPLOT---IDOUBL--KSSOUT--MAXOUT--IPUN----MEMSAV--ICAT----NENERG--IPRSUP--
       1     1000
C TRANSFORMER AT ENS
C TRANSFORMER BUS3--       IST---PSIST-BUST--RMAG--                              0
  TRANSFORMER                    1.73   TENS-1
C +CUR----------FLUX-----------
          9999
C BUS1--BUS2--             RK----LK----VOLT--                                    0
 1ENS-R1                    0.1    22. 380.
 2BENS-1                    0.62  -1.4220.
 3DENS-1                    0.5    33.9 85.
  TRANSFORMER TENS-1                    TENS-2
 1ENS-R2
 2BENS-2
 3DENS-2DENS-1
  TRANSFORMER TENS-1                    TENS-3
 1ENS-R3
 2BENS-3
 3      DENS-2
C BUS1--BUS2--BUS3--BUS4--R-----L----------R-----L----------R-----L----------
C INFEED ENS
51BRON-4BENS-1              5.49        54.9
52BRON-5BENS-2              3.56        35.65
53BRON-6BENS-3
C INFEED DIEMEN
51BRON-1DIM-R1             100.          194.
52BRON-2DIM-R2             100.           92.5
53BRON-3DIM-R3
C INFEED KRIMPEN
51BRON-1KIJ-R1             100.          194.
52BRON-2KIJ-R2             100.           92.5
53BRON-3KIJ-R3
C INFEED GEERTRUIDENBERG
51BRON-1GTB-R1             100.           81.
52BRON-2GTB-R2             100.           92.5
53BRON-3GTB-R3
C INFEED MAASVLAKTE
51BRON-1MVL-R1               2.1          68.
52BRON-2MVL-R2               8.1         257.
53BRON-3MVL-R3
```

```
C INFEED EINDHOVEN
51BRON-1EHV-R1                67.          130.
52BRON-2EHV-R2                67.           61.
53BRON-3EHV-R3
C TRANSMISSIONLINE DIEMEN-ENS
-1DIM-11ENS-1                  2.                    -2 6
      11      0.54488725738666300000E+03
 -0.66550112317763710OE+03  0.11310644724440860OE+05  0.30498126976339880OE+05
  0.68300901073626210OE+06  0.52696612183308850OE+07  0.15048409266969450OE+08
  0.22996150397032160OE+08  0.14733841944808480OE+08  0.22956298311596640OE+08
  0.32889484125591760OE+08  0.73117682293571170OE+08
  0.25775900806863820OE+01  0.31317920897603720OE+02  0.49278982281455180OE+03
  0.11632843262573320OE+05  0.98731240220843830OE+05  0.60603484649316990OE+06
  0.19332393216187440OE+07  0.49390539353262160OE+07  0.78225414668145190OE+07
  0.11351093192865390OE+08  0.25173583376436810OE+08
      12      0.26000446311681450000E-03
  0.14034629114847550OE+00  0.45640907505540220OE+01  0.54833133619565130OE+01
  0.65794581408572040OE+01  0.45044244388043480OE+02  0.53860572259034400OE+03
  0.37695346411184390OE+03  0.37403967327036220OE+04  0.23545907688454140OE+05
  0.18666035619359870OE+07  0.18114381548713840OE+09 -0.18303868272413620OE+09
  0.28505706221252480OE+02  0.85199526920169740OE+03  0.11776931845553270OE+04
  0.11273619709713690OE+04  0.20974464064963380OE+04  0.79720905918741770OE+04
  0.15621158415215170OE+05  0.12836406848978050OE+05  0.35937918746168240OE+05
  0.91902825042361510OE+05  0.83950989354809240OE+05  0.84034940344163990OE+05
-2DIM-12ENS-2                  2.                    -2 6
      11      0.37916763180759080000E+03
  0.15059728868446240OE+04  0.47796587861261890OE+03  0.29453883984532780OE+03
  0.29623954424538490OE+03  0.11304414738999120OE+03  0.27754408993046330OE+04
  0.97735332522282380OE+05  0.61470612598721450OE+06  0.16187756739931740OE+07
  0.45772273518762680OE+07  0.25988309474639030OE+08
  0.40460047231220400OE+01  0.79284505701286570OE+01  0.12685020221332040OE+02
  0.21443018222587600OE+02  0.31615556663595650OE+02  0.11149028101688900OE+04
  0.39243178794292150OE+05  0.24689868337585600OE+06  0.65682187727970680OE+06
  0.18730685184755070OE+07  0.10712249957294590OE+08
       7      0.24594959509923860000E-03
  0.24894288402682040OE+05  0.75659851362892320OE+05  0.93626537296881400OE+06
  0.18484658993995090OE+09 -0.18291810002689030OE+09  0.22257343257452700OE+09
 -0.22553874200032560OE+09
  0.88987807363111610OE+05  0.21336540895587340OE+06  0.46420491656320450OE+06
  0.10068430275445350OE+07  0.10078498705720790OE+07  0.73066647539724220OE+06
  0.73139714187263900OE+06
-3DIM-13ENS-3                  2.                    -2 6
      11      0.25924782813320220000E+03
  0.90930226835431860OE+03  0.59404392935138950OE+03  0.80487694470604690OE+03
  0.36639304171074360OE+03  0.47726200965851480OE+03  0.16034798841060160OE+03
  0.23324202927775600OE+03  0.43261876659053970OE+03  0.55438281224075470OE+04
  0.13772263405717560OE+05  0.42972645060404900OE+06
  0.26451805482907770OE+01  0.47238429853371590OE+01  0.93813344907331400OE+01
  0.16164402798665800OE+02  0.29663971358326280OE+02  0.35886936002396950OE+02
  0.63392370726982160OE+02  0.37186661151617830OE+03  0.46025460747833910OE+04
  0.11550192342841870OE+05  0.36120928280562740OE+06
      14      0.24286694181224860000E-03
  0.47314796475279870OE+01  0.82691580539328340OE+02  0.52376200527537960OE+02
  0.66901012808931010OE+02  0.46682799925511970OE+04  0.48431488804387630OE+04
  0.33463761484989130OE+05 -0.11349371208088410OE+07  0.20694204969589160OE+07
  0.20020293310146700OE+07  0.70997579025662160OE+09 -0.70414751191216770OE+09
  0.55325548874634930OE+10 -0.55413628604057440OE+10
  0.85613194103721500OE+03  0.13364871508804530OE+05  0.93401893860298010OE+04
  0.13935157229548800OE+05  0.20156731530702810OE+06  0.10414122298592150OE+06
  0.38161315770152350OE+06  0.23010645586521420OE+07  0.20895137534598190OE+07
  0.60572034691422170OE+07  0.50616539704387390OE+08  0.50667156244091730OE+08
  0.23703258917257470OE+08  0.23726962176174720OE+08
```

```
-4DIM-14ENS-4                    2.                    -2 6
      11      0.26416919383049050000E+03
  0.12583633117932330 0E+04  0.15939888588671340 0E+03  0.96627421525444030 0E+03
  0.23078128264040890 0E+03  0.79339564300732900 0E+02  0.18256356770788760 0E+03
  0.18037288933181170 0E+03  0.87254889182506530 0E+02  0.17101610924280580 0E+03
  0.33827382925512040 0E+04  0.51620183379697450 0E+05
  0.29467439034249710 0E+01  0.41825884254387530 0E+01  0.92883083845980660 0E+01
  0.14061000891306340 0E+02  0.17686807859687030 0E+02  0.29941143083793990 0E+02
  0.49342366337047420 0E+02  0.85860237554391050 0E+02  0.15815128122608050 0E+03
  0.28688642788500050 0E+04  0.44065596313212020 0E+05
      10      0.24534323660721550000E-03
  0.42770651421329630 0E+01  0.10386844081947710 0E+03  0.64238224867139210 0E+02
  0.10279591236992400 0E+03  0.37057045694261940 0E+04  0.66078183778761830 0E+04
  0.19545537925648050 0E+06  0.24316280488836750 0E+06  0.22894893897808520 0E+07
  0.19288801629661340 0E+08
  0.96080197577277090 0E+03  0.24619294610304080 0E+05  0.14228265074181150 0E+05
  0.22310672458859340 0E+05  0.23846268863869680 0E+06  0.17778357826716880 0E+06
  0.33748724268895090 0E+07  0.16861657651925320 0E+07  0.98699281586130930 0E+07
  0.39080989963226590 0E+08
-5DIM-15ENS-5                    2.                    -2 6
      11      0.24772378961513770000E+03
  0.10075823059527990 0E+04  0.48679479379932850 0E+03  0.94687503869214020 0E+03
  0.17628617924272130 0E+03  0.82613321369675130 0E+02  0.18453027666968300 0E+03
  0.17158674040519680 0E+03  0.82559563638247540 0E+02  0.14168339152404340 0E+03
  0.25990126613582270 0E+04  0.41552411127664760 0E+05
  0.26757531603127300 0E+01  0.45012559168304640 0E+01  0.93970763581254210 0E+01
  0.14042232027018350 0E+02  0.18051881019340820 0E+02  0.30693437855276520 0E+02
  0.49039722851442210 0E+02  0.80194482582362740 0E+02  0.13974451776192560 0E+03
  0.22195266003693490 0E+04  0.35534153161753300 0E+05
      10      0.24043774504465650000E-03
  0.14632047265820260 0E+02  0.23789558012221150 0E+03  0.63816448036021980 0E+03
  0.18861708918864560 0E+03  0.73499194915942900 0E+04  0.40742002392977090 0E+05
  0.16283266183281900 0E+06  0.91410662651071530 0E+06  0.50862261762309400 0E+07
  0.58373284866340940 0E+07
  0.21854196197633560 0E+04  0.36278716977401510 0E+05  0.95132595366268000 0E+05
  0.27403308315994660 0E+05  0.26786605217373920 0E+06  0.74271864634981120 0E+06
  0.45663719572179060 0E+07  0.33360428456764000 0E+07  0.13573789936330380 0E+08
  0.28524147158989080 0E+08
-6DIM-16ENS-6                    2.                    -2 6
      13      0.27355815795272550000E+03
  0.10117349819996390 0E+04  0.37077791419969950 0E+03  0.82477414445609720 0E+03
  0.79971352517286290 0E+03  0.39447563654705640 0E+03  0.36452676575181120 0E+03
  0.15306900843940720 0E+03  0.19216399934408050 0E+03  0.20971842689207260 0E+04
  0.50216396076548580 0E+04  0.12622662386591740 0E+05  0.49961885862445250 0E+05
  0.76901738439365700 0E+06
  0.28070151766059690 0E+01  0.43883131111709220 0E+01  0.95222636628149570 0E+01
  0.21523540142803920 0E+02  0.31668058729822160 0E+02  0.50848471302225990 0E+02
  0.78230710441632970 0E+02  0.17146726857710800 0E+03  0.17157183946363520 0E+04
  0.40692424406561540 0E+04  0.10279078021783240 0E+05  0.40754485636065200 0E+05
  0.63071348234717280 0E+06
      12      0.24885121183501520000E-03
  0.31442858797406590 0E+02  0.25354685227610930 0E+01  0.45090704685532710 0E+02
  0.27257090382506870 0E+03 -0.21263353633919130 0E+04  0.53152479950064230 0E+04
  0.47205117657343130 0E+05  0.69010742920907840 0E+05  0.54730993913125680 0E+06
  0.14387492921979150 0E+07  0.24095577380643440 0E+10 -0.24116635537088270 0E+10
  0.55871660475658840 0E+04  0.45859212778119700 0E+03  0.83152946860200720 0E+04
  0.38610133635527460 0E+05  0.50528026279729360 0E+05  0.49772639746792180 0E+05
  0.67479832256518000 0E+06  0.36371058138124350 0E+06  0.17646208554367400 0E+07
  0.44688434620670540 0E+07  0.16861728086974150 0E+08  0.16878589815061110 0E+08
  0.46015820 -0.29980357  0.52972831  0.24608396  0.58249064  0.15796441
  0.00000000  0.00000000  0.00000000  0.00000000  0.00000000  0.00000000
  0.24073124 -0.19460909 -0.38184398  0.54342128 -0.34475269  0.46890384
```

```
 0.00000000  0.00000000  0.00000000  0.00000000  0.00000000  0.00000000
 0.47989885 -0.61011894 -0.27126204 -0.37965247 -0.20457329 -0.50514991
 0.00000000  0.00000000  0.00000000  0.00000000  0.00000000  0.00000000
 0.46015820  0.29980357  0.52972831 -0.24608396 -0.58249064  0.15796441
 0.00000000  0.00000000  0.00000000  0.00000000  0.00000000  0.00000000
 0.24073124  0.19460909 -0.38184398 -0.54342128  0.34475269  0.46890384
 0.00000000  0.00000000  0.00000000  0.00000000  0.00000000  0.00000000
 0.47989885  0.61011894 -0.27126204  0.37965247  0.20457329 -0.50514991
 0.00000000  0.00000000  0.00000000  0.00000000  0.00000000  0.00000000
C TRANSMISSIONLINE DIEMEN-FAULT
-1DIM-1 FLT-1                    2.                    -2 6
      11      0.54488725738666300000E+03
 -0.66550112317763710 0E+03  0.11310644724440860 0E+05  0.30498126976339880 0E+05
  0.68300901073626210 0E+06  0.52696612183308850 0E+07  0.15048409266969450 0E+08
  0.22996150397032160 0E+08  0.14733841944808480 0E+08  0.22956298311596640 0E+08
  0.32889484125591760 0E+08  0.73117682293571170 0E+08
  0.25775900806863820 0E+01  0.31317920897603720 0E+02  0.49278982281455180 0E+03
  0.11632843262573320 0E+05  0.98731240220843830 0E+05  0.60603484649316990 0E+06
  0.19332393216187440 0E+07  0.49390539353262160 0E+07  0.78225414668145190 0E+07
  0.11351093192865390 0E+08  0.25173583376436810 0E+08
      11      0.41962079931353280000E-04
  0.65674177269175700 0E+01  0.45201449716810010 0E+02  0.13328819971188460 0E+03
  0.37813870293095110 0E+03  0.92820986799796910 0E+03  0.52963012752412170 0E+05
  0.38487380893956420 0E+04  0.18406727414918320 0E+05  0.31058568839023380 0E+06
  0.32901777230790700 0E+08 -0.33289072803075730 0E+08
  0.11958986245080090 0E+04  0.75035383788577340 0E+04  0.14483184506168020 0E+05
  0.13393823262474470 0E+05  0.20943058236965270 0E+05  0.11329901578648530 0E+06
  0.12448560744582420 0E+06  0.16366487560085700 0E+06  0.49710882976761260 0E+06
  0.10754144723821600 0E+07  0.10764898868545420 0E+07
-2DIM-2 FLT-2                    2.                    -2 6
      11      0.37916763180759080000E+03
  0.15059728868446240 0E+04  0.47796587861261890 0E+03  0.29453883984532780 0E+03
  0.29623954424538490 0E+03  0.11304414738999120 0E+03  0.27754408993046330 0E+04
  0.97735332522282380 0E+05  0.61470612598721450 0E+06  0.16187756739931740 0E+07
  0.45772273518762680 0E+07  0.25988309474639030 0E+08
  0.40460047231220400 0E+01  0.79284505701286570 0E+01  0.12685020221332040 0E+02
  0.21443018222587600 0E+02  0.31615556663595650 0E+02  0.11149028101688900 0E+04
  0.39243178794292150 0E+05  0.24689868337585600 0E+06  0.65682187727970680 0E+06
  0.18730685184755070 0E+07  0.10712249957294590 0E+08
       7      0.41105368978686840000E-04
  0.17760489262119990 0E+05  0.35358745040874070 0E+06 -0.10412289457001050 0E+07
  0.12997958509287200 0E+07  0.24445384590187450 0E+07  0.38046881067958030 0E+09
 -0.38354326398349460 0E+09
  0.17517570327304680 0E+06  0.99280640659044380 0E+06  0.13263407310202820 0E+07
  0.12577928554788060 0E+07  0.43673667701435070 0E+07  0.10120302850025010 0E+08
  0.10130423152875030 0E+08
-3DIM-3 FLT-3                    2.                    -2 6
      11      0.25924782813320220000E+03
  0.90930226835431860 0E+03  0.59404392935138950 0E+03  0.80487694470604690 0E+03
  0.36639304171074360 0E+03  0.47726200965851480 0E+03  0.16034798841060160 0E+03
  0.23324202927775600 0E+03  0.43261876659053970 0E+03  0.55438281224075470 0E+04
  0.13772263405717560 0E+05  0.42972645060404900 0E+06
  0.26451805482907770 0E+01  0.47238429853371590 0E+01  0.93813344907331400 0E+01
  0.16164402798665800 0E+02  0.29663971358326280 0E+02  0.35886936002396950 0E+02
  0.63392370726982160 0E+02  0.37186661151617830 0E+03  0.46025460747833910 0E+04
  0.11550192342841870 0E+05  0.36120928280562740 0E+06
      14      0.40853434047356420000E-04
  0.10877034898047420 0E+02  0.69649096090511490 0E+02  0.22485328744456340 0E+03
  0.38135929307610460 0E+03  0.45396156313069790 0E+03  0.59529755166446080 0E+03
  0.48020661522064260 0E+03  0.48472549365354150 0E+03 -0.59657512168830650 0E+04
  0.77576017744233730 0E+05  0.61672377554933350 0E+06  0.11778636827362440 0E+07
  0.50510975135726660 0E+07  0.49098379539491620 0E+08
```

```
  0.45303652471399960OE+04  0.28961408073759210OE+05  0.92822041456801950OE+05
  0.15335337876745390OE+06  0.19710420601913030OE+06  0.25149902803862510OE+06
  0.18622759750532440OE+06  0.20931103700747490OE+06  0.12761930779392690OE+07
  0.12372895438371780OE+07  0.64153304208847270OE+07  0.97008194102285360OE+07
  0.33203116131468720OE+08  0.88832461849922880OE+08
-4DIM-4 FLT-4                 2.                  -2 6
      11      0.26416919383049050000E+03
  0.12583633117932330OE+04  0.15939888588671340OE+03  0.96627421525444030OE+03
  0.23078128264040890OE+03  0.79339564300732900OE+02  0.18256356770788760OE+03
  0.18037288933181170OE+03  0.87254889182506530OE+02  0.17101610924280580OE+03
  0.33827382925512040OE+04  0.51620183379697450OE+05
  0.29467439034249710OE+01  0.41825884254387530OE+01  0.92883083845980660OE+01
  0.14061000891306340OE+02  0.17686807859687030OE+02  0.29941143083793990OE+02
  0.49342366337047420OE+02  0.85860237554391050OE+02  0.15815128122608050OE+03
  0.28688642788500050OE+04  0.44065596313212020OE+05
       7      0.41264059130453280000E-04
  0.22864725223195560OE+03  0.52874771993589970OE+04  0.87624191268682430OE+04
  0.33296433041947690OE+04  0.47626888992593390OE+05 -0.43415263822704160OE+07
  0.79847846991652800OE+08
  0.38145769101596490OE+05  0.87031722108168520OE+06  0.14065506402034950OE+07
  0.54632565592574060OE+06  0.20466519965404390OE+07  0.57889721951027860OE+09
  0.83216063374364880OE+08
-5DIM-5 FLT-5                 2.                  -2 6
      11      0.24772378961513770000E+03
  0.10075823059527990OE+04  0.48679479379932850OE+03  0.94687503869214020OE+03
  0.17628617924272130OE+03  0.82613321369675130OE+02  0.18453027666968300OE+03
  0.17158674040519680OE+03  0.82559563638247540OE+02  0.14168339152404340OE+03
  0.25990126613582270OE+04  0.41552411127664760OE+05
  0.26757531603127300OE+01  0.45012559168304640OE+01  0.93970763581254210OE+01
  0.14042232027018350OE+02  0.18051881019340820OE+02  0.30693437855276520OE+02
  0.49039722851442210OE+02  0.80194482582362740OE+02  0.13974451776192560OE+03
  0.22195266003693490OE+04  0.35534153161753300OE+05
       8      0.40432852140582170000E-04
  0.11998779597756660OE+03  0.16499642733996450OE+04  0.17267600617847940OE+04
  0.36694741766658510OE+04  0.12441569200904700OE+06  0.16674257895118680OE+06
  0.74941696244871720OE+06  0.83868103673813240OE+08
  0.26595103576847840OE+05  0.39003655750078690OE+06  0.36605561645187360OE+06
  0.78943359414966950OE+06  0.66169090924331640OE+07  0.42533656602377850OE+07
  0.10848507459694970OE+08  0.98148988148576230OE+08
-6DIM-6 FLT-6                 2.                  -2 6
      13      0.27355815795272550000E+03
  0.10117349819996390OE+04  0.37077791419969950OE+03  0.82477414445609720OE+03
  0.79971352517286290OE+03  0.39447563654705640OE+03  0.36452676575181120OE+03
  0.15306900843940720OE+03  0.19216399934408050OE+03  0.20971842689207260OE+04
  0.50216396076548580OE+04  0.12622662386591740OE+05  0.49961885862445250OE+05
  0.76901738439365700OE+06
  0.28070151766059690OE+01  0.43883131111709220OE+01  0.95222636628149570OE+01
  0.21523540142803920OE+02  0.31668058729822160OE+02  0.50848471302225990OE+02
  0.78230710441632970OE+02  0.17146726857710800OE+03  0.17157183946363520OE+04
  0.40692424406561540OE+04  0.10279078021783240OE+05  0.40754485636065200OE+05
  0.63071348234717280OE+06
      13      0.41850274073413540000E-04
  0.10769272899578870OE+02  0.66501665471676870OE+02  0.10652232304007730OE+03
  0.19622436566243190OE+03  0.31256836913523170OE+03  0.51364654918972460OE+03
  0.12575510335509650OE+04  0.62120232150083000OE+04  0.21340653484582350OE+06
  0.18078419292682400OE+06  0.13815012325927140OE+07 -0.71330974700223180OE+07
  0.39401560251750570OE+08
  0.39958985377712720OE+04  0.24515778287518700OE+05  0.39482817861560040OE+05
  0.72291673436084980OE+05  0.11614919776434860OE+06  0.18107412127765730OE+06
  0.22159604928601710OE+06  0.29672325258876200OE+06  0.48284579837058180OE+07
  0.20539009201829460OE+07  0.93244672055747160OE+07  0.52270014430240710OE+09
  0.57103675491092470OE+08
```

```
  0.46015820 -0.29980357  0.52972831  0.24608396  0.58249064  0.15796441
  0.00000000  0.00000000  0.00000000  0.00000000  0.00000000  0.00000000
  0.24073124 -0.19460909 -0.38184398  0.54342128 -0.34475269  0.46890384
  0.00000000  0.00000000  0.00000000  0.00000000  0.00000000  0.00000000
  0.47989885 -0.61011894 -0.27126204 -0.37965247 -0.20457329 -0.50514991
  0.00000000  0.00000000  0.00000000  0.00000000  0.00000000  0.00000000
  0.46015820  0.29980357  0.52972831 -0.24608396 -0.58249064  0.15796441
  0.00000000  0.00000000  0.00000000  0.00000000  0.00000000  0.00000000
  0.24073124  0.19460909 -0.38184398 -0.54342128  0.34475269  0.46890384
  0.00000000  0.00000000  0.00000000  0.00000000  0.00000000  0.00000000
  0.47989885  0.61011894 -0.27126204  0.37965247  0.20457329 -0.50514991
  0.00000000  0.00000000  0.00000000  0.00000000  0.00000000  0.00000000
C TRANSMISSIONLINE KRIMPEN-FAULT
-1KIJ-1 FLT-1                    2.                    -2 6
      11       0.54488725738666300000E+03
 -0.66550112317763710 0E+03  0.11310644724440860 0E+05  0.30498126976339880 0E+05
  0.68300901073626210 0E+06  0.52696612183308850 0E+07  0.15048409266969450 0E+08
  0.22996150397032160 0E+08  0.14733841944808480 0E+08  0.22956298311596640 0E+08
  0.32889484125591760 0E+08  0.73117682293571170 0E+08
  0.25775900806863820 0E+01  0.31317920897603720 0E+02  0.49278982281455180 0E+03
  0.11632843262573320 0E+05  0.98731240220843830 0E+05  0.60603484649316990 0E+06
  0.19332393216187440 0E+07  0.49390539353262160 0E+07  0.78225414668145190 0E+07
  0.11351093192865390 0E+08  0.25173583376436810 0E+08
      11       0.16448554767177770000E-03
  0.45671532629534510 0E+00  0.23479863561931310 0E+02  0.16295390427660710 0E+02
  0.89346597311421750 0E+02  0.13447969154333730 0E+04  0.13457075278350850 0E+04
  0.67682155574441190 0E+04  0.29900631633708370 0E+05  0.11003864427447550 0E+07
 -0.14607123912258710 0E+09  0.14493136374964190 0E+09
  0.81503979064270750 0E+02  0.21397742308138730 0E+04  0.21706230848143180 0E+04
  0.36743011491416730 0E+04  0.15117221629027740 0E+05  0.28669066321664670 0E+05
  0.22086608137958750 0E+05  0.56222933193454350 0E+05  0.13593650949937090 0E+06
  0.15823685430698400 0E+06  0.15839509116129090 0E+06
-2KIJ-2 FLT-2                    2.                    -2 6
      11       0.37916763180759080000E+03
  0.15059728868446240 0E+04  0.47796587861261890 0E+03  0.29453883984532780 0E+03
  0.29623954424538490 0E+03  0.11304414738999120 0E+03  0.27754408993046330 0E+04
  0.97735332522282380 0E+05  0.61470612598721450 0E+06  0.16187756739931740 0E+07
  0.45772273518762680 0E+07  0.25988309474639030 0E+08
  0.40460047231220400 0E+01  0.79284505701286570 0E+01  0.12685020221332040 0E+02
  0.21443018222587600 0E+02  0.31615556663595650 0E+02  0.11149028101688900 0E+04
  0.39243178794292150 0E+05  0.24689868337585600 0E+06  0.65682187727970680 0E+06
  0.18730685184755070 0E+07  0.10712249957294590 0E+08
       6       0.15719827892272640000E-03
  0.36335236871885930 0E+05  0.77921630949076250 0E+05  0.28523636205089840 0E+06
  0.38816894770566140 0E+08 -0.26457319310248160 0E+10  0.26065155430244070 0E+10
  0.13471854508535550 0E+06  0.27641447675961130 0E+06  0.50272909288790380 0E+06
  0.11681160596219650 0E+07  0.12539627619397970 0E+07  0.12552167247017350 0E+07
-3KIJ-3 FLT-3                    2.                    -2 6
      11       0.25924782813320220000E+03
  0.90930226835431860 0E+03  0.59404392935138950 0E+03  0.80487694470604690 0E+03
  0.36639304171074360 0E+03  0.47726200965851480 0E+03  0.16034798841060160 0E+03
  0.23324202927775600 0E+03  0.43261876659053970 0E+03  0.55438281224075470 0E+04
  0.13772263405717560 0E+05  0.42972645060404900 0E+06
  0.26451805482907770 0E+01  0.47238429853371590 0E+01  0.93813344907331400 0E+01
  0.16164402798665800 0E+02  0.29663971358326280 0E+02  0.35886936002396950 0E+02
  0.63392370726982160 0E+02  0.37186661151617830 0E+03  0.46025460747833910 0E+04
  0.11550192342841870 0E+05  0.36120928280562740 0E+06
      11       0.15553036999004810000E-03
  0.68424305822101140 0E+01  0.10417616959632270 0E+03  0.72143003389585450 0E+02
  0.90183890256704460 0E+02  0.26585822225572100 0E+04  0.64966919881612250 0E+04
  0.13189808781765830 0E+06  0.17994441735949080 0E+06  0.86603647099375810 0E+06
  0.57620186010385690 0E+07 -0.35480631445318930 0E+06
```

```
 0.1498272114812229OOE+04  0.235341088494294800E+05  0.154292963208264000E+05
 0.195179505120160600E+05  0.185825042833254600E+06  0.158456791763291800E+06
 0.193137645494754000E+07  0.108568983617190100E+07  0.370414422689246500E+07
 0.121547529849864500E+08  0.212869303708525400E+08
-4KIJ-4 FLT-4              2.                       -2 6
   11      0.264169193830490500000E+03
 0.125836331179323300E+04  0.159398885886713400E+03  0.966274215254440300E+03
 0.230781282640408900E+03  0.793395643007329000E+02  0.182563567707887600E+03
 0.180372889331811700E+03  0.872548891825065300E+02  0.171016109242805800E+03
 0.338273829255120400E+04  0.516201833796974500E+05
 0.294674390342497100E+01  0.418258842543875300E+01  0.928830838459806600E+01
 0.140610008913063400E+02  0.176868078596870300E+02  0.299411430837939900E+02
 0.493423663370474200E+02  0.858602375543910500E+02  0.158151281226080500E+03
 0.286886427885000500E+04  0.440655963132120200E+05
   14      0.157085213186240200000E-03
 0.279595041448791800E+01  0.369147323191925100E+02  0.508129579105908600E+02
 0.125296551826468800E+03  0.214289909419186500E+03  0.311022597391346200E+03
 0.389190760385108000E+03  0.575789915751979600E+03  0.541040800869759000E+04
 0.206674703172800500E+06  0.155109713862968500E+06  0.146072000505443500E+07
-0.683757546056907600E+07  0.358637995703530100E+08
 0.980203374997697400E+03  0.128319082238484200E+05  0.179267206404139300E+05
 0.437047227279413800E+05  0.754422414618611200E+05  0.105579021282733200E+06
 0.134936878148858800E+06  0.189007156522978900E+06  0.243229786248258800E+06
 0.447205968383503300E+07  0.169720405682457400E+07  0.926079446918128200E+07
 0.523019955999905200E+09  0.534354797395568200E+08
-5KIJ-5 FLT-5              2.                       -2 6
   11      0.247723789615137700000E+03
 0.100758230595279900E+04  0.486794793799328500E+03  0.946875038692140200E+03
 0.176286179242721300E+03  0.826133213696751300E+02  0.184530276669683000E+03
 0.171586740405196800E+03  0.825595636382475400E+02  0.141683391524043400E+03
 0.259901266135822700E+04  0.415524111276647600E+05
 0.267575316031273000E+01  0.450125591683046400E+01  0.939707635812542100E+01
 0.140422320270183500E+02  0.180518810193408200E+02  0.306934378552765200E+02
 0.490397228514422100E+02  0.801944825823627400E+02  0.139744517761925600E+03
 0.221952660036934900E+04  0.355341531617533000E+05
   10      0.153935254430618700000E-03
 0.886098692725687100E+01  0.126842311111289700E+03  0.392086869521513100E+03
 0.729746643855802100E+03  0.242568556304202700E+04  0.576595320144207700E+05
 0.433621910386592100E+06  0.400702692967472000E+06  0.302188955036122800E+07
 0.196631462798831600E+08
 0.206566505889988500E+04  0.294110357191962900E+05  0.890458166628229500E+05
 0.140172849273867900E+06  0.151362377256962000E+06  0.143998572385894100E+07
 0.632857118527732500E+07  0.286220271957292700E+07  0.128224790388994600E+08
 0.409345328322973000E+08
-6KIJ-6 FLT-6              2.                       -2 6
   13      0.273558157952725500000E+03
 0.101173498199963900E+04  0.370777914199699500E+03  0.824774144456097200E+03
 0.799713525172862900E+03  0.394475636547056400E+03  0.364526765751811200E+03
 0.153069008439407200E+03  0.192163999344080500E+03  0.209718426892072600E+04
 0.502163960765485800E+04  0.126226623865917400E+05  0.499618858624452500E+05
 0.769017384393657000E+06
 0.280701517660596900E+01  0.438831311117092200E+01  0.952226366281495700E+01
 0.215235401428039200E+02  0.316680587298221600E+02  0.508484713022259900E+02
 0.782307104416329700E+02  0.171467268577108000E+03  0.171571839463635200E+04
 0.406924244065615400E+04  0.102790780217832400E+05  0.407544856360652000E+05
 0.630713482347172800E+06
   12      0.159324533758076800000E-03
 0.636843179108117500E+01  0.491304601788395800E+02  0.912401768680968800E+02
 0.467940941057095400E+03  0.115767491125934000E+04  0.333659296955149100E+04
-0.880810115067377900E+05  0.284728404790996000E+06  0.929679876780359400E+06
 0.248831030454549500E+07  0.683501564691058200E+10 -0.683863539343308100E+10
 0.124236880812735000E+04  0.948136395451614400E+04  0.177629540526711600E+05
```

```
  0.652116852606797600E+05  0.847111954506622300E+05  0.743155655231731500E+05
  0.910345255949329600E+06  0.844258723058883900E+06  0.323591942451258700E+07
  0.824478647763683900E+07  0.364889756152280700E+08  0.365254645908433000E+08
  0.46015820 -0.29980357  0.52972831  0.24608396  0.58249064  0.15796441
  0.00000000  0.00000000  0.00000000  0.00000000  0.00000000  0.00000000
  0.24073124 -0.19460909 -0.38184398  0.54342128 -0.34475269  0.46890384
  0.00000000  0.00000000  0.00000000  0.00000000  0.00000000  0.00000000
  0.47989885 -0.61011894 -0.27126204 -0.37965247 -0.20457329 -0.50514991
  0.00000000  0.00000000  0.00000000  0.00000000  0.00000000  0.00000000
  0.46015820  0.29980357  0.52972831 -0.24608396 -0.58249064  0.15796441
  0.00000000  0.00000000  0.00000000  0.00000000  0.00000000  0.00000000
  0.24073124  0.19460909 -0.38184398 -0.54342128  0.34475269  0.46890384
  0.00000000  0.00000000  0.00000000  0.00000000  0.00000000  0.00000000
  0.47989885  0.61011894 -0.27126204  0.37965247  0.20457329 -0.50514991
  0.00000000  0.00000000  0.00000000  0.00000000  0.00000000  0.00000000
C TRANSMISSIONLINE KRIMPEN-MAASVLAKTE
-1KIJ-11MVL-1                2.                -2 6
      12       0.540895585929157300000E+03
 -0.193523734743956600E+03 -0.118424098651530500E+04  0.115397660311143800E+05
  0.580624107241017900E+05  0.826912157720395700E+06  0.549385376593773600E+07
  0.146467124020816000E+08  0.220198503209170400E+08  0.165936135554690300E+08
  0.203227756620327000E+08  0.317760571021511600E+08  0.672543607665423500E+08
  0.138150163925774500E+01  0.347612936750384600E+01  0.316348008140862800E+02
  0.985232102979461600E+03  0.150121355443224200E+05  0.109510614456763800E+06
  0.624065350997398800E+06  0.195702719159214900E+07  0.578782021082655800E+07
  0.739895415891676300E+07  0.115371727697519900E+08  0.244302385924156500E+08
      12       0.298318950631355700000E-03
  0.154304190264672000E+00  0.701435397585872200E+01  0.966140341732372200E+01
  0.656685714824822600E+02  0.854894194405262400E+03  0.668383251109299600E+03
  0.327847695597521100E+04  0.426249537120198400E+05  0.246429284590677700E+09
 -0.240122555289785200E+09  0.340391954523529800E+09 -0.346746193031169900E+09
  0.273812555224966400E+02  0.117713923301281900E+04  0.802950639129322800E+03
  0.252890009154552900E+04  0.856729293286989000E+04  0.150804909787404800E+05
  0.115638094487558400E+05  0.388908594147081900E+05  0.861810344497921800E+05
  0.862672154842419700E+05  0.784945911611700000E+05  0.785730857523311000E+05
-2KIJ-12MVL-2                2.                -2 6
      15       0.368114219784831800000E+03
  0.682567347038873800E+03  0.162015824223811900E+03  0.157100976708574000E+03
  0.489917151476643300E+02  0.763832819033596300E+02  0.163704358296304900E+03
  0.228422293329377800E+03  0.948174271499565100E+04  0.925317817805468400E+05
  0.291633863494937400E+06  0.598068356078248000E+06  0.114243002677270100E+07
  0.232511376937853500E+07  0.534399108309072200E+07  0.232107834909580300E+08
  0.351593134471536000E+01  0.544072595303305700E+01  0.886535016579220400E+01
  0.119853181058247900E+02  0.273323434592900700E+02  0.104712861082594400E+03
  0.151786253080691000E+03  0.598745163505429900E+04  0.582906066888354800E+05
  0.184612396361138700E+06  0.380086983072432400E+06  0.730606706658926000E+06
  0.149835016797845000E+07  0.346686482311350400E+07  0.151070646210042800E+08
      12       0.281986923772908000000E-03
  0.223601152100819000E+02  0.124520168910722200E+03  0.446780431442207500E+03
  0.177701226864031400E+04  0.869859355508917200E+04  0.396030674332240000E+05
  0.158861862424405000E+05  0.901523176541290700E+06  0.159054457493567600E+09
 -0.157274423335993200E+09  0.227312295647024900E+09 -0.230060411501352500E+09
  0.411672323845263100E+04  0.201040116441725500E+05  0.329810123564311900E+05
  0.556247079474647500E+05  0.949818182964343300E+05  0.136174791793402000E+06
  0.154983419274067700E+06  0.406177883277453700E+06  0.851476116593895700E+06
  0.852327592710488800E+06  0.623625561152606600E+06  0.624249186713758900E+06
-3KIJ-13MVL-3                2.                -2 6
      10       0.241162706439141500000E+03
  0.663273320139283200E+03  0.915999998921096800E+02  0.337969677302542700E+03
  0.349921491274651700E+03  0.220415677707486400E+03  0.258565926122312200E+03
  0.998044162035100700E+02  0.188311671679273200E+03  0.568811474413470100E+04
  0.136107900166260000E+06
```

```
 0.2535072898333390100E+01  0.3391183711560612000E+01  0.6340153539666304000E+01
 0.1371591803770529000E+02  0.2141518422738493000E+02  0.4214164720124600000E+02
 0.6436758000257558000E+02  0.1134845127839190000E+03  0.3145839841040736000E+04
 0.7568410516091636000E+05
   13      0.2794149932825857000E-03
 0.6152096152310805000E+01  0.6056141298336696000E+02  0.4868979009063074000E+02
 0.8723892141157292000E+02  0.3731721038898403000E+04  0.3906609207995730000E+04
 0.3038506356413609000E+05  0.4008358950572759000E+06  0.5103697649303295000E+06
 0.2286438386928089000E+07  0.2153256822178083000E+07  0.2057462994784829000E+09
-0.2111354263836075000E+09
 0.1138488401490318000E+04  0.1397592986932730000E+05  0.8868416959621811000E+04
 0.1358603561460872000E+05  0.1683708577040257000E+06  0.8672104517789812000E+05
 0.3494986123294963000E+06  0.3160182173374627000E+07  0.1438042729565112000E+07
 0.6295125488804737000E+07  0.1560992981345259000E+08  0.3231866074425494000E+08
 0.3235097940499917000E+08
-4KIJ-14MVL-4                     2.                         -2 6
   9       0.2402222156929791000E+03
 0.2460588703735432000E+04 -0.1658524150919338000E+04  0.2726662076709682000E+03
 0.1828034332780117000E+03  0.1031599130123973000E+03  0.9402837971870650000E+02
 0.9160230200372875000E+02  0.9008816686489315000E+02  0.1434395829988528000E+05
 0.2908045015911502000E+01  0.3078957796980396000E+01  0.5601297123690770000E+01
 0.9482825965716515000E+01  0.1331475181843341000E+02  0.1987364890322183000E+02
 0.3266120719206920000E+02  0.5817645115461954000E+02  0.8123524678316013000E+04
   11      0.2835339303512609000E-03
 0.1120528974971207000E+02  0.1773854842134837000E+03  0.1097808687540424000E+03
 0.2832372424178511000E+03  0.4758786242480895000E+04  0.1147701540710939000E+05
 0.3693371452859989000E+06  0.3102229518223149000E+06  0.2194594885022345000E+07
-0.1454100016720983000E+08  0.2751040318668575000E+08
 0.2212100232996088000E+04  0.3494411460510004000E+05  0.2154515009650988000E+05
 0.5584284208375060000E+05  0.3058024780491813000E+06  0.2564800266130228000E+06
 0.4699392810663657000E+07  0.1907498394518724000E+07  0.9365885305134289000E+07
 0.6856982341744883000E+08  0.4204149689786295000E+08
-5KIJ-15MVL-5                     2.                         -2 6
   9       0.2312465779331537000E+03
 0.1167412114099001000E+04 -0.3247805703807436000E+03  0.2441586984650296000E+03
 0.2188200887457527000E+03  0.7005839863537597000E+02  0.9397066661765527000E+02
 0.8979387818355814000E+02  0.7836840446407999000E+02  0.9873130041532519000E+04
 0.2811663060970027000E+01  0.3302766455344382000E+01  0.5596492835133215000E+01
 0.1001695199739616000E+02  0.1278659409806771000E+02  0.2005537414072326000E+02
 0.3235109677608415000E+02  0.5249240434758042000E+02  0.5646622070782730000E+04
   10      0.2752501666012248000E-03
 0.1844402700093074000E+02  0.1431086398619034000E+03  0.7970165171605863000E+03
 0.1926168129814878000E+04  0.5038892049067846000E+04  0.5321941646701015000E+05
 0.4794362039756702000E+05  0.9175663911524623000E+06  0.4801543678996810000E+07
 0.8501181352233818000E+07
 0.3022412973160542000E+04  0.2344771940878692000E+05  0.1251641005390270000E+06
 0.3222931658752583000E+06  0.2043994976938899000E+06  0.1010392879691435000E+07
 0.4259502771040691000E+07  0.3415562684079352000E+07  0.1387703995935099000E+08
 0.3140483977293064000E+08
-6KIJ-16MVL-6                     2.                         -2 6
   10      0.2482764292507087000E+03
 0.6640624034958618000E+03  0.5480031994745198000E+02  0.4072121935915791000E+03
 0.4193538426547140000E+03  0.4685118707398454000E+03  0.3580037735596703000E+03
 0.1903042617694237000E+03  0.4951066057208483000E+04  0.2283755162671852000E+05
 0.4903347716937221000E+06
 0.2558427457158475000E+01  0.3334034955154938000E+01  0.6935345538930020000E+01
 0.1610981569540386000E+02  0.3520526182247179000E+02  0.5789979140058002000E+02
 0.1147911371337127000E+03  0.2694023020565561000E+04  0.1254046731254050000E+05
 0.2708840260455612000E+06
   12      0.2867545516013102000E-03
 0.3351467410674114000E+01  0.4635180437989214000E+02  0.4448250059801015000E+02
 0.4318611986067825000E+02  0.5995986307245992000E+03  0.2242012617603819000E+04
```

```
 0.10773119919562060OE+05  0.18932229708824210OE+06  0.22084851706575860OE+06
 0.90721466322660460OE+06  0.18202254499587840OE+10 -0.18215565875392580OE+10
 0.62882876160819520OE+03  0.84089895127900890OE+04  0.90929277878938190OE+04
 0.74550224315327220OE+04  0.27341190275177600OE+05  0.11743503088385650OE+06
 0.10063706524171960OE+06  0.14779558087606460OE+07  0.64606374478314340OE+06
 0.28733256950056580OE+07  0.11312157258904430OE+08  0.11323469416163330OE+08
 0.45419355 -0.29644042  0.52813697  0.29681271  0.55068345  0.22763805
 0.00000000  0.00000000  0.00000000  0.00000000  0.00000000  0.00000000
 0.24290185 -0.19963279 -0.40742081  0.48028460 -0.41401739  0.42483453
 0.00000000  0.00000000  0.00000000  0.00000000  0.00000000  0.00000000
 0.48859734 -0.61239374 -0.23990309 -0.40190508 -0.15321058 -0.54097502
 0.00000000  0.00000000  0.00000000  0.00000000  0.00000000  0.00000000
 0.45618287  0.30387064  0.52316666 -0.30594582 -0.56464260  0.16672992
 0.00000000  0.00000000  0.00000000  0.00000000  0.00000000  0.00000000
 0.24385705  0.20344184 -0.40995350 -0.49672378  0.38304759  0.43549804
 0.00000000  0.00000000  0.00000000  0.00000000  0.00000000  0.00000000
 0.47792309  0.60292436 -0.23613748  0.42351372  0.19057053 -0.50752848
 0.00000000  0.00000000  0.00000000  0.00000000  0.00000000  0.00000000
C TRANSMISSIONLINE KRIMPEN-GEERTRUIDENBERG
-1KIJ-21GTB-11                2.                -2 6
      11      0.54488725738666300000E+03
-0.66550112317763710OE+03  0.11310644724440860OE+05  0.30498126976339880OE+05
 0.68300901073626210OE+06  0.52696612183308850OE+07  0.15048409266969450OE+08
 0.22996150397032160OE+08  0.14733841944808480OE+08  0.22956298311596640OE+08
 0.32889484125591760OE+08  0.73117682293571170OE+08
 0.25775900806863820OE+01  0.31317920897603720OE+02  0.49278982281455180OE+03
 0.11632843262573320OE+05  0.98731240220843830OE+05  0.60603484649316990OE+06
 0.19332393216187440OE+07  0.49390539353262160OE+07  0.78225414668145190OE+07
 0.11351093192865390OE+08  0.25173583376436810OE+08
      11      0.11647074230328710000E-03
 0.12539904532836250OE+01  0.24674886347155980OE+02  0.36213197191037700OE+02
 0.11237451336568610OE+03  0.17140385501002680OE+04  0.18548551445776630OE+04
 0.95550457700733280OE+04  0.34220612103477040OE+05  0.10977495660911940OE+07
-0.17302213141764070OE+09  0.17187686278339250OE+09
 0.21836081380868750OE+03  0.30851366435399450OE+04  0.32263394931400940OE+04
 0.46640697277898630OE+04  0.20244452984030150OE+05  0.40275427405307260OE+05
 0.30923571776997570OE+05  0.76309792075814140OE+05  0.20080644485544440OE+06
 0.24366900059320050OE+06  0.24391266959379350OE+06
-2KIJ-22GTB-12                2.                -2 6
      11      0.37916763180759080000E+03
 0.15059728868446240OE+04  0.47796587861261890OE+03  0.29453883984532780OE+03
 0.29623954424538490OE+03  0.11304414738999120OE+03  0.27754408993046330OE+04
 0.97735332522282380OE+05  0.61470612598721450OE+06  0.16187756739931740OE+07
 0.45772273518762680OE+07  0.25988309474639030OE+08
 0.40460047231220400OE+01  0.79284505701286570OE+01  0.12685020221332040OE+02
 0.21443018222587600OE+02  0.31615556663595650OE+02  0.11149028101688900OE+04
 0.39243178794292150OE+05  0.24689868337585600OE+06  0.65682187727970680OE+06
 0.18730685184755070OE+07  0.10712249957294590OE+08
      11      0.11214834596335050000E-03
 0.62420829184867830OE+02  0.27584241198739650OE+03  0.51029834837302300OE+03
 0.25694514202416540OE+04  0.16952670436976390OE+05  0.12564774349006380OE+07
-0.11189055398243090OE+07  0.20107704214737090OE+06  0.23404602386368560OE+07
-0.49712126732459380OE+09  0.49442178746528190OE+09
 0.11033970441202470OE+05  0.39997014375381380OE+05  0.43680989847076290OE+05
 0.91633451988075480OE+05  0.20181917520227520OE+06  0.34351374504057130OE+06
 0.34615465988577170OE+06  0.58923775007571130OE+06  0.14203740574035270OE+07
 0.20582937845960710OE+07  0.20603520783806660OE+07
-3KIJ-23GTB-13                2.                -2 6
      11      0.25924782813320220000E+03
 0.90930226835431860OE+03  0.59404392935138950OE+03  0.80487694470604690OE+03
 0.36639304171074360OE+03  0.47726200965851480OE+03  0.16034798841060160OE+03
 0.23324202927775600OE+03  0.43261876659053970OE+03  0.55438281224075470OE+04
```

```
  0.137722634057175600E+05  0.429726450604049000E+06
  0.264518054829077700E+01  0.472384298533715900E+01  0.938133449073314000E+01
  0.161644027986658000E+02  0.296639713583262800E+02  0.358869360023969500E+02
  0.633923707269821600E+02  0.371866611516178300E+03  0.460254607478339100E+04
  0.115501923428418700E+05  0.361209282805627400E+06
      10      0.111302808992371400000E-03
  0.202581044483005600E+03  0.293819892063599500E+02  0.747691694297594800E+03
  0.798756994967382400E+03  0.498528345844728700E+04  0.105451375485101900E+06
  0.134477746837289100E+06  0.690339015836507000E+06  0.385298664281670100E+07
  0.783653549950912100E+07
  0.308011535641850500E+05  0.449352095381115400E+04  0.105946904158235800E+06
  0.121559915731069100E+06  0.192976300969741400E+06  0.202793098244054100E+07
  0.115189151919733100E+07  0.378819946967576600E+07  0.117734218469987900E+08
  0.292040126324520400E+08
-4KIJ-24GTB-14                 2.                    -2 6
      11      0.264169193830490500000E+03
  0.125836331179323300E+04  0.159398885886713400E+03  0.966274215254440300E+03
  0.230781282640408900E+03  0.793395643007329000E+02  0.182563567707887600E+03
  0.180372889331811700E+03  0.872548891825065300E+02  0.171016109242805800E+03
  0.338273829255120400E+04  0.516201833796974500E+05
  0.294674390342497100E+01  0.418258842543875300E+01  0.928830838459806600E+01
  0.140610008913063400E+02  0.176868078596870300E+02  0.299411430837939900E+02
  0.493423663370474200E+02  0.858602375543910500E+02  0.158151281226080500E+03
  0.286886427885000500E+04  0.440655963132120200E+05
      12      0.112400472990698800000E-03
  0.142159034233472800E+02  0.131905449348325200E+03  0.536934798579827200E+03
  0.704535423516504900E+04  0.111043107562636400E+04 -0.546922234659165900E+04
  0.215207954739149200E+04  0.350093839727638900E+05  0.243479230344971800E+06
  0.106300167285918000E+07 -0.893724031643906000E+07  0.527613297477025200E+08
  0.348203487768058900E+04  0.322626452499911200E+05  0.128021204833519300E+06
  0.188473391944682500E+06  0.260192354293167400E+06  0.188571442320570000E+06
  0.282333561190790800E+06  0.106741170691966300E+07  0.363398225698996600E+07
  0.897316654334271100E+07  0.222043489432800000E+09  0.669130010721031800E+08
-5KIJ-25GTB-15                 2.                    -2 6
      11      0.247723789615137700000E+03
  0.100758230595279900E+04  0.486794793799328500E+03  0.946875038692140200E+03
  0.176286179242721300E+03  0.826133213696751300E+02  0.184530276669683000E+03
  0.171586740405196800E+03  0.825595636382475400E+02  0.141683391524043400E+03
  0.259901266135822700E+04  0.415524111276647600E+05
  0.267575316031273000E+01  0.450125591683046400E+01  0.939707635812542100E+01
  0.140422320270183500E+02  0.180518810193408200E+02  0.306934378552765200E+02
  0.490397228514422100E+02  0.801944825823627400E+02  0.139744517761925600E+03
  0.221952660036934900E+04  0.355341531617533000E+05
       9      0.110168171885171700000E-03
  0.458587956959647600E+02  0.120604678407963300E+04  0.613498751772846700E+03
  0.810047274193741700E+03  0.154270940401019900E+06  0.333238171682168500E+06
  0.175329075105780600E+06  0.197470689848212300E+07  0.335028524001336800E+08
  0.746889837787586300E+04  0.200466639339049300E+06  0.976886918206073900E+05
  0.132919276814744900E+06  0.247637436405486800E+07  0.639080003341068600E+07
  0.265175161441891400E+07  0.116583449603684000E+08  0.536314632180739600E+08
-6KIJ-26GTB-16                 2.                    -2 6
      13      0.273558157952725500000E+03
  0.101173498199963900E+04  0.370777914199699500E+03  0.824774144456097200E+03
  0.799713525172862900E+03  0.394475636547056400E+03  0.364526765751811200E+03
  0.153069008439407200E+03  0.192163999344080500E+03  0.209718426892072600E+04
  0.502163960765485800E+04  0.126226623865917400E+05  0.499618858624452500E+05
  0.769017384393657000E+06
  0.280701517660596900E+01  0.438831311117092200E+01  0.952226366281495700E+01
  0.215235401428039200E+02  0.316680587298221600E+02  0.508484713022259900E+02
  0.782307104416329700E+02  0.171467268577108000E+03  0.171571839463635200E+04
  0.406924244065615400E+04  0.102790780217832400E+05  0.407544856360652000E+05
  0.630713482347172800E+06
```

```
     9      0.11401743693626850000E-03
  0.26586471467277890OE+02  0.19666817935845170OE+03  0.15482957258757060OE+04
  0.25542955578252480OE+04  0.85201492666183610OE+05  0.74000892198855120OE+05
  0.68961297013081420OE+06  0.31487607580984570OE+07  0.63865573926835110OE+07
  0.36219168239274110OE+04  0.26410079315118620OE+05  0.11548933481937160OE+06
  0.83871663937104090OE+05  0.14880256273040480OE+07  0.62366414709757980OE+06
  0.33261983394484400OE+07  0.99241807394546080OE+07  0.26612899318352480OE+08
  0.46015820 -0.29980357  0.52972831  0.24608396  0.58249064  0.15796441
  0.00000000  0.00000000  0.00000000  0.00000000  0.00000000  0.00000000
  0.24073124 -0.19460909 -0.38184398  0.54342128 -0.34475269  0.46890384
  0.00000000  0.00000000  0.00000000  0.00000000  0.00000000  0.00000000
  0.47989885 -0.61011894 -0.27126204 -0.37965247 -0.20457329 -0.50514991
  0.00000000  0.00000000  0.00000000  0.00000000  0.00000000  0.00000000
  0.46015820  0.29980357  0.52972831 -0.24608396 -0.58249064  0.15796441
  0.00000000  0.00000000  0.00000000  0.00000000  0.00000000  0.00000000
  0.24073124  0.19460909 -0.38184398 -0.54342128  0.34475269  0.46890384
  0.00000000  0.00000000  0.00000000  0.00000000  0.00000000  0.00000000
  0.47989885  0.61011894 -0.27126204  0.37965247  0.20457329 -0.50514991
  0.00000000  0.00000000  0.00000000  0.00000000  0.00000000  0.00000000
C TRANSMISSIONLINE GEERTRUIDENBERG-EINDHOVEN
-1GTB-R1EHV-1                    2.                    -2
    12       .24346604962400000000E+03
  -.62417101513600000OE+02  .20305029539500000OE+04  .28200883487900000OE+04
   .78786948872800000OE+04  .20436064014200000OE+06  .18729468188100000OE+07
   .56888401749600000OE+07  .10731350952000000OE+08  .98380233591200000OE+07
   .15245639908400000OE+08  .32766772239900000OE+08  .34037404842100000OE+09
   .15109699946600000OE+01  .16709321392800000OE+02  .41100166284000000OE+02
   .24240796097300000OE+03  .65057424725600000OE+04  .66406737868800000OE+05
   .43896708778300000OE+06  .17308507405600000OE+07  .63321684642400000OE+07
   .99985010163200000OE+07  .21507295949200000OE+08  .22500278586500000OE+09
    12      .22714398157100000000E-03
   .12960650510300000OE+00  .34571407121200000OE+01  .48167898421900000OE+01
   .44240911935600000OE+01  .30247022598500000OE+02  .35633270776400000OE+03
   .26530149810500000OE+03  .36708488612400000OE+04  .87478393920000000OE+04
   .64026957492800000OE+05  .60642010498400000OE+08 -.60719120810400000OE+08
   .29015171561600000OE+02  .71738216845600000OE+03  .10399501409000000OE+04
   .91297458414400000OE+03  .16029726194800000OE+04  .66472283248800000OE+04
   .14845533840400000OE+05  .12550733563000000OE+05  .26021027357400000OE+05
   .13851801666600000OE+06  .81861071918400000OE+05  .81942932990400000OE+05
-2GTB-R2EHV-2                    2.                    -2
    13       .98460046012000000000E+02
   .49668462860000000OE+03 -.25433998184600000OE+02  .24181117358200000OE+03
   .15538021368800000OE+03  .79805265220800000OE+02  .50732102772900000OE+02
   .32082874955000000OE+02  .39521316452300000OE+02  .65542480860000000OE+02
   .36060394078400000OE+04  .23389796453200000OE+05  .14543602591100000OE+06
   .21519020044800000OE+07
   .17204120325200000OE+01  .24475340577900000OE+01  .56655514220800000OE+01
   .11404575310600000OE+02  .16822347061800000OE+02  .23197697817100000OE+02
   .39694731289600000OE+02  .79833816220000000OE+02  .12717484954300000OE+03
   .63819816336000000OE+04  .41606484945200000OE+05  .26035778932200000OE+06
   .38726091829500000OE+07
    11       .21937075217600000000E-03
   .41979674767100000OE+02  .80256880779200000OE+01  .35419465664600000OE+03
   .47500093542000000OE+03  .39515897952900000OE+04  .19743612068000000OE+06
  -.19577086058900000OE+06  .13447550543800000OE+06  .41291138758000000OE+06
   .15253185950200000OE+10 -.15258724791400000OE+10
   .84343024989600000OE+04  .16518105600300000OE+04  .35236139890600000OE+05
   .23036531940800000OE+05  .86512787455200000OE+05  .30241059736600000OE+06
   .34309746264600000OE+06  .33363778301200000OE+06  .82208989715200000OE+07
   .25724206480400000OE+07  .25749930687200000OE+07
-3GTB-R3EHV-3                    2.                    -2
    13       .98460046012000000000E+02
```

```
    .4966846286000000000E+03  -.2543399818460000000E+02   .2418111735820000000E+03
    .1553802136880000000E+03   .7980526522080000000E+02   .5073210277290000000E+02
    .3208287495500000000E+02   .3952131645230000000E+02   .6554248086000000000E+02
    .3606039407840000000E+04   .2338979645320000000E+05   .1454360259110000000E+06
    .2151902004480000000E+07
    .1720412032520000000E+01   .2447534057790000000E+01   .5665551422080000000E+01
    .1140457531060000000E+02   .1682234706180000000E+02   .2319769781710000000E+02
    .3969473128960000000E+02   .7983381622000000000E+02   .1271748495430000000E+03
    .6381981633600000000E+04   .4160648494520000000E+05   .2603577893220000000E+06
    .3872609182950000000E+07
      11       .2193707521760000000E-03
    .4197967476710000000E+02   .8025688077920000000E+01   .3541946566460000000E+03
    .4750009354200000000E+03   .3951589795290000000E+04   .1974361206800000000E+06
   -.1957708605890000000E+06   .1344755054380000000E+06   .4129113875800000000E+06
    .1525318595020000000E+10  -.1525872479140000000E+10
    .8434302498960000000E+04   .1651810560030000000E+04   .3523613989060000000E+05
    .2303653194080000000E+05   .8651278745520000000E+05   .3024105973660000000E+06
    .3430974626460000000E+06   .3336377830120000000E+06   .8220898971520000000E+07
    .2572420648040000000E+07   .2574993068720000000E+07
C   TRANSMISIONLINE   EINDHOVEN-MAASBRACHT SIMULATED BY WAVE IMPEDANCE
C BUS1--BUS2--BUS3--BUS4--R-----L----------R-----L----------R-----L----------
51BRON-1EHV-1              330.
52BRON-2EHV-2              130.
53BRON-3EHV-3
C TRANSFORMER CAPACITANCE DIEMEN
C BUS1--BUS2--BUS3--BUS4--R-----L-----C-----                                  0
  DIM-R1                              2.0E-2
  DIM-R2                              2.0E-2
  DIM-R3                              2.0E-2
C STATION CAPACITANCE MAASVLAKTE
  MVL-R1                              1.4E-1
  MVL-R2                              1.4E-1
  MVL-R3                              1.4E-1
C TRANSFORMER CAPACITANCE KRIMPEN
C BUS1--BUS2--BUS3--BUS4--R-----L----------R-----L----------R-----L----------
  KIJ-R1                              2.0E-2
  KIJ-R2                              2.0E-2
  KIJ-R3                              2.0E-2
C TRANSFORMER CAPACITANCE EINDHOVEN
C BUS1--BUS2--BUS3--BUS4--R-----L----------R-----L----------R-----L----------
  EHV-R1                              3.0E-2
  EHV-R2                              3.0E-2
  EHV-R3                              3.0E-2
C BUS1--BUS2--BUS3--BUS4--R-----L----------R-----L----------R-----L----------
C TRANSFORMER CAPACITANCE GEERTRUIDENBERG
  GTB-R1                              2.0E-2
  GTB-R2                              2.0E-2
  GTB-R3                              2.0E-2
C 220 KV TRANSMISSIONLINES ENS
C BUS1--BUS2--BUS3--BUS4--R-----L----------R-----L----------R-----L----------
51BRON-1BENS-1             539.
52BRON-2BENS-2             177.
53BRON-3BENS-3
C BUS1--BUS2--BUS3--BUS4--R-----L-----C-----                                  0
C TRANSFORMER CAPACITANCES ENS
  ENS-R1                              2.1E-2
  ENS-R2                              2.1E-2
  ENS-R3                              2.1E-2
  ENS-R1BENS-1                        1.9E-2
  ENS-R2BENS-2                        1.9E-2
  ENS-R3BENS-3                        1.9E-2
  BENS-1                              4.3E-2
```

```
  BENS-2                                4.3E-2
  BENS-3                                4.3E-2
BLANK CARD TERMINATING BRANCHES
C SWITCHES
C BUS1--BUS2--TCLOSE----TOPEN-----IEPS------                                  0
C  FAULT POSITION
  FLT-1 FLT-2          0       1E21
C DIEMEN
  DIM-R1DIM-1         -1       1E21                                           1
  DIM-R2DIM-2         -1       1E21                                           1
  DIM-R3DIM-3         -1       1E21                                           1
  DIM-R1DIM-4         -1       1E21                                           1
  DIM-R2DIM-5         -1       1E21                                           1
  DIM-R3DIM-6         -1       1E21                                           1
  DIM-R1DIM-11        -1       1E21                                           1
  DIM-R2DIM-12        -1       1E21                                           1
  DIM-R3DIM-13        -1       1E21                                           1
  DIM-R1DIM-14        -1       1E21                                           0
  DIM-R2DIM-15        -1       1E21                                           0
  DIM-R3DIM-16        -1       1E21                                           0
C ENS
  ENS-R1ENS-1         -1       1E21                                           1
  ENS-R2ENS-2         -1       1E21                                           1
  ENS-R3ENS-3         -1       1E21                                           1
  ENS-R1ENS-4         -1       1E21                                           0
  ENS-R2ENS-5         -1       1E21                                           0
  ENS-R3ENS-6         -1       1E21                                           0
C KRIMPEN
  KIJ-R1KIJ-1         -1       1E21                                           1
  KIJ-R2KIJ-2         -1       1E21                                           1
  KIJ-R3KIJ-3         -1       1E21                                           1
  KIJ-R1KIJ-4         -1       1E21                                           1
  KIJ-R2KIJ-5         -1       1E21                                           1
  KIJ-R3KIJ-6         -1       1E21                                           1
  KIJ-R1KIJ-11        -1       1E21                                           1
  KIJ-R2KIJ-12        -1       1E21                                           1
  KIJ-R3KIJ-13        -1       1E21                                           1
  KIJ-R1KIJ-14        -1       1E21                                           0
  KIJ-R2KIJ-15        -1       1E21                                           0
  KIJ-R3KIJ-16        -1       1E21                                           0
  KIJ-R1KIJ-21        -1       1E21                                           1
  KIJ-R2KIJ-22        -1       1E21                                           1
  KIJ-R3KIJ-23        -1       1E21                                           1
  KIJ-R1KIJ-24        -1       1E21                                           0
  KIJ-R2KIJ-25        -1       1E21                                           0
  KIJ-R3KIJ-26        -1       1E21                                           0
C MAASVLAKTE
  MVL-R1MVL-1         -1       1E21                                           1
  MVL-R2MVL-2         -1       1E21                                           1
  MVL-R3MVL-3         -1       1E21                                           1
  MVL-R1MVL-4         -1       1E21                                           0
  MVL-R2MVL-5         -1       1E21                                           0
  MVL-R3MVL-6         -1       1E21                                           0
C GEERTRUIDENBERG
  GTB-R1GTB-11        -1       1E21                                           1
  GTB-R2GTB-12        -1       1E21                                           1
  GTB-R3GTB-13        -1       1E21                                           1
  GTB-R1GTB-14        -1       1E21                                           0
  GTB-R2GTB-15        -1       1E21                                           0
  GTB-R3GTB-16        -1       1E21                                           0
BLANK CARD TERMINATING SWITCHES
C BUS1--I-AMPL------FREQ------PHI-------                  TSTART----TSTOP-----
```

```
C SOURCES 380KV = 1000 UNITS AMPLITUDE
14BRON-1 0       1.E3       50.0        30.                                  -1
14BRON-2 0       1.E3       50.0       150.                                  -1
14BRON-3 0       1.E3       50.0       270.                                  -1
C SOURCES 220KV
14BRON-4 0       578.       50.0        30.                                  -1
14BRON-5 0       578.       50.0       150.                                  -1
14BRON-6 0       578.       50.0       270.                                  -1
BLANK CARD TERMINATING SOURCES
C NAM1--NAM2--NAM3--NAM4--NAM5--NAM6--NAM7--NAM8--NAM9--NAM10-NAM11-NAM12-NAM13-
  DIM-1 DIM-2 DIM-3 ENS-1 ENS-2 ENS-3 KIJ-1 KIJ-2 KIJ-3 MVL-1 MVL-2 MVL-3 GTB-R1
  GTB-R2GTB-R3
BLANK CARD TERMINATING OUTPUT
BLANK CARD TERMINATING DATA CASE
```

Appendix E: Situations studied during complex network study

Run	Fault-type	Fault-init.-angle	Distance to Diemen
43	R-N	0°	12 km
44	R-N	90°	12 km
45	R-N	30°	12 km
45a	R-S	30°	12 km
46	R-S	120°	12 km
48	R-S-N	120°	12 km
50	R-S-N	24°	12 km
52	R-S-N	50°	12 km
54	R-S-N	139°	12 km
56	R-V	30°	12 km
58	R-V	120°	12 km
60	S-N	60°	12 km
62	S-N	150°	12 km
64	T-N	120°	12 km
66	T-N	30°	12 km
68	R-T	150°	12 km
70	R-T	30°	12 km
72	S-T	90°	12 km
74	S-T	0°	12 km
76	R-T-N	150°	12 km
78	S-T-N	96°	12 km
80	R-S-T	35°	12 km
82	R-S-T-U-V-W	35°	12 km
84	R-V-N	96°	12 km
86	R-S-T-V	149°	12 km
88	R-S-U-N	30°	12 km
90	R-S-T-W-N	90°	12 km
92	R-S-U-V-N	15°	12 km
94	S-T-W-N	12°	12 km
119	R-T	60°	12 km
122	R-V-N	106°	12 km
124	R-W-N	85°	12 km
126	R-S-T-U-N	90°	12 km
129	R-N	0°	28.85 km
130	R-N	0°	2 km
131	R-S	30°	2 km
132	R-S-T	35°	2 km
133	R-S-T-U-V-W	35°	2 km
135	R-S-T	60°	2 km
136	R-S-T-U-V-W	60°	2 km

Appendix F: Multiple reflections

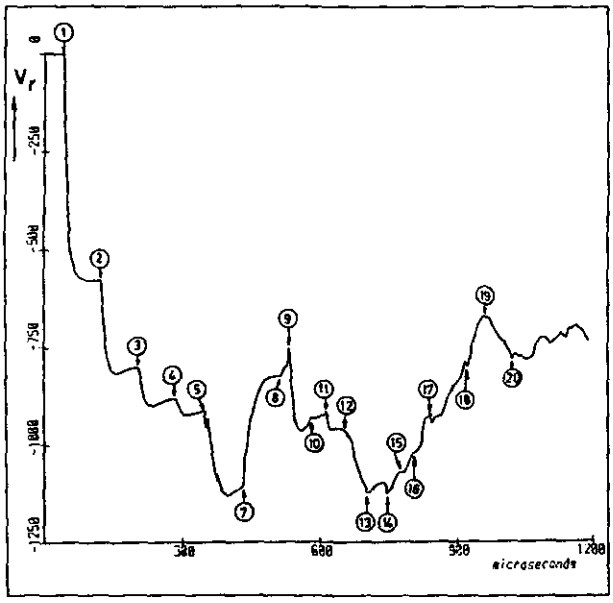

Figure 81: Voltages Diemen

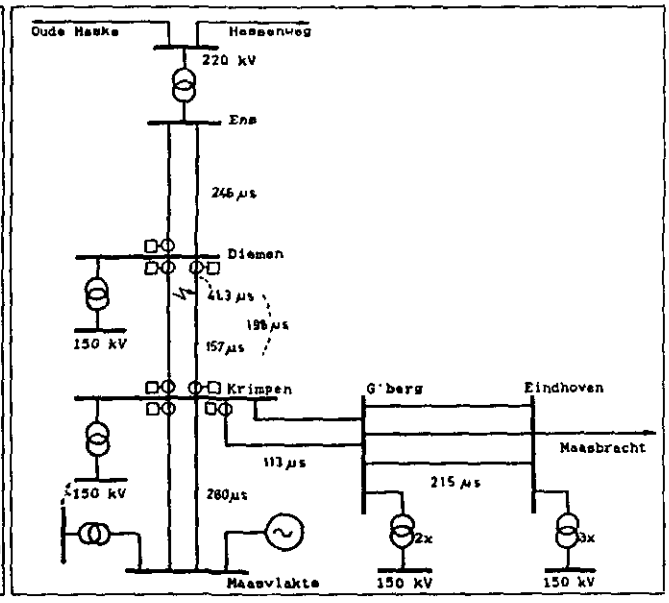

Figure 82: Dutch 380 kV grid.

Figure 81 shows the voltage behaviour of phase R in the station of Diemen after an R-N fault with a fault-initiation-angle of 0^{o}. Figure 82 shows the configuration of the Dutch 380 kV grid with the travel times of the different lines. Every peak or change in the voltage in figure 81 represents a travelling wave arriving in the station. the explanation of the most pronounced peaks is given in table 13.

No.	Time (microsec.)	Travelling wave path
1	41,3	Arrival Fault-Diemen
2	124	1e reflection Fault-Diemen (F-D-F-D)
3	207	2e reflection Fault-Diemen (F-D-F-D-F-D)
4	289	3e reflection Fault-Diemen
5	355	1e reflection Fault-Krimpen, Diemen (F-K-D)
7	437	Fault-Diemen-Krimpen-Diemen
8	520	1e reflection Fault-Diemen, Krimpen-Diemen
9	533	Fault-Ens-Diemen
10	581	Fault-Geertruidenberg-Diemen
11	616	1e reflection Fault-diemen, Ens-Diemen
12	669	2e reflection Fault-Krimpen, Krimpen-Diemen
13	700	2e reflection Fault-Diemen, Ens-Diemen
14	738	1e reflection Fault-Krimpen, G'berg-Diemen
15	779	1e refl. Fault-Krimpen, Diemen-G'berg-Diemen
16	825	2e reflection Fault-Diemen, G'berg-Diemen
17	847	1e reflection Fault-Krimpen, Diemen-Ens-Diemen
18	915	Fault-Maasvlakte-Diemen
19	970	1e reflection Fault-Diemen, Krimpen-Ens-Diemen
20	1011	Fault-Eindhoven-Diemen

Table 13: Travelling waves arriving at the station Diemen.

Eindhoven University of Technology Research Reports
Faculty of Electrical Engineering

ISSN 0167-9708
Coden: TEUEDE

(188) Jóźwiak, J.
THE FULL DECOMPOSITION OF SEQUENTIAL MACHINES WITH THE STATE AND OUTPUT BEHAVIOUR REALIZATION.
EUT Report 88-E-188. 1988. ISBN 90-6144-188-9

(189) Pineda de Gyvez, J.
ALWAYS: A system for wafer yield analysis.
EUT Report 88-E-189. 1988. ISBN 90-6144-189-7

(190) Siuzdak, J.
OPTICAL COUPLERS FOR COHERENT OPTICAL PHASE DIVERSITY SYSTEMS.
EUT Report 88-E-190. 1988. ISBN 90-6144-190-0

(191) Bastiaans, M.J.
LOCAL-FREQUENCY DESCRIPTION OF OPTICAL SIGNALS AND SYSTEMS.
EUT Report 88-E-191. 1988. ISBN 90-6144-191-9

(192) Worm, S.C.J.
A MULTI-FREQUENCY ANTENNA SYSTEM FOR PROPAGATION EXPERIMENTS WITH THE OLYMPUS SATELLITE.
EUT Report 88-E-192. 1988. ISBN 90-6144-192-7

(193) Kersten, W.F.J. and G.A.P. Jacobs
ANALOG AND DIGITAL SIMULATION OF LINE-ENERGIZING OVERVOLTAGES AND COMPARISON WITH MEASUREMENTS IN A 400 kV NETWORK.
EUT Report 88-E-193. 1988. ISBN 90-6144-193-5

(194) Hosselet, L.M.L.F.
MARTINUS VAN MARUM: A Dutch scientist in a revolutionary time.
EUT Report 88-E-194. 1988. ISBN 90-6144-194-3

(195) Bondarev, V.N.
ON SYSTEM IDENTIFICATION USING PULSE-FREQUENCY MODULATED SIGNALS.
EUT Report 88-E-195. 1988. ISBN 90-6144-195-1

(196) Liu Wen-Jiang, Zhu Yu-Cai and Cai Da-Wei
MODEL BUILDING FOR AN INGOT HEATING PROCESS: Physical modelling approach and identification approach.
EUT Report 88-E-196. 1988. ISBN 90-6144-196-X

(197) Liu Wen-Jiang and Ye Dau-Hua
A NEW METHOD FOR DYNAMIC HUNTING EXTREMUM CONTROL, BASED ON COMPARISON OF MEASURED AND ESTIMATED VALUE.
EUT Report 88-E-197. 1988. ISBN 90-6144-197-8

(198) Liu Wen-Jiang
AN EXTREMUM HUNTING METHOD USING PSEUDO RANDOM BINARY SIGNAL.
EUT Report 88-E-198. 1988. ISBN 90-6144-198-6

(199) Jóźwiak, L.
THE FULL DECOMPOSITION OF SEQUENTIAL MACHINES WITH THE OUTPUT BEHAVIOUR REALIZATION.
EUT Report 88-E-199. 1988. ISBN 90-6144-199-4

(200) Huis in 't Veld, R.J.
A FORMALISM TO DESCRIBE CONCURRENT NON-DETERMINISTIC SYSTEMS AND AN APPLICATION OF IT BY ANALYSING SYSTEMS FOR DANGER OF DEADLOCK.
EUT Report 88-E-200. 1988. ISBN 90-6144-200-1

(201) Woudenberg, H. van and R. van den Born
HARDWARE SYNTHESIS WITH THE AID OF DYNAMIC PROGRAMMING.
EUT Report 88-E-201. 1988. ISBN 90-6144-201-X

(202) Engelshoven, R.J. van and R. van den Born
COST CALCULATION FOR INCREMENTAL HARDWARE SYNTHESIS.
EUT Report 88-E-202. 1988. ISBN 90-6144-202-8

(203) Delissen, J.G.M.
THE LINEAR REGRESSION MODEL: Model structure selection and biased estimators.
EUT Report 88-E-203. 1988. ISBN 90-6144-203-6

(204) Kalasek, V.K.I.
COMPARISON OF AN ANALYTICAL STUDY AND EMTP IMPLEMENTATION OF COMPLICATED THREE-PHASE SCHEMES FOR REACTOR INTERRUPTION.
EUT Report 88-E-204. 1988. ISBN 90-6144-204-4

Eindhoven University of Technology Research Reports
Faculty of Electrical Engineering

ISSN 0167-9708
Coden: TEUEDE

(205) Butterweck, H.J. and J.H.F. Ritzerfeld, M.J. Werter
FINITE WORDLENGTH EFFECTS IN DIGITAL FILTERS: A review.
EUT Report 88-E-205. 1988. ISBN 90-6144-205-2

(206) Bollen, M.H.J. and G.A.P. Jacobs
EXTENSIVE TESTING OF AN ALGORITHM FOR TRAVELLING-WAVE-BASED DIRECTIONAL DETECTION AND PHASE-SELECTION BY USING TWONFIL AND EMTP.
EUT Report 88-E-206. 1988. ISBN 90-6144-206-0

(207) Schuurman, W. and M.P.H. Weenink
STABILITY OF A TAYLOR-RELAXED CYLINDRICAL PLASMA SEPARATED FROM THE WALL BY A VACUUM LAYER.
EUT Report 88-E-207. 1988. ISBN 90-6144-207-9

(208) Lucassen, F.H.R. and H.H. van de Ven
A NOTATION CONVENTION IN RIGID ROBOT MODELLING.
EUT Report 88-E-208. 1988. ISBN 90-6144-208-7

(209) Jóźwiak, L.
MINIMAL REALIZATION OF SEQUENTIAL MACHINES: The method of maximal adjacencies.
EUT Report 88-E-209. 1988. ISBN 90-6144-209-5

(210) Lucassen, F.H.R. and H.H. van de Ven
OPTIMAL BODY FIXED COORDINATE SYSTEMS IN NEWTON/EULER MODELLING.
EUT Report 88-E-210. 1988. ISBN 90-6144-210-9

(211) Boom, A.J.J. van den
H_∞-CONTROL: An exploratory study.
EUT Report 88-E-211. 1988. ISBN 90-6144-211-7